LAPPEENRANNAN TEKNILLINEN YLIOPISTO
Faculty of Technology
Master's Degree Program in Chemical Engineering

*Tuomas Sihvonen*

# Determination of collector chemicals from flotation process waters using capillary electrophoresis

Examiners: Professor Heli Sirén
Ph.D. Jaakko Leppinen

Supervisors: M.Sc. (tech.) Annukka Aaltonen
Professor Heli Sirén
Ph.D. Jaakko Leppinen

## ABSTRACT

LAPPEENRANNAN TEKNILLINEN YLIOPISTO
Faculty of Technology
LUT Kemia

Tuomas Sihvonen

**Determination of collector chemicals from flotation process waters using capillary electrophoresis**

Master's thesis

2012

58 pages, 27 figures, 17 tables and 11 appendices

Examiners: Professor Heli Sirén
Ph.D. Jaakko Leppinen

**Keywords:** Capillary electrophoresis, flotation, xanthate, ditiophophinate, ditiophosphate

Froth flotation is a widely used process for separating valuable minerals from ore. This process depends heavily on collector chemicals that bind the valuable minerals to air bubbles, thus separating them from the gangue. Analyzing of these chemicals from the process waters is needed for better understanding of the collector behavior in the process and for better process control. In the literature part of this work different kinds of analysis methods for these compounds have been collected and compared. In the experimental part two analytical separation methods using capillary electrophoresis were developed. These methods were able to detect sodium diiosobutylditiophosphate (DTP) with detection limits of 2.7 $mgL^{-1}$ in pure water and 6.7 $mgL^{-1}$ in process water; sodium diisobutyldithiophosphinate (DTPI) with limits of 4.5 $mgL^{-1}$ and 6.7 $mgL^{-1}$ respectively; ethyl xanthate with limits of 0.025 $mgL^{-1}$ and 0.16 $mgL^{-1}$ and isobutyl xanthate with limits of 0.41 $mgL^{-1}$ and 0.62 $mgL^{-1}$. In future these methods can be further optimized for collector decomposition studies as well as for on-line process analysis.

**TIIVISTELMÄ**

LAPPEENRANNAN TEKNILLINEN YLIOPISTO
Teknillinen tiedekunta
LUT Kemia

Tuomas Sihvonen

**Kokoojakemikaalien määritys vahdotusprosessivesitä kapillaarielektroforeesilla**

Diplomityö

2012

58 sivua, 27 kuvaa, 17 taulukkoa ja 11 liitettä

Tarkastajat: Professor Heli Sirén
Ph.D. Jaakko Leppinen

**Hakusanat:** Kapillaarielektroforeesi, vaahdotus, ksantaatti, ditiofosfinaatti, ditiofosfaatti

Vaahdotusprosessia käytetään yleisesti erottamaan arvokkaita mineraaleja malmeista. Toimiakseen tehokkaasti prosessi tarvitsee kokoojakemikaaleja, joiden tehtävänä on sitoa halutut mineraalit ilmakupliin. Jotta näiden kemikaalien käyttäytymistä prosessissa voitaisiin ymmärtää paremmin ja prosessin ohjausta tehostaa, pitää kokoojia pystyä analysoimaan prosessivesistä. Työn kirjallisuusosassa on koottu ja vertailtu erilaisia kirjallisuudesta löytyneitä analyysimenetelmiä kokoojakemikaaleille. Kokeellisessaosassa on kehitetty kaksi kapillaarielektroforeesimenetelmää näiden kemikaalien tutkimiseen. Menetelmien toteamisrajat tutkituille kemikaaleille olivat seuraavanlaiset: natrium diiosobutylditiofosfaattille (DTP) 2,7 $mgL^{-1}$ puhtaassa vedessä ja 6,7 $mgL^{-1}$ prosessivedessä; natrium diisobutyldithiofosfinaatille (DTPI) vastaavasti 4,5 $mgL^{-1}$ ja 6,7 $mgL^{-1}$; etyyli ksantaatille 0,025 $mgL^{-1}$ ja 0,16 $mgL^{-1}$; ja isobutyyli ksantaatille 0,41 $mgL^{-1}$ ja 0,62 $mgL^{-1}$. Näitä menetelmiä voidaan tulevaisuudessa kehittää kokoojien hajoamistuotteiden analysointia varten sekä prosessien on-line mittauksiin.

# Contents

# Literature part

## 1 Introduction

Froth flotation is a process for separating valuable minerals form ores. First the ore is crushed and ground. Then the slurry is treated with flotation chemicals in a conditioning stage. In the flotation stage air bubbles generated in a flotation machine carry selected minerals to the top of the cell where they are collected for further processing. Surface active collector chemicals have a central role in the flotation process as they render the mineral particles hydrophobic. Particles having sufficient hydrophophibicity will be attached to the air bubbles while hydrophilic particles remain in the pulp [1–3]. This process can be used for many different kinds of ores, but in this work the collectors used mainly for sulfide ores are studied.

The most commonly used collector chemicals in froth flotation of sulfide minerals and gold are xanthates, dialkyl dithiophosphinates and dialkyl dithiophosphates, often referred as thiol or sulfhydryl collectors. Many times these collectors are used as mixtures to improve the process [3–6]. It has been noted in some studies that the decomposition products from xanthates are detrimental to the flotation process, but no mechanisms for this were given [1].

The purpose of this work was to develop an analytical separation method for determining organic collectors and their decomposition products from flotation process waters. Main focus was in chromatographic methods, because with these techniques it is possible to separate the collectors from the sample matrix and from one another so to be able to qualify and to quantify all the different species of collectors present. This is important because these kind of analysis methods can be used for the study of flotation phenomena or for process control.

Previously thiol collectors such as xanthates have been studied by ultraviolet–visible (UV/VIS) spectrophotometry [7,8], titration [9] and fourier transform infrared (FTIR) spectrometry [10]. Unfortunately these methods usually only give information on the sum of of different collectors present in the sample. Chromatography can be used to separate the different compounds especially in complex process solutions. There are already some chromatographic methods used for determining thiol collectors. These are mainly different kinds of high performance liquid chromatography (HPLC) methods [11–15]. In many of the methods the samples need derivatization before analysis. This leads to complex mixtures to be analyzed. In this work cap-

illary electrophoresis (CE) was used. A few articles about the use of CE for these compounds have already been published and they provided a starting point for this work [16, 17].

# 2 Thiol collectors

Xanthates, dialkyl dithiophosphinates and dialkyl dithiophosphates are collectors used in froth flotation of all kinds of sulfides. The first commercial patent to use xanthates as collectors in froth flotation is from the year 1925 [18]. Since then xanthates have been the most used group of collectors for sulfide minerals.

Table 1: Collectors used in this study

| IUPAC and trivial name | Abbreviation | Structure | CAS no. |
|---|---|---|---|
| Potassium o-ethyl carbonodithioate, Potassium ethyl xanthate | KEX | 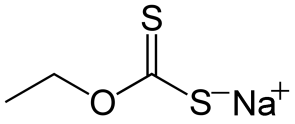 | 140-90-9 |
| Sodium O-isobutyl carbonodithioate, Sodium isobutyl xanthate | SIBX | 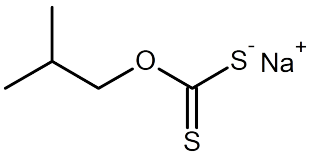 | 25306-75-6 |
| Sodium diisobutylphosphinodithioate, Sodium diisobutyldithiophosphinate | DTPI | 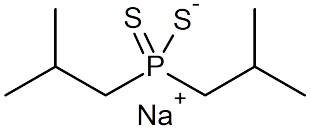 | 13360-78-6 |
| Sodium o,o-diisobutyl phosphorodithioate, Sodium diisobutyldithiophosphate | DTP | 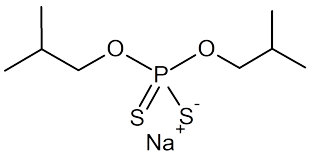 | 53378-51-1 |

Dithiophosphates and dithiophosphinates are often called promoters in the literature. This is because they are usually used together with xanthates, not alone [5]. Information on collectors examined in this study is presented in Table 1.

While a lot of information about xanthates is available the same can not be said about dithiophosphates and dithiophosphinates. So most of the discussion in the

thesis will be about xanthates and information about dithiophosphates and dithiophosphinates is given, when it is available.

## 2.1 Function in froth flotation

This section is meant to give a very general overview of the collector mineral interactions, to help the reader understand the function of the chemicals in the flotation process. In addition some basic information on suggested adsorption mechanisms is given, to showcase that the adsorption process can affect either pH or ionic strength of the process water.

The main interaction mechanism of collectors on mineral surfaces is adsorption, either chemisorption or physisorption, or combination of these two. In the flotation process the purpose of collector chemicals is to attach the desired minerals to air bubbles, so the minerals will float to the surface of the flotation cell. The collectors thiol end adsorbs to a mineral surface while the carbon chain create the necessary hydrophobicity for bubble-particle attachment. [2, 3, 19]

Waters can be circulated in the process, to save water and water purification costs. In this kind of process some collectors, their complexes or decomposition species can accumulate in the process to such a concentrations that have an effect on the process. Also in a process where different minerals are floated in succession, the minerals are exposed to collectors many times. Then the collectors decomposed on the surfaces may affect the minerals floatability. [1, 20]

Valdivieso et al. have studied xanthate adsorption mechanism on pyrite [21]. The study was performed by floating mineral samples in a laboratory scale flotation cell and then assaying samples from the flotation pulp. Three different xanthates were used. Assaying was done using UV/VIS spectrophotometry, surface area and electrokinetic studies. They compared the amount of $Fe^{2+}$ ions in the solution to the adsorption density of xanthates, and found a linear dependency between the two. This lead them to conclude that xanthates adsorb to pyrite surface forming dixanthogen reducing $Fe(OH)_3$ species on the surface to $Fe^{2+}$. The whole mechanism is presented in Figure 1. Earlier also Leppinen came to the conclusion that xanthate adsorbs on pyrite mainly by forming dixanthogen [22].

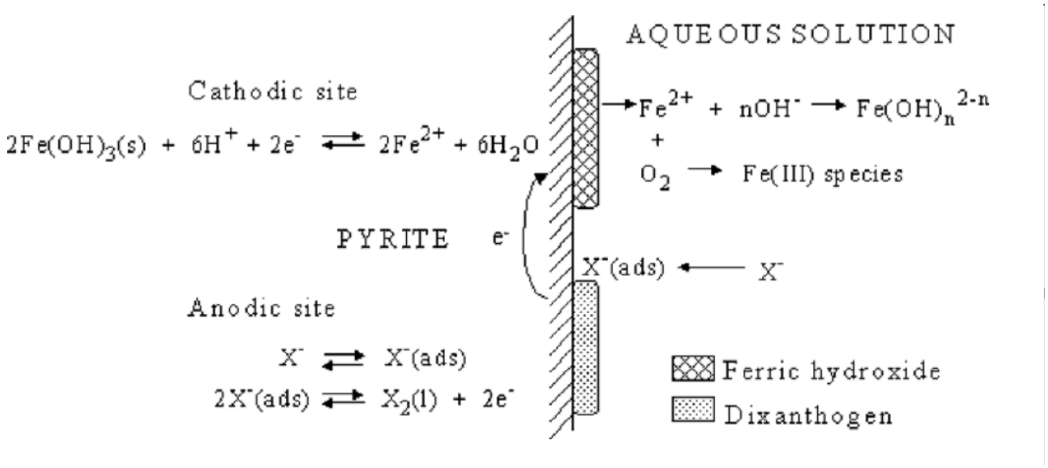


Figure 1: Xanthate adsorption mechanism on pyrite [21].

## 2.2 Chemical characteristics

Xanthates are produced through the (i) and (ii) reaction system, where alkali metal hydroxide is dissolved to alcohol followed by an addition of carbon disulfide. [23]

$$\mathrm{ROH} + \mathrm{NaOH} \longrightarrow \mathrm{RONa} + \mathrm{H_2O} \tag{i}$$

$$\mathrm{RONa} + \mathrm{CS_2} \longrightarrow \mathrm{ROCS_2} \tag{ii}$$

The used alcohol determines the length of the carbon chain at the end of the xanthate molecule.

Dialkyl dithiophosphate acid is produced through the following reaction,

$$\mathrm{P_4S_{10}} + 8\,\mathrm{R{-}OH} \longrightarrow 4\,\mathrm{R_2O_2{-}P{-}S_2H} + 2\,\mathrm{H_2S} \tag{iii}$$

where phosphorous pentasulphide ($P_4S_{10}$) reacts with alcohol in an inert media. This reaction produces $H_2S$, which is highly toxic. These acids react with alkali forming the corresponding dialkyl dithiophosphate. Shorter chained xanthates and dithiophosphates are more selective than long chained and are usually considered as weaker collectors. Dithiophosphates are more selective than xanthates with the same alkyl group. [19]

## 2.3 Decomposition

Information on decomposition is valuable to both the process and to analytics. In processes it is important to know the concentrations of various collectors in the slurry. In analysis it is important to know how long the samples stay representative and what species can be expected to be found in the samples. Based on his kinetic studies Trudgett has come to the conclusion that samples containing xanthates should have a pH of 8 or above and should be stored in cold to maximize the xanthate preservation [24].

There is information available on the decomposition xanthates such as kinetics at different pH:s [25] and decomposition mechanisms [23]. However it is largely unknown, how the decomposition products affect the flotation process or nature. Unfortunately there is not much information available on dithiophosphates and dithiophosphinates.

### 2.3.1 Decomposition in acidic conditions

Decomposition kinetics for xanthates depend heavily on pH. Sun and Forsling have studied the decomposition kinetics at pH 3–12 by UV-Visible spectroscopy. They found that at pHs lower than 7 the degradation is the fastest, then at pH 7–8 xanthates are at their most stable point. After that degradation gets faster at pH 9–10 and again slows down after pH 10. They also give a reaction mechanism for the degradation at pH 3–5 given in reactions (iv) and (v) [25]. Dialkyl dithiophosphates are more stable in acidic conditions than xanthates as their respective dialkyl dithiophosphoric acids are more stable [23].

Iwasaki and Cooke have studied xanthate decomposition kinetics in acidic solutions [26]. Their study was done by following the UV response at 301 nm. The study covered pH ranges of 2.68–4.71 and 0.1–1.11. For the former range they suggested the same mechanism as Sun and Forsling, given in equations (iv) and (v). They made the assumption that the determining step was the decomposition of xanthic acid (v) as the first reaction is ionic and thus very fast. From their measurements they were able to calculate the following dissociation constant to xanthic acid $K = 0.020 \pm 0.001$.

$$\mathrm{ROCS_2^-} + \mathrm{H^+} \rightleftharpoons \mathrm{ROCS_2H} \qquad \text{(iv)}$$

$$\mathrm{ROCS_2H} \longrightarrow \mathrm{ROH} + \mathrm{CS_2} \qquad \text{(v)}$$

Typically froth flotation processes of sulfide minerals are not operated at pHs below 5 and consequently the above decomposition products are not a priority in this work. On the contrary oxidation reactions and their products are more interesting for this study. It is known that these reactions need an oxidizing agent. The most common oxidant in the processes is oxygen from air. Usually this oxidation takes place catalyzed by the mineral surface.

### 2.3.2 Decomposition in alkaline conditions

Accordingly to Sun and Forsling [25] dixanthogens are formed at pH 6–12. The most widely recognized model for dixanthogen formation is presented in the following reactions. First the xanthate oxidizes to dixanthogen (vi). The electrons given off at this reaction are conducted by the mineral surface or other catalyst back to the solution through the cathodic reduction of oxygen (vii). The overall reaction is presented in equation (viii). [23, 27]

$$2\,\mathrm{ROCS_2^-} \rightleftharpoons (\mathrm{ROCS_2})_2 + 2\,\mathrm{e^-} \qquad \text{(vi)}$$

$$\tfrac{1}{2}\,\mathrm{O_2} + \mathrm{H_2O} + 2\,\mathrm{e^-} \rightleftharpoons 2\,\mathrm{OH^-} \qquad \text{(vii)}$$

$$2\,\mathrm{ROCS_2^-} + \tfrac{1}{2}\,\mathrm{O_2} + \mathrm{H_2O} \rightleftharpoons (\mathrm{ROCS_2})_2 + 2\,\mathrm{OH^-} \qquad \text{(viii)}$$

The above reaction mechanism is similar to the one suggested for pyrite by Valdivieso et al. [21], presented in Figure 1, except in their mechanism the cathodic reduction of oxygen is replaced by the reduction of surface-ferric hydroxide species.

Tipman and Leja have studied the formation and decomposition of dixanthogen in basic solutions [28]. Measurements were made by following UV absorption at 301 nm. They propose that in solutions of pH 7–10 xanthate decomposes according to the following reaction,

$$\mathrm{ROCS_2^-} + \mathrm{H_2O} \longrightarrow \mathrm{ROH} + \mathrm{CS_2} + \mathrm{OH^-} \qquad \text{(ix)}$$

and that no dixanthogen is formed by oxidation by oxygen, when no catalyst is present. In the presence of a oxidizing agent, it was found that the rate constant of xanthate decomposition increased by $10^6$ at pH 8. No dixanthogen was detected during the decomposition, so it was concluded that the reaction followed equation (ix). Dixanthogen was found to decompose in basic media following the next reaction,

$$(\mathrm{ROCS_2})_2 + \mathrm{OH^-} \longrightarrow \mathrm{ROCS_2OH} + \mathrm{ROCS_2^-} \tag{x}$$

where $ROCS_2OH$ is a sulfenic acid, that is highly unstable and decomposes further. Based on some other semiquantitative tests and knowledge of base strengths the following order or dixanthogen reactivity with nucleophiles was proposed: $HS^- > CN^- > OH^- > SO_3^{2-} > S_2O_3^{2-} > EtX^- > SCN^- > I^-$. [28]

The solubility of dixanthogen in water was measured in two ways. First by analyzing the dixanthogen in aqueous phase of a dixanthogen water system that was agitated so that it was likely in equilibrium. Second way was to measure the turbidity when dixanthogen saturates a solution of xanthate that is titrated with $KI_3$. With both methods the solubility at pH 2.8–8.4 was $1.25 \pm 0.05 \times 10^{-5}$ mol/L. [28]

At pH 9–11 perxanthate is formed [25] and for it the following reaction has been proposed [23].

$$\mathrm{ROCS_2^-} + \mathrm{H_2O_2} \longrightarrow \mathrm{ROCS_2O^-} + \mathrm{H_2O} \tag{xi}$$

Monothiocarbonate also needs a mineral surface, most likely a sulfide surface, to form. The exact reaction mechanism seems to be unknown, but the next mechanism has been given in [23].

$$\mathrm{Pb(X)_2} + \mathrm{O_2} \longrightarrow \mathrm{Pb(MTC)_2} + 2\,\mathrm{S^0} \tag{xii}$$

$$\mathrm{Pb(MTC)_2} + 2\,\mathrm{X^-} \longrightarrow \mathrm{Pb(X)_2} + 2\,\mathrm{MTC} \tag{xiii}$$

Information on decomposition species of ethyl xanthate is presented in Table 2 and it is very likely that other xanthates produce similar degradation products, as all the degradation reactions seem to be only depended on the functional thiol group. Also there seems to be very little difference in xanhtate decomposition kinetics between xanthates of different alkyl groups [24].

Table 2: Decomposition products of ethyl xanthate [14].

| Name, abbreviation | Structure | UV | $pK_a$ |
|---|---|---|---|
| Xanthate ion, $EX^-$ | 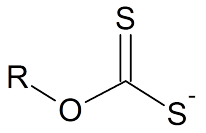 | 301 | 1.6 |
| Dixanthogen, $(EX)_2$ | 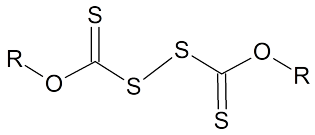 | 283 | 0.843 |
| Ethyl perxanthate, $EPX^-$ | 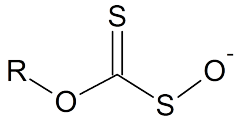 | 347 | 5.1 |
| Ethyl monothiocarbonate, $ETC^-$ | 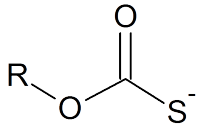 | 222 | <7 |
| Ethyl xanthyl thiosulfate, $EXT^-$ | 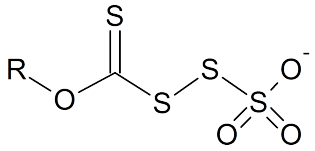 | 283 | <2 |

### 2.3.3 Decomposition on mineral surfaces

Many of xanthate decomposition species form only in heterogeneous systems where some mineral surface or oxidizing agent is present [23, 28]. These conditions are obviously met in froth flotation. The phenomena happening on mineral surfaces are very complex and it seems that there is not a clear picture of the reactions taking place. Hao et al. have given a reaction scheme for the decomposition of ethyl xanthate on mineral surfaces in Figure 2.

Vreugdenhil et al. have studied xanthate decomposition on mineral surfaces [29]. They analyzed the gas phase decomposition products of potassium ethyl xanthate on variety of sulphide mineral surfaces. Analysis was done using a head space IR method they had developed themselves. In their setup dry mineral sample treated

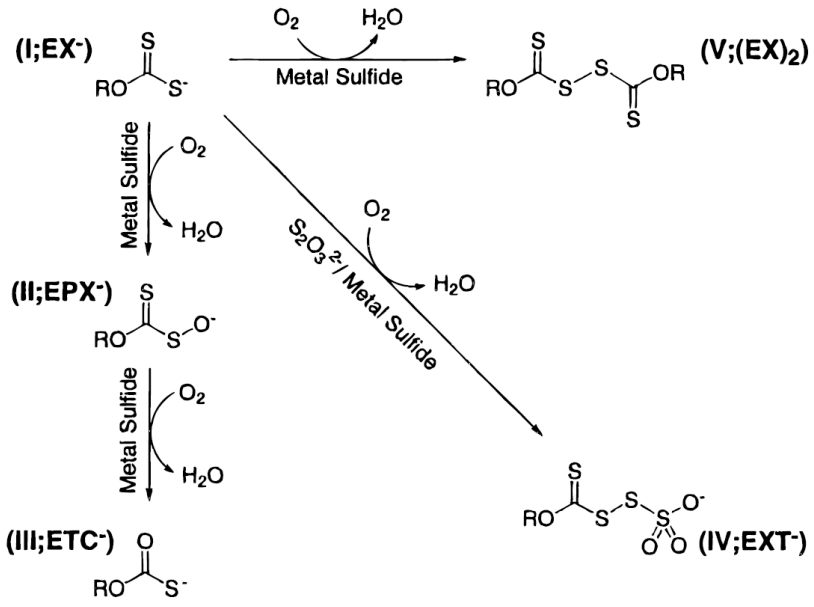


Figure 2: Ethyl xanthate decomposition scheme [14].

with xanthate is placed in the measurement cell and heated to release the gaseous decomposition species, from which the IR spectrum was recorded.

For the formation of $CS_2$ Vreugdenhil et al. [29] have postulated the following mechanism (xiv), which is basically the reverse of the xanthate synthesize reaction (ii). For COS they have produced a mechanism (xv). In all of the mechanisms M is either a metal atom in the mineral lattice or oxidized metal atom on the mineral surface.

$$\mathrm{EtOCS_2M} \longrightarrow \mathrm{EtOM} + \mathrm{CS_2} \tag{xiv}$$

$$\mathrm{EtOCS_2M} \longrightarrow \mathrm{EtSCOSM} \longrightarrow \mathrm{EtOM} + \mathrm{COS} \tag{xv}$$

Isotope studies were made to find out the origin of $CO_2$ so that the C1 of ethyl xanthate was replaced with $^{13}C$. As a result most of the $CO_2$ was suspected to have desorbed from the sample boat or mineral surface. Still there was some labeled $CO_2$ present, the amount of which depended on the mineral in question and the temperature. It was found that at 130 °C on chalcocite sample 40% of carbon dioxide released was labeled and in the same conditions galena and pyrite samples produced only 13% of labeled $CO_2$. From these findings they proposed that $CO_2$ was produced by the following mechanism. [29]

$$\mathrm{EtOCS_2M + COS \longrightarrow EtSCOSM \longrightarrow EtSCO_2M \longrightarrow EtSM + CO_2} \qquad \text{(xvi)}$$

## 2.4 Metal complexes

Flotation process waters usually contain many different metals dissolved. These metals are free to produce complexes with the collectors added to the process.

Xanthate can exist either as soluble (ionic) or insoluble complexes. The ionic complexes can be either cationic $M(X)^{(n-m)+}$ or anionic $M(X)_m^{(m-n)-}$, where $M^{n+}$ is the metal cation and $X^-$ the xanthate ion. Ionic complexes are produced when xanthates and metal ions are non stoichiometric concentrations and after the solubility of the complex MXn is exceeded. Xanthate has been found to form 1:1 complexes at least with the following metals: $Pb^{2+}$, $Cd^{2+}$, $Zn^{2+}$, $Ni^{2+}$, $Co^{2+}$ and $Cu^{2+}$. As for the stoichiometric complexes, it can be seen from Table 3 that their solubilities are quite low. [23]

Table 3: Solubilities of xanthate metal complexes in water, at 20 °C [23].

| Metal complex | Solubility, [mol/L] |
|---|---|
| $Zn(EX)_2$ | $9.0 \times 10^{-4}$ |
| $Ni(EX)_2$ | $6.3 \times 10^{-5}$ |
| $As(EX)_2$ | $5.5 \times 10^{-5}$ |
| $Cd(EX)_2$ | $3.3 \times 10^{-5}$ |
| $Co(EX)_2$ | $7.6 \times 10^{-8}$ |
| $Cu_2(EX)_2$ | $4.1 \times 10^{-8}$ |

Readiness of xanthates to form complexes has also been used in analysis. Eggers and Rüssel [11] have used xanthates for analyzing metal ions through xanthate complexes. They found that some solvents caused the complexes to decompose rapidly. Also Vregdenhil at al. have studied xanthate complex decomposition [20]. They found that Fe(III) and Zn(II) complexes decompose fast, even at low temperatures, producing $CS_2$ and COS. Pb(II), Ni(II) and Cu(I) complexes were found to be more stable and only decompose rapidly in higher temperatures.

Dithiophosphates have been found to produce complexes with $Pb^{2+}$, $Hg^{2+}$, $Fe^{3+}$, $Ni^{2+}$, $As^{3+}$, $Cu^{2+}$, $Cd^{2+}$ and $Bi^{3+}$. These complexes dissolve to water much more than

equivalent xanthate metal complexes. Complexes of $Mn^{2+}$, $Fe^{2+}$, $Co^{2+}$, $Zn^{2+}$ and $Ga^{3+}$ do not precipitate in aqueous solutions with diethyl dithiophosphate ion, but some of these complexes can still be found form the solution. The Fe(III) complex is unstable and forms a Fe(II) ion and bis-(O,O-dialkylthiophosphoryl)disulphide (analogous to dixanthogen) molecule. [23]

# 3 Analytical methods

In this section methods for analyzing collectors from flotation process water are reviewed. Thus far, many methods are used only to determine the bulk amount of collectors present in the process waters, or to analyze the amounts of different collectors present. Only one article was found in the literature in which a method for analyzing xanthate decomposition species have been developed and tested on process water samples [7].

There is a number of different methods for analyzing xanthates and other thiol collectors, which are discussed in this section. The objective is to give an overview on what has been done and where these methods might be used. Table 4 can be used for easy comparison between different types of analysis methods.

### 3.0.1 UV/VIS spectrophotometry

UV/VIS spectrophotometry is one of the most used analysis methods in chemistry and UV/VIS detectors are widely used with liquid chromatography and capillary electrophoresis [37]. This is why it is good to know the spectroscopic behavior of the analytes. All thiol collectors have quite distinctive UV spectra by which they can be identified. UV spectra of different collectors and also xanthate decomposition species are given in Figure 3.

Jones and Woodcock have determined dixanthogens from flotation liquors [8]. Because dixanthogen has a low solubility to water, they propose to extract dixanthogen to isooctane and then measure the UV absorbances at 241 nm and 286 nm. They note that when different xanthates are used as a mixture also asymmetrical dixanthogens are formed and that the spectra for them might differ from symmetrical ones used in calibration. In symmetrical dixanthogen two xanthates with the same alkyl groups have connected together and in asymmetrical case the alkyl groups are different.

Table 4: Comparison of the analysis methods found in literature.

| Method | Analytes studied | Sample preparation | Analysis time | Detection | Sensitivity | Pros and cons | Ref |
|---|---|---|---|---|---|---|---|
| Normal and reverse phase HPLC | Xantahates | Derivation to dixanthogen or to metalcomplex | 10–20 min | UV | 0.005 mg/L 0.20–100 ng | Possible to analyze many compounds at a time. Derivation generates more complex matrices. | [11–13, 30] |
| Ion interaction HPLC | Xanthates and their oxidation products. DTP and DTPI | Removing solids by filtration | 8–16 min | UV | 0.017–0.1 mg/L | Possible to analyze many compounds at a time. | [14, 15, 24] |
| CZE | ethyl, isopropyl and hexyl xanthates | Removing solids by filtration | 15 min | UV | 0.010-0.040 mg/L | Possible to analyze many compounds at a time. | [16, 17] |
| Voltammetry | Ethyl xanthate, diethyl DTP, diphenyl DTP | $N_2$ purging, pH adjustment | 10 min | | 0.002 mg/L | Measurements are fast, but sample preparation takes time. Gives a sum result if many analytes in a sample. | [31–33] |
| Xanthate selective electrode | Isopropy and isobutyl xanthates | none | instant | | 1.58 mg/L | Fast and does not need sample preparation. Different electrodes for different collectors. | [34–36] |
| UV/VIS spectrophotometry | All types of collectors | removal of UV absorbing solids | 0.5 min | | 0.2 mg/L (KEX) | Fast but gives the sum spectrum of the sample. | [7, 8] |

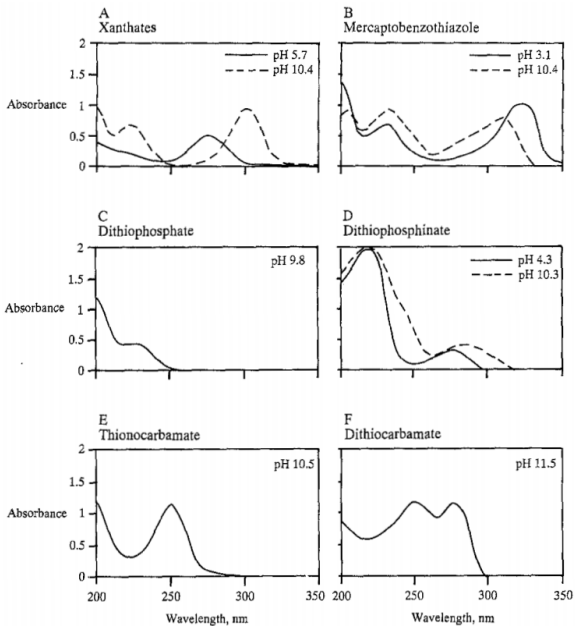


(a) UV spectra of common collectors [15].

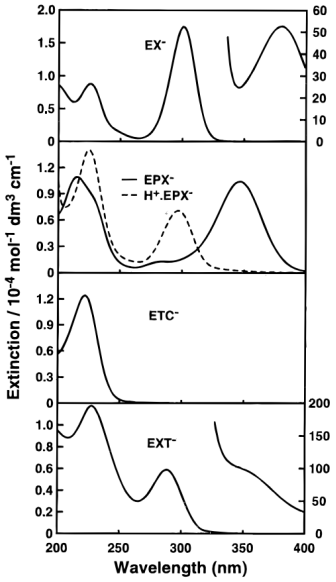


(b) UV spectra of decomposition products of ethyl xanthate. In pH 8–11 at 25 °C [14]

Figure 3: UV spectra of collectors and ethyl xanthate oxidation products in water.

One of the biggest problems for using UV/VIS spectrophotometry for analyzing industrial samples is the interference from the matrix. Even when only xanthates are present UV/VIS spectrophotometry only gives the sum absorbance of xanthates with various chain lengths [7]. Still UV/VIS spectrophotometry is used for example to check the purity of industrial grade collectors [15].

### 3.0.2 Voltammetry

Leppinen and Vahtila have studied thiol collectors in waters by differential pulse polarography [32]. With this method they wanted to analyze xanthates and dithiophosphates in the presence of sulphides, as they are usually present in flotation of sulfide minerals. They studied ethyl xanthate diethyl dithiophosphate and diphenyl dithiophosphate. The problem with this method is that in different concentrations of analytes also different peaks are observed. Even in the concentration ranges where only one peak is present the peak height or area might not be linearly dependent on analyte concentration. All samples were purged with $N_2$ prior to experiments. To determine sulphides simultaneously to thiol collectors, they propose that first the polarogram of sulphide is recorded in basic conditions and then the pH is adjusted to 5.3 using acetic acid to remove the sulphides as $H_2S$. With this method sulphide

can be analyzed in the range of $1\times10^{-6}$–$5\times10^{-4}$ M and that it can be determined simultaneously with ethyl xanthate or dithiophosphates. One thing to note about this method is that xanthate decomposes rapidly in acidic condition, so some xanthate will be lost during sulphide removal. Lastly, they compared the results from their method to UV/VIS spectrophotometry and noted that while that gave more precise measurements and lower deviations over the whole concentration range, polarography could give better results, if the samples have suspended solids, that absorb UV.

Ivaska and Leppinen have analyzed ethyl xanthate from aqueous solution by cathodic stripping voltammetry [31]. They wanted to study adsorption of ethyl xanthate and diethyl dithiophosphate on $Cu_2S$-surface and for this they needed a method with high sensitivity. The method was calibrated between $1 \times 10^{-8}$–$7 \times 10^{-5}$ M for ethyl xanthate and $1 \times 10^{-7}$–$1 \times 10^{-5}$ M for diethyl dithiophosphate. The draw back of this analysis method is that the peak shapes change with concentration. This causes problems for calibration and also interpreting the voltamperograms can be hard. Then again peak changes can give more information about the adsorption and redox reactions happening on the mercury surface. The method was also tested on samples from a flotation plant. No ethyl xanthate was found from flotation plant process or effluent waters but they were able to find both ethyl xanthate and ethyl dixanthogen from the flotation liquor. One reason for not finding any collectors in the waters may be that the samples were taken from the plant and only assayed the next day in the laboratory. The authors did not record the pH or temperature of the samples, but they mentioned some problems in sampling from the slurry.

Zakharova and Zakharov have also developed a cathodic stripping voltammetry method for determining xanthates [33]. While Ivaska and Leppinen used a mercury drop as the working electrode, Zakharova and Zakharov used a silver electrode. Still they observed similar peak changes as in [31]. Their method has a detection limit of $1.8 \times 10^{-5}$ M for ethyl xanthate.

Voltammetry seems to be a good tool at least when studying adsorption, because peaks at different potentials can give ideas about the phenomena happening at the mercury surface and this information can be applied to other surfaces. But when it comes to studying of process waters or other more complex matrices, this method is hardly the best. When used as a detector in some chromatographic method voltammetry could give some information about the reactions of analytes, to help identify some unknown species, and simultaneously help achieve low detection limits. The use of chromatography would remove the problems of sample matrix having

species which overlap. This kind of detection has been used in study of xanthate complexes [38]. Furthermore it is possible to detect very small amounts ($10^{-6}$–$10^{-9}$ M) with voltammetry [37] and this has been shown to work also in xanthate analysis [31].

### 3.0.3 Xanthate ion-selective electrodes

Bugajski and Gamsjäger have developed a xanthate ion specific electrode [34]. They note that their cell is easier to regenerate than silver metal based electrodes, which can be easily poisoned by xanthate decomposition products. Their cell consists of an anode made by dipping a silver wire first to saturated silver amalgam and then to finely ground silver xanthate. Cell was calibrated between $10^{-1}$–$10^{-5}$ mol/L. The cell was tested against a titration method and results were found to be quite similar.

Cabrera et al. have produced a PVC membrane based isopropyl xanthate ion-selective electrode [35]. These kind of electrodes have a polymer disk that has a liquid ion exchanger held in. This disk is fastened at the end of a tube housing the internal reference electrode, there the polymer disk works as a membrane between the analyte solution and the reference solution [37]. Cabrera et al. used two kinds of plasticizers to form the PVC membranes and in both cases they used trioctylmethylammonium-isopropyl xanthate complex as the held in ion exchanger. For both membranes the limits of detection were between $10^{-4}$ and $10^{-5}$ M. Calomel electrode was used a reference electrode. They found that while the electrodes were not much interfered by chloride, nitrate, carbonate or acetate; they were strongly interfered by isobutyl xanthate and they could not distinguish between isopropyl and isobutyl xanthates. So it seems that this kind of electrode could be used in process conditions as long as the process has only one kind of xanthate present.

A similar type of PVC membrane electrode was also used by Huang et al. in an on-line application [36]. Their membrane had trioctyldodecylammonium-isobutyl xanthate complex held in. Calibration were linear in the range of $10^{-1}$–$10^{-6}$ M for IBX. They tested the electrode in laboratory scale flotation cell and reported no problems. Electrode was also compared to UV-spectroscopy and found that the error in water samples was about 2 % and in flotation pulp samples about 5 %. All of the errors seem to be so that UV method has detected less xanthate than the electrode and the authors note that this could be because the UV samples needed some filtering and were studied a few hours later while the electrode readings were

taken on-line.

## 3.1 Chromatographic methods

In comparison to the previous analytical methods, chromatography offers many advantages. The main advantage is to be able to analyze different collectors simultaneously. In addition analyzing from complex matrices is possible when the species that would otherwise interfere are separated from the analytes. On the other hand, chromatographic methods are not so straight forward as some other analysis methods and they require more expertise and work to optimize.

### 3.1.1 High performance liquid chromatography

Xanthates and other thiol collectors are ionic in most sample matrices and thus do not retain well enough in the reverse-phase column. So to counter this, in most of the high performance liquid chromatography (HPLC) methods described here, two kinds of derivations have been done. One method has been to oxidize the xanthates to corresponding dixanthogens and the other method is to create metal complexes from xanthates. The derivation steps adds extra work to the analysis and can lead to some more complex matrices. In more advanced methods ion pairing reagents are used in the mobile phase to remove the need for derivation.

Regardless of the few drawbacks, at least in the older methods, HPLC is still one of the most used and studied chromatographic method for analyzing xanthates. That is why it is good to evaluate and compare some of the suggested methods. For easy comparison, main points of the different methods have been compiled in Table 5. It should be noted that many authors have given absolute limits of detections, which means the total amount of analyzed compound that has been injected to the separation column. The concentration of the sample can then be calculated from the volume of sample injected. Unfortunately, these injection volumes are not always given in the papers discussed here.

Table 5: Comparison of HPLC methods found from literature

| Method | Studied compounds | UV-det., nm | LOD, $mgL^{-1}$ | LOD, ng | Ref. |
|---|---|---|---|---|---|
| Dixanthogen | Dibutyl dixanthogen | 254 | | 10.00 | [30] |
| | Butyl xanthate | 254 | | 100.00 | |
| Metal complexes | As(III)ethylxanthate | 228 | | 3.3–330 | [11] |
| | Te(II)ethylxanthate | 249 | | 3.3–330 | |
| Metal complexes (A) and Dixanthogen (B) | Etyl xanthate Isopropy xanthate Isobutyl xanthate | 301 (A), 240 (B) | | 2.00 | [13] |
| Dixanthogen | Etyl xanthate | 245 | | 0.38 | [12] |
| | Isopropy xanthate | 245 | | 0.38 | |
| | Isobutyl xanthate | 245 | | 0.35 | |
| | Amyl xanthate | 245 | | 0.31 | |
| | Octyl xanthate | 245 | | 0.20 | |
| Metal complexes | Ethyl xanthate | 287 | | | [39] |
| Ion-pairing | Etyl xanthate | 300 | 0.017 | 0.34 | [24] |
| | Isopropy xanthate | 300 | 0.021 | 0.41 | |
| | Propyl xanthate | 300 | 0.019 | 0.38 | |
| | Sec-butyl xanthate | 300 | 0.021 | 0.43 | |
| | Isobutyl xanthate | 300 | 0.022 | 0.44 | |
| | Butyl xanthate | 300 | 0.020 | 0.40 | |
| | Octyl xanthate | 300 | 0.021 | 0.41 | |

One of the first HPLC methods for xanthates were created by Eckhardt et al. [30]. In their method xanthates were derived to dixanthogens and separated in a reversed-phase column using a gradient elution of water and methanol. All dixanthogens eluate in less than 20 minutes. This method is able to separate and detect different xanthates as corresponding dixanthogens, but problems arise when dealing with mixtures of xanthates. Then through the oxidation also asymmetrical dixanthogens are produced. They found that asymmetrical species form even when dixanthogens of different xanthates are formed separately and then mixed. The system of dixanthogens converge towards some kind of equilibrium point whether xanthate mixture is oxidized or the already made dixanthogens are mixed.

Another derivation method for analyzing xanthates with HPLC is to create metal complexes. This same method can also be used the other way around, so that xanthates are used for the analysis of metals. Eggers and Rüssel have studied xanthate complexes with HPLC and thin layer chromatography (TLC). They wanted to use xanthates to form complexes with various metals and thus analyze those metals with HPLC and TLC. They noted that some solvents such as methanol cause rapid decomposition of xanthate complexes during analysis. Xanthates of different alkyl chain lengths were tested as the complex ligands and found that butylxanthate gave good resolution while still eluting in a reasonable time of 10 minutes. However, the authors did not try to separate different xanthates from each other using this method. The complex method has the same problem as the dixanthogen method, namely that when the complexes are created also asymmetrical species form. [11]

Zhou et al. have compared and optimized metal complex and dixanthogen methods [13]. For the metal complex method they tried many different thiophilic metal ions, but decided on the copper(I)-complex as it gave the best resolution and sensitivity. They found that either method works equally well for analyzing xanthates with detection limits, given for ethyl xanthate, of $3.1 \times 10^{-8}$ mol/L for the metal complex method and $1.6 \times 10^{-8}$ mol/L for the dixanthogen method. Analysis times for both methods were under 10 minutes. Both methods were applied for flotation solutions, in which they seemed to work well. Although some problems appear when the dixanthogen method is applied to a flotation sample of copper sulfide ore or a sample where copper has been used as a depressant. Then both dixanhogens and copper complexes are formed in the same sample.

In another article Zhou et al. have developed a normal-phase HPLC method for analyzing xanthate mixtures as dixanthogens [12]. With this method they have achieved better limit of detection and the peak insensitivities are not so much dependent on the proportions of the mobile phase. Dixanthogens are more stable and soluble in the n-hexane mobile phase. This method has shorter analysis time and it is more sensitive than the reverse-phase methods. In this normal-phase method the less polar longer chained diaxanthogens eluate a lot quicker than in the reversed-phase method. For this reason this method is better at least for xanthates with longer carbon chains. A detection limit of 0.41 ng was achieved for potassium ethyl xanthate. Analysis times presented are under 10 minutes. Method was tested on real process waters and compared to the results gained from the previous reversed-phase method. It was noted that both methods give similar results.

Barnes et al. have developed an HPLC method based on ion-pairing to study vari-

ous thiol collectors [15]. The collectors studied were mercaptanes, xanthates, dialkyl dithiophosphates, dialkyl dithiophosphinates, dialkyl dithiocarbamates and thinocarbamates. To obtain an optimal separation they looked at the effects of mobile phase, column support material, column lenght, flow rate and temperature. From their comparison of tree different ion-pairing reagents, tetrabutylammonium hydroxide (TBAOH), tetrapropylammonium hyhdorxide (TPAOH) and cetyltrimethylammonium hydroxide (CTMOH), they came to the conclusion that TBAOH works best in either silica or polymer based columns. From column support materials the silica one gave better selectivity and efficiency. The method was able to separate xanthates of various chain lengths, up to amyl xanthate, from one another in 24 minutes. Analysis of dibutyl dithiophosphinates was achieved in about 14 minutes and dibutyl dithiophosphate had first the analysis time of over 50 minutes, but after some optimization it was lowered to 16 minutes. The calibration range for studied thiol collectors were between 0.1–100 $mgL^{-1}$.

Ion-pairing can also be used for the study of xanthate oxidation products, as Hao et al. have done [14]. Their method is able to separate and identify ethyl xanthate $EX^-$ and its decomposition species $EPX^-$, $ETC^-$ and $EXT^-$ given in Table 2. They found that increasing the concentration of ion-pairing agent, tetrabutylammonium ion ($TBA^+$), also increased the retention factor. Still it was necessary to have $TBA^+$ concentration at 5 mmol/L to achieve adequate separation. Phosphoric acid was used as the pH modifier, mainly to neutralize the hydroxide from TBAOH. The amount of phosphate had no other major effect on the method. Acetonitrile was the organic modifier in the eluent. Increase in its concentration caused the retention factors (k') to get very big. To keep the analysis times reasonable a low amount was used. In the optimized method they used a gradient method for acetonitrile to eluate $EXT^-$ faster. Ethyl xanthate oxidation products could be analyzed in under 13 minutes with the method. The optimized method was then tested by analyzing a flotation suspension of pentlandite. From those samples the method was able to determine all the species it was optimized for.

In his masters thesis Mark Trudgett did a very comprehensive study on the analysis of xanthate mixtures [24]. He made a comparison between suggested ion-pairing based HPLC methods. He concluded that tetrabutylammonium (TBAB) was the best ion-pairing reagent. With this method absolute detection limits of 0.08–0.42 ng were calculated for ethyl xanthate and amyl xanthate respectively, when detected at 227 nm. Analysis time for studied xanthates was under 9 minutes, amyl xanthate being the last to migrate. The optimized method was tested on mine tailings waters

and sludges. He noted that his method has the capacity to separate different oxidation products from xanthates, but no further analysis was done. He showed that his method is able to separate some xanthate metal complexes from tailings sludges. At the moment his method seems to be the most accessible and sensitive. It has the advantages of no need for pretreatment of samples, other than the filtration of solid material.

In conclusion, it can be said about the HPLC methods that at the moment those methods employing ion-interaction give the best results. These methods have even been tested on some real samples from flotation plants. Although Trudgetts study seems to be only one where samples from waters that circulate back to the plant from tailings was studied. Some of the older methods, such as derivation to metal complexes or to dixanthogens, can still be helpful when the analysis of either of those compounds is needed. As for the study of only xanthates the derivation methods have no advantages over the ion-paring methods.

### 3.1.2 Capillary electrophoresis

Because capillary electrophoresis (CE) is not so well known method in everyday laboratory work, some of the concepts will be presented here. The main focus will be on capillary zone electrophoresis (CZE), as it will be used in the experimental part of this work. Other types of electrophoresis under the term CE are capillary gel electrophoresis (CGE) and micellar electrokinetic chromatography (MEKC); according to Kuhn capillary isoelectric focusing (CIEF) and capillary isotachophoresis (CITP) should not go under the term CE [40].

As in the HPLC methods the detection limits can be given either as absolute values or as the concentrations present in the sample. Because in CE the injected amounts of sample are usually in the nL range, the absolute values of detection are also very low, in the pg range. This is why limits given this way do not give much information about the applicability of the method, so detection limits given as the concentrations of the analyte in the sample are preferred.

Capillary zone electrophoresis is a separation method based on the different electrophoretic movements of ions in a electric field. The separation occurs in a fused silica capillary, which is filled with a background electrolyte, when a voltage of up to $\pm 30$ kV is applied between the capillary ends. The voltage is usually applied so that the negative electrode is at the outlet and positive at the inlet. This is called normal polarity and when the electrode potentials are switched it is called reversed

polarity. When the pH of the electrolyte is above 2 the silanol ($SiO^-$) groups on the capillary walls are ionized and thus negatively charged. Positive ions in the electrolyte form a electrical double layer (Stern layer) on this negatively charged surface. After the Stern layer a diffusion layer forms consisting mostly on the positive ions that do not have space in the double layer. When a direct current (dc) high voltage is applied the positively-charged ions in the diffusion layer migrate towards the negative electrode (cathode) and carry solvent molecules in the same direction. This overall solvent movement is called electroosmotic flow (EOF). During a separation, uncharged (neutral) molecules move at the same velocity as the electroosmotic flow (with very little separation). Positively charged ions (cations) move faster and negatively charged ions (anions) move slower. [37, 40–42]

Capillary electrophoresis equipment consists of high voltage power supply, that usually produces voltages between $\pm 30$ kV; the capillary itself; electrolyte vials, which house the capillary ends and electrodes; and a detector. Usually detection happens through the capillary, from a spot where the polyimide housing the capillary has been burned off to form a window [41]. A schematic drawing of the main components in a CE equipment can be seen in Figure 4.

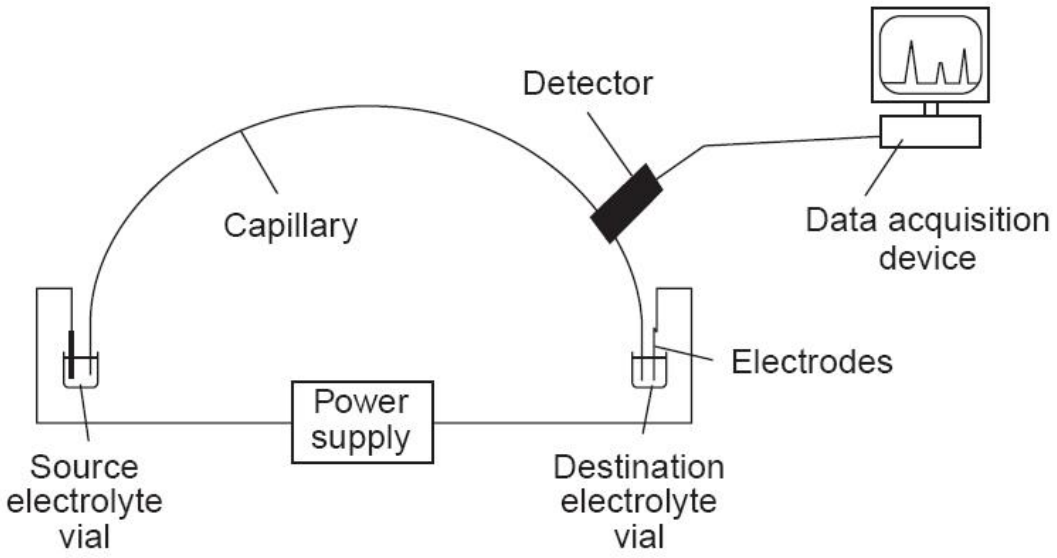


Figure 4: Capillary electrophoresis instrumentation schematic [41].

Most used injection method in capillary electrophoresis is hydrodynamic injection, in which the sample is introduced to the capillary by pressure. This can be done by pressurizing the sample vial, by introducing a vacuum to the outlet vial or by siphoning. Injection can also be done electrokinetically. In this injection method, usually called field amplified sample injection (FASI), sample is introduced to the capillary by applying a voltage between the capillary ends, while the capillary inlet

is in the sample vial. The analytes migrate to the capillary according to their electrophoretic mobilities aided or hindered by the EOF. If the EOF moves towards the outlet, it can help pump sample in to the capillary, but if the EOF is moving to the opposite direction, it can move the analytes away from the capillary. [40, 42]

In cases where the EOF removes the analytes from the capillary during FASI, pressure assisted field amplified sample injection (PA-FASI) can be used. In this method a small pressure is applied to the inlet vial to stop the electroosmotic flow from moving the analytes away from the capillary. The biggest problem with FASI and PA-FASI is that they do not give uniform injection of the sample. This causes complication for example in calibration, as the molecules with higher elecrophoretic mobilities migrate more rapidly to the capillary. In addition, the difference in ionic strength between the sample and the buffer in the capillary has an effect on the migration to the capillary. This quality can also be used as an advantage, if ions of only certain charge are needed to analyze. [37, 40–42]

To overcome the problems of FASI and PA-FASI a stacking method can be used. First in stacking some amount of sample is injected to the capillary hydrodynamically, to get larger amounts of the analytes to the capillary. Sample can be injected up to two-thirds of the total column length. After that a opposite polarity of what would be used in the separation normally is applied. This causes the electro-osmotic flow to move towards the inlet while the analytes try to migrate towards the outlet. The EOF pushes the sample matrix out of the capillary, while the analytes stay at the sample matrix buffer interface. If the voltage is picked so that the electro-osmosis does not take the analytes with it to the inlet vial, then they will stack accordingly to their electrophoretic mobilities. After stacking normal separation voltage is applied. Because the sample is introduced to the capillary by pressure it represents the sample better. [37, 42]

Hissner et al. have used capillary electrophoresis to study the tailings waters from a former tin mine [17]. They developed the method for styrene phosphonate, etyl xanthate, isopropyl xanthate and hexyl xanthate. They evaluated three different sample injection modes and their effect on detection limits. These injection methods were hydrodynamic, pressure assisted field amplified and stacking. From these injection modes stacking was found to have the best sensitivity. PA-FASI gave better results than the hydrodynamic injection especially to species that have a high electrophoretic mobility as they migrate faster to the capillary. Because of the difficulties in calibration and in the automation, PA-FASI method was not validated further. Hydrodynamic injection gave a detection limit of 200 ppb and for stacking

the limit was 20 ppb to ethyl xanthate. Analysis time for the compounds was under 15 minutes. The optimized method was tested on samples from a tailings bond outlet, which lead to a river. From the water samples they were able to find styrene phosphate, but xanthates were not used at the plant for a couple of years, so any traces of them were not found.

Malik and Faubel, studied ethyl xanthate and dithiocarbamates [16]. Samples were injected in the capillary by vacuum, so that the injection volume was 13.1 nL. They compared borate, phosphate and acetate buffers, which had pHs 9.0, 7.0 and 4.5, respectively. These buffers were studied in the concentration range of 1.5–50 mM. At buffer pHs below 7.0 no peaks were observed, so borate was chosen as the buffer. Concentration of 20 mM was chosen for the buffer, because at concentrations above 25 nM the separation times grew too large. With the optimized method the analysis time was under 12 minutes. Separation voltage was +25 kV. For the injection volume of 13.1 nL, the detection limit for ethyl xanthate was 3.7 pg or 0.28 ppm. This is about one order of magnitude larger than in Hissners method, although here the injection volumes are much smaller.

Capillary electrophoresis has also been used to analyze dialkyl dithiophosphates [43]. Although this method was developed for the study of lubricant additives and thus is nonaqueous and can not be used in the flotation samples as such, it may still offer some help in the analysis of dithiophosphates.

From the CE-methods Hisner et al. have reported the lowest detection limits for xanthates, which are around the same amounts as Trudgett has reported for his HPLC-method.

## 3.2 On-line analysis

It has been proven through kinetic studies that xanthates stay intact in samples even for long periods of time, if the pH is eight or above [24]. So it would seem that the samples could just be analyzed at a laboratory. For process control analyses done in a laboratory take usually too much time. The collectors can also continue to react with the ions or solids in the process sample, while the sample is taken to the laboratory. So the only way to really know which species are present and might affect the process, is to use on-line analytics. On-line analytics used at concentrator plants are usually only pH and temperature measurements, in addition also particle sizes and inorganic elements are analyzed on-line. Normally collectors end up in the concentrate with the valuable minerals, if they are found in the waters that have

gone past the process, they are most likely being over dosed to the process.

Stén et al. have studied how pH and the concentrations of $Ca^{2+}$, $CO_3^{2-}$ and $HCO_3^-$ ions change in the Siilinjärvi apatite flotation plant [44]. The study was done with a process titrator with sampling from water circulated back from the tailings bond and from the thickener overflow. They have showed that there is variation in pH, from around 8.9 during the winter to about 9.8 during the summer. They suggest that this variation is from biological activity brought on by the increasing sunlight during the summer.

In a paper by Luukkanen et al. the same research group has studied the process waters of a different concentration plant [9]. They used the same process titration equipment as before, but this time they studied the concentrations of $Ca^{2+}$, $Mg^{2+}$, $SO_4^{2-}$ and xanthate. When titrating xanthate from the pyrite circuit tailings waters, they noticed some species that were titrated ahead of xanthate. These species were believed to be some kind of xanthate degradation products. Unfortunately, the titration equipment was not capable of separating and identifying what products were present. The concentrations of xanthate in the tailings from copper circuit was found to be lower than in the pyrite tailings. The amounts of xanthate found in tailings was compared to the amounts added to the process and they seem to vary in a similar fashion. Ion chromatography was selected for a reference method for the xantahate titrations. An additional peak was observed also in the chromatograms and it was thought to belong to the same degradation product that was seen on the titration curves. No attempt was made to identify this compound.

Hao et al. have developed an UV spectrophotometry based system for monitoring the xanthate concentrations in flotation pulps [7]. Their aim was to develop a faster way for monitoring xanthate concentration during flotation experiments in the laboratory. Samples were taken from the flotation cell by a filter fitted in the cell. Filtrate was then pumped to a UV spectrometer, where a signal was recorded at 301 nm. From there the sample was returned back to the flotation cell. The UV spectrophotometric measurements gave linear calibrations within the range of xanthate concentrations used in flotation. There are some components that might interfere the UV detection of xanthates. In this study they were not a problem, but this should be taken into consideration when applying the method on industrial scale.

It can be seen in the studies published on on-line analytics of flotation processes that there is not a robust method that could give deeper knowledge about xanthates and their degratation products in the process waters to the operators or to the scientists studying the phenomena happening at these plants. The currently used on-line

methods give only information about the total amounts of collectors in the process waters or in the laboratory flotation experiments. More information about the reactions happening in the process could be gained by using chromatographic methods on-line as with them it is possible to detect also the side products of these reactions.

# Experimental part

## 4 Water samples

Knowledge of the inorganic content of the samples is needed for the development of the capillary electrophoresis method, because the ionic strength of the sample also affects the analysis. Similarly ionic organic species affect the analysis, but in the case of flotation process waters, their concentrations should be much smaller than that of inorganic ions. Preparation of artificial samples is made by using this information. However, in this work it was chosen to use the process samples themselves as the sample matrix. The main advantage of this approach is that the sample matrix is basically the same that would be found when doing the measurements at the concentrator. This helps to produce a method that would work robustly enough for the process samples.

Two process water samples from Vammala gold concentrator were analyzed and used in the method development. The water samples were from two different circulation from the plant. One from the thickener overflow which is circulated back to the beginning of the process (process water A). The other sample is from the water circulated back from the tailings pond (process water B). These sampling points can be seen in the flowchart of the plant in Figure 23. Both samples were stored in a freezer and melted when needed.

The sample from the thickener overflow has some particles that can be seen with naked eye. The water sample from the tailings bond did not have visible particles but a slight brownish coloration. Both samples were filtered through a 45 $\mu$m syringe filter. Even though the tailings water seemed to be free of particles it fouled the filter much faster. After filtration both samples were clear colorless liquids. The filtered samples were stored in a refrigerator in closed containers and let to warm to room temperature before use.

## 4.1 ICP-AES analysis

Filtered water samples from a concentrating plant were assayed for inorganic content with inductively coupled plasma atomic emission spectrometry (ICP-AES). Study was done using a Iris intrepid II XDL (Thermo Electron Corporation) ICP-AES equipment with ASX-520 Autosampler (Cetac). Calibration samples were prepared using ICP standards from Romil. A multi standard was used for the following metals Ca, Cd, Co, Cr, Cu, Fe, Mg, Mn, Mo, Ni, Pb, Se, V and Zn. A separate calibration mixture was made for Na and S. From both mixtures a calibration series of 0.01, 0.05, 0.1, 1, 2, 5, 10 and 20 $mgL^{-1}$ were made. For iron the detection limit was raised to 1 $mgL^{-1}$ as the smaller concentration calibration points did not fall to the calibration curve. All standards and samples were made in 6 % nitric acid. Both water samples were diluted to 1:10 and 1:100 and also analyzed undiluted. The results of ICP-AES analysis are presented in Table 6. Knowledge of the inorganic metal cations in the sample solutions gives information on what kind of complexes could be found during CE analysis.

Table 6: Results from ICP-AES analysis of two different process waters form the Vammala concentrator plant.

| Element | Detection wavelength | Thickener overflow, $mgL^{-1}$ | Tailings water, $mgL^{-1}$ |
|---|---|---|---|
| Ca | 317.9 | 133.3 | 124.0 |
| Cd | 222.8 | – | – |
| Co | 238.7 | < 0.01 | 0.02 |
| Cr | 206.1 | < 0.01 | < 0.01 |
| Cu | 324.7 | < 0.01 | < 0.01 |
| Fe | 239.5 | < 1 | < 1 |
| Mg | 279.5 | 92.08 | 107.9 |
| Mn | 257.6 | 0.32 | 0.860 |
| Mo | 203.8 | 0.14 | 0.007 |
| Na | 589.5 | 53.9 | 53.1 |
| Ni | 231.6 | 0.14 | 0.500 |
| Pb | 220.3 | < 0.01 | < 0.01 |
| S | 182.0 | 296.3 | 306.3 |
| Se | 196.0 | 0.046 | – |
| V | 310.2 | 0.144 | 0.640 |
| Zn | 213.8 | 0.02 | 0.05 |

It can be seen from Table 6 that there is very little or no difference between the inorganic content of the two water samples. Still everyday practice at the concentration plant and some laboratory flotation experiments have shown that there is a difference on how these waters work in the flotation process. ICP-AES analysis does not give the species in which these metals occur. Still it seems likely that the differences in flotation performance are the result of organic species in the process waters. From the organics the collectors chemicals, their complexes and degradation products are the most interesting.

# 5 Capillary electrophoresis method

The aim of this thesis was the developing of a capillary electrophoresis method for the analysis of collector chemicals from flotation process waters. As described in the literature part of this work the analysis of xanthates using CE has already been studied. The methods developed in this work differ from the ones found in the literature. Firstly, both of those methods use buffers based on sodium tetraborate, while in this work CAPS was used as the buffer. In Malik and Faubels work the sample matrix was also totally different. They used their method to study fertilizers from wheat grains [16]. Hissner et al. on the other hand did use their method to study tailings waters from a tin mine [17]. They reported no interference from the sample matrix and were able to quantify sturene phosphate from the tailings waters. The authors did not give other information about the water samples so for example the salt content of the sample matrix is unknown.

## 5.1 Instrumentation and reagents

All dilutions were made in a low conductivity water purified by Elga Centra-R 60/120. In this work this water is called pure water. For method development industrial grade collector reagents were used. Names and information given by the suppliers is in Table 7.

Table 7: Reagents used in the method development.

| Chemical | Product name | Purity | Provider |
|---|---|---|---|
| Potassium ethyl xanthate | PEX | 85 % | Alkemin |
| Sodium isobutyl xanthate | SIBX | 82 % | Alkemin |
| Sodium diisobutyldithiophosphate | Danafloat 245 | 50 % (water) | Cheminova |
| Sodium diisobutyldithiophosphinate | Aerophine 3418A | 50–52 % (water) | Cytec |

From these reagents both xanthates were in the form of solids while Aerophine and Danafloat were in about 50 % water solutions. Xanthates dissolved to water easily and no visible impurities were seen. Aerophine was a clear slightly viscose liquid with no visible impurities and a strong smell. Danafloat was a brownish liquid with some fine dark particles.

When diluted Aerophine formed a white cloudy liquid and when left to mix on a magnetic stirrer the cloudiness disappeared as the small white particles aggregated to bigger ones. This liquid was filtered and continued dilutions from the filtered sample did not form particles anymore. There were no problems in the dilutions of Danafloat, but it was also filtered to get rid of the impurities which could be seen.

### 5.1.1 Electrolyte solution

The electrolyte solution, background electrolyte or buffer solution as it is sometimes called, is an important part of the CE-method. In the methods the background electrolyte used was a 60 mM CAPS (3-(cyclohexylamino)propane-1-sulfonic acid) and 40 mM NaOH solution. The pH of the electrolyte was measured using Orion model 410A pH meter with VWR pH electrode to be 10.7.

CAPS is a zwitterionic compound with a $pK_a$ of 10.4 [45]. Zwitterions are compounds that can have simultaneously a negative and a positive charge in its structure. For example amino acids are zwitterionic. CAPS has a sulfonic acid group in it and also a secondary amine group as can be seen in Figure 5. When pH is over the $pK_a$ CAPS is mostly negatively charged as the sulfonic group dissociates. Information on the chemicals used in the buffer solution is presented in Table 8.

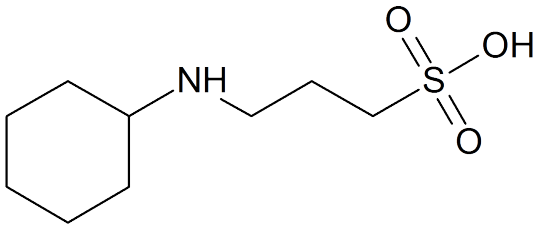


Figure 5: Molecular structure of 3-(cyclohexylamino)propane-1-sulfonic acid (CAPS).

Table 8: Chemicals used in the electrolyte solution.

| Chemical | Purity | Provider |
|---|---|---|
| CAPS | $\geq 98\%$ | Sigma-Aldrich |
| Sodium hydroxide | $\geq 99\%$ | Merk |

### 5.1.2 Instrumentation

The method was developed on a Beckman Coulter P/ACE MDQ capillary electrophoresis system with a diode array detection. Capillary used was a Polymicro Technologies fused silica capillary with inner diameter of 49 $\mu m$, total length of 60 cm and 50 cm length to detector. The schematic diagram of a typical CE-instrumentation can be seen in Figure 4.

## 5.2 Method development

During method development mostly different injections were tried. First case was to use pressure injection. Pressure injection gives the most uniform representation of the sample as all types of analytes have a similar driving force for migrating to the capillary. For this method different injection pressures and times were tested. It was noticed that with higher injection pressures and times the migration time of the analytes starts decreasing hindering separation. To counter this longer voltage ramp up times were tested in the separation step. Longer ramp up should help the sample plug to mix with the running buffer and so help the separation [46]. But in this case no efficient enhancement in separation was noticed with increasing ramp up times.

The optimized method is presented in Table 9. This method is able to detect DTP and DTPI in the concentration range of about 5 – 10,000 $\text{mgL}^{-1}$. This is already

quite good result at least considering that the method works also with samples prepared using the process waters described earlier. However, this method can be further optimized to be more sensitive with lover LODs, especially for xanthates for which detection limits were not determined using this method. This method is able to separate all of the analytes in under 20 minutes.

Table 9: Parameters of method 1

| Instrument parameters | | Background electrolyte | |
|---|---|---|---|
| Capillary | 50/60 cm | CAPS | 60 mM |
| Voltage | 20 kV | NaOH | 40 mM |
| Injection pressure | 1 psi | pH | 10.7 |
| Injection time | 5 s | Temperature | 20°C |
| Detection | 214, 225 and 301 nm | | |

Some of the seemingly low sensitivity can be attributed to the fact that the inner diameter of the capillary is just 49 $\mu m$. Detection is made through the capillary; in in-line mode. The i.d. of the capillary is then the path lenght of the light in the sample. The injected sample volume is only 10.55 nL. Therefore, the ammounts of analytes in the capillary are very low. These two factors cause low absorbance resulting in low sensitivity.

The sensitivity can be increased by using a capillary with larger inner diameter, injecting more sample or using a different detection method. From these options increasing the injection was the most applicable as it does not need any modification to the instrument and larger capillaries were not available. But as mentioned earlier, just increasing the amount injected by pressure does not work. This is why electrokinetic injections modes were tested.

To get lower detection limits than in method 1 a field amplified sample injection (FASI) method was tried. In the method all of the the collertors are anions. Therefore sample injection was done with reverce polarity. In that case the inlet electrode is the cathode and the outlet is the anode. This way negative ions are more likely to migrate to the capillary. After the injection the separation voltage of 20 kV was applied. Other instrument parameters and buffer composition was the same as in method 1.

Different injection voltages and times were tested. Even with rising voltages and injection times the analyte peaks did not seem to grow. The reversed polarity also reverses the flow of the EOF and it seems the EOF carries some of the analytes

away from the capillary. Even though the negative species want to migrate to the capillary the EOF is stronger and only a little amount of the analytes stay in the capillary during injection. Figure 6 shows that this method gives quite poor peaks in for a sample in the concentration of 100 $mgL^{-1}$.

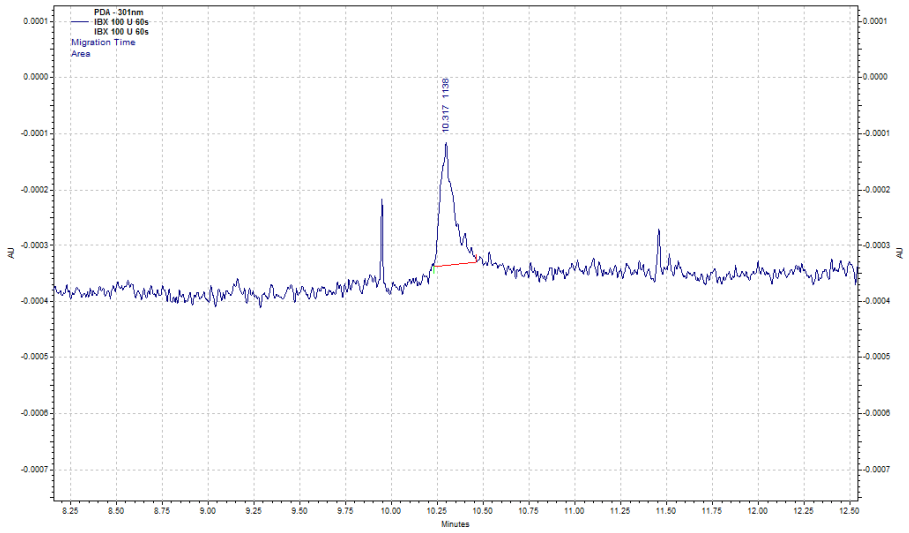


Figure 6: Electropherogram of isobityl xanthate in the concentration of 100 mg/L in water, using FASI method. Detection 301 nm.

A small pressure was applied to the inlet vial to resolve the problem of EOF carrying the analytes away from the capillary during electrokinetic injection. This kind of injection is called pressure assisted field amplified sample injection (PA-FASI). With this method a few different injection voltages, times and pressures were tested. In the end the parameters presented in Table 10 gave satisfactory results.

Table 10: Parameters of method 2

| Instrument parameters | | Background electrolyte | |
|---|---|---|---|
| Capillary | 50/60 cm | CAPS | 60 mM |
| Voltage | 20 kV | NaOH | 40 mM |
| Injection voltage | -10 kV | pH | 10.7 |
| Injection pressure | 2 psi | Temperature | 20°C |
| Injection time | 60 s | | |
| Detection | 214, 225 and 301 nm | | |

The results of PA-FASI method can be seen in Figures 7, 8, 9 and 10. These figures show that applying pressure during electrokinetic injection improves the results.

Even when the injection time is as high as one minute the sample peaks still separate. This is quite good result, if compared to the purely pressure injected samples, where increasing the injection time or pressure resulted in none of the analytes separating. For this method injection was varied by changing the injection time. Figure 11 illustrates a series of electropherograms with different injection times. The sample used was 0.1 $\mathrm{mgL}^{-1}$ IBX and from the series it can be seen that even with a injection time of 5 min only a badly shaped peak forms.

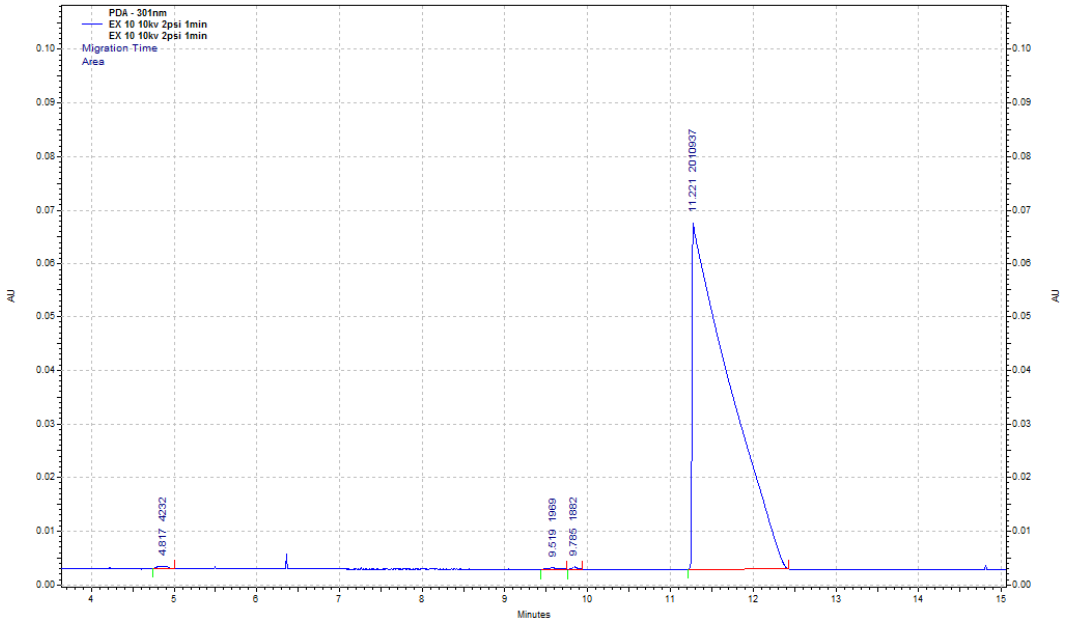


Figure 7: Electropherogram of ethyl xanthate in the concentration of 10 mg/L in water, using method 2. Detection 301 nm.

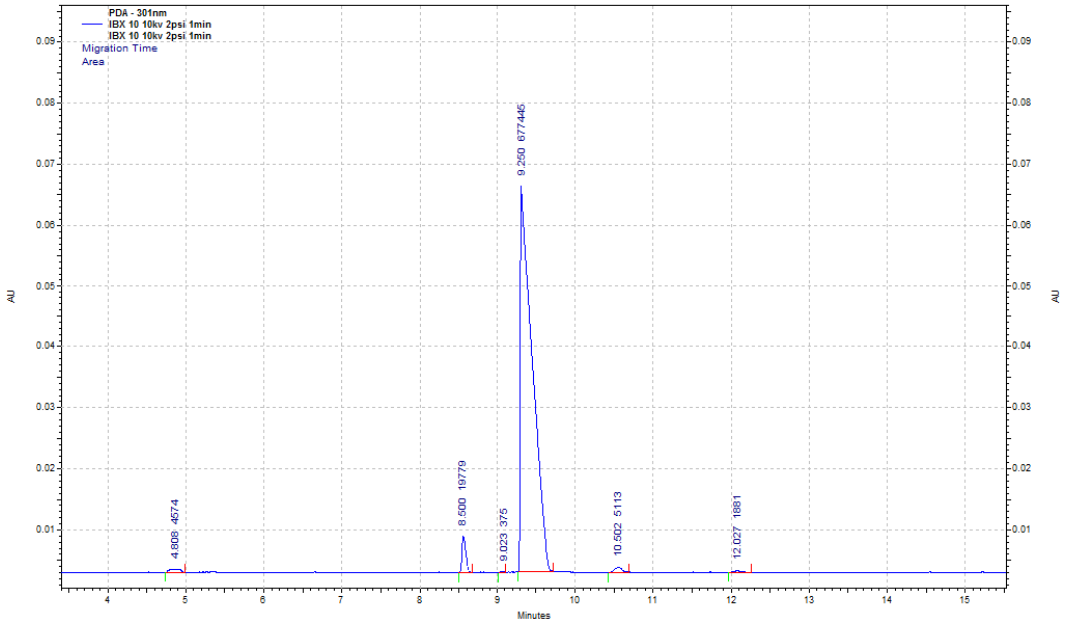


Figure 8: Electropherogram of isobutyl xanthate in the concentration of 10 mg/L in water, using method 2. Detection 301 nm.

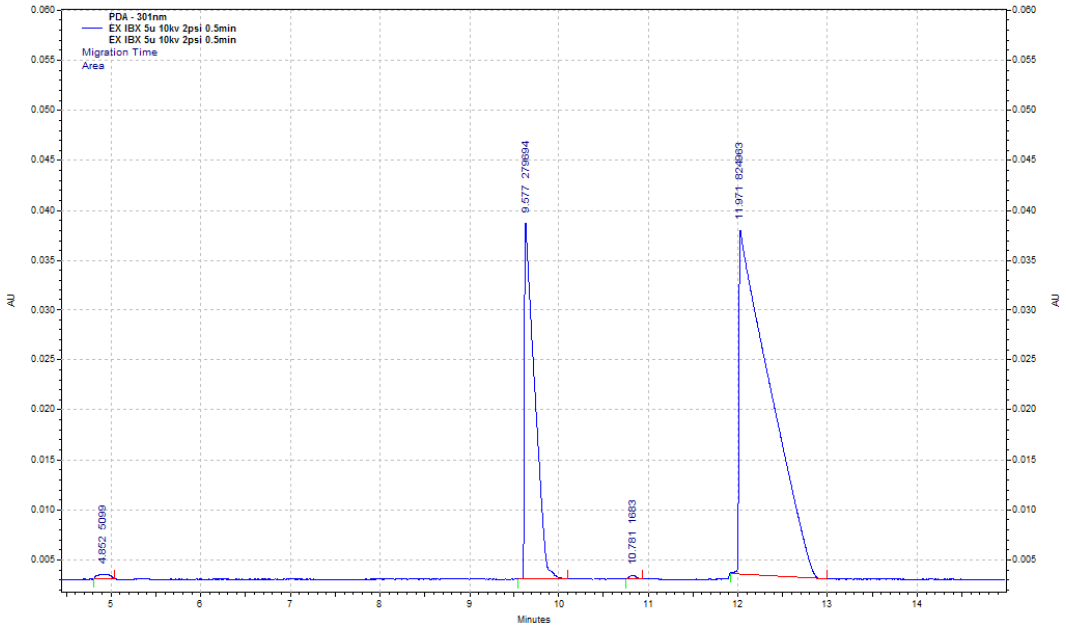


Figure 9: Electropherogram of ethyl xanthate and isobutyl xanthate in the concentration of 5 mg/L in water, using method 2. Detection 301 nm.

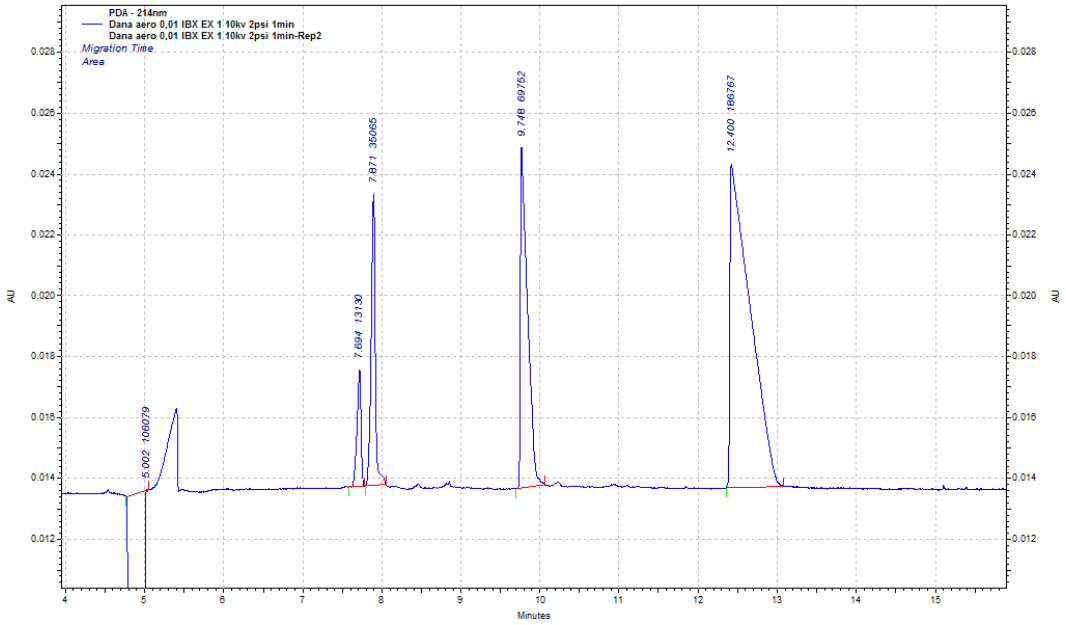


Figure 10: Electropherogram of sodium diisobutyldithiophosphate, sodium diisobutyldithiophosphinate, isobutyl xanthate and ethyl xanthate, using method 2. DTP and DTPI in the concentration of 10 mg/L; and both xanthates in the concentration of 1 mg/L in water. Detection at 214nm.

Use of this method was also tested with samples dissolved in process water. Results are shown in Figures 12, 13 and 14. It can be seen that the peaks are smaller than in the pure water samples and also some unknown peaks appear. These unknown peaks were also observed during the calibration of this method and can be seen clearer in Figure 19. Figure 15 indicates that DTP and DTPI do not separate in the process water samples using this method even though they did separate in pure water.

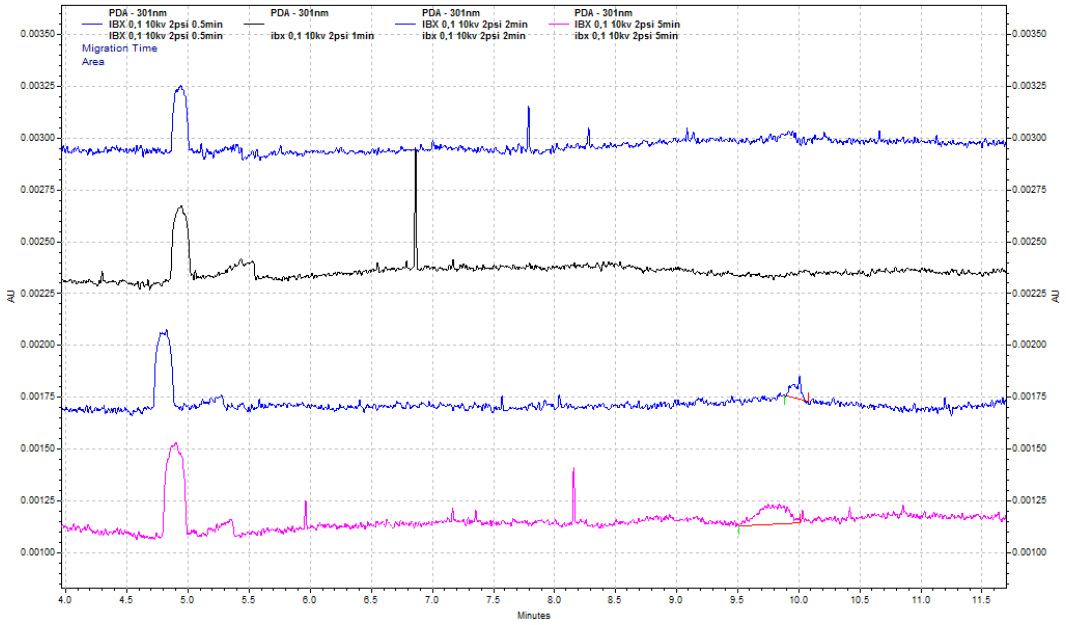


Figure 11: Electropherogram of isobutyl xanthate in the concentration of 0.1 mg/L in pure water, with various injection times. From top the injection times were 0.5 min, 1 min, 2 min and 5 min, otherwise the same parameters as in method 2. Detection 301 nm.

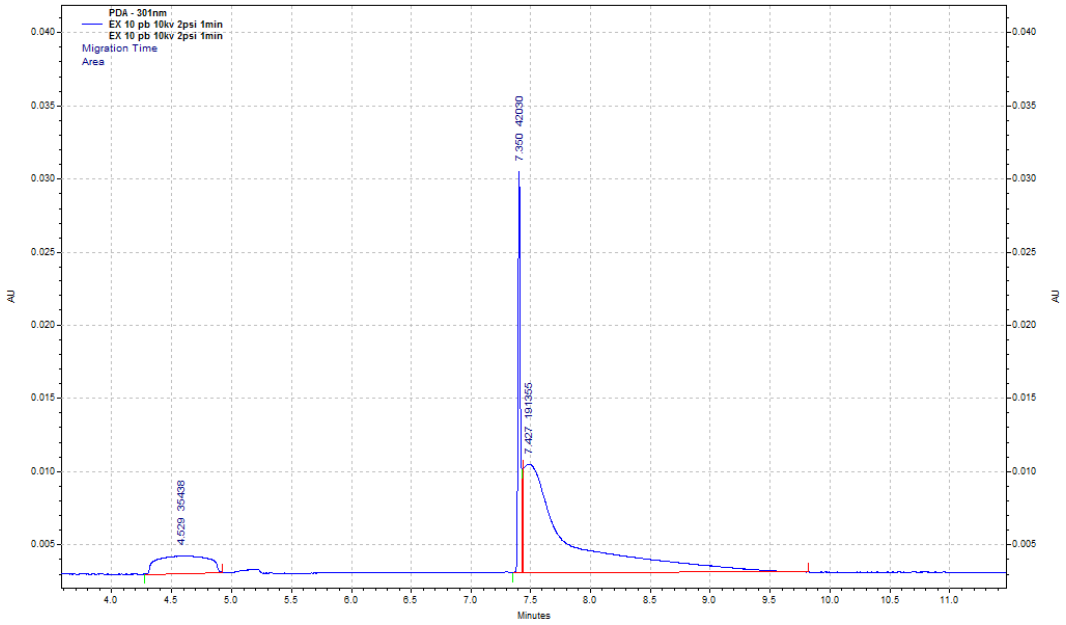


Figure 12: Electropherogram of ethyl xanthate sample in concentration of 10 mg/L in process water, using method 2. Detection 301 nm.

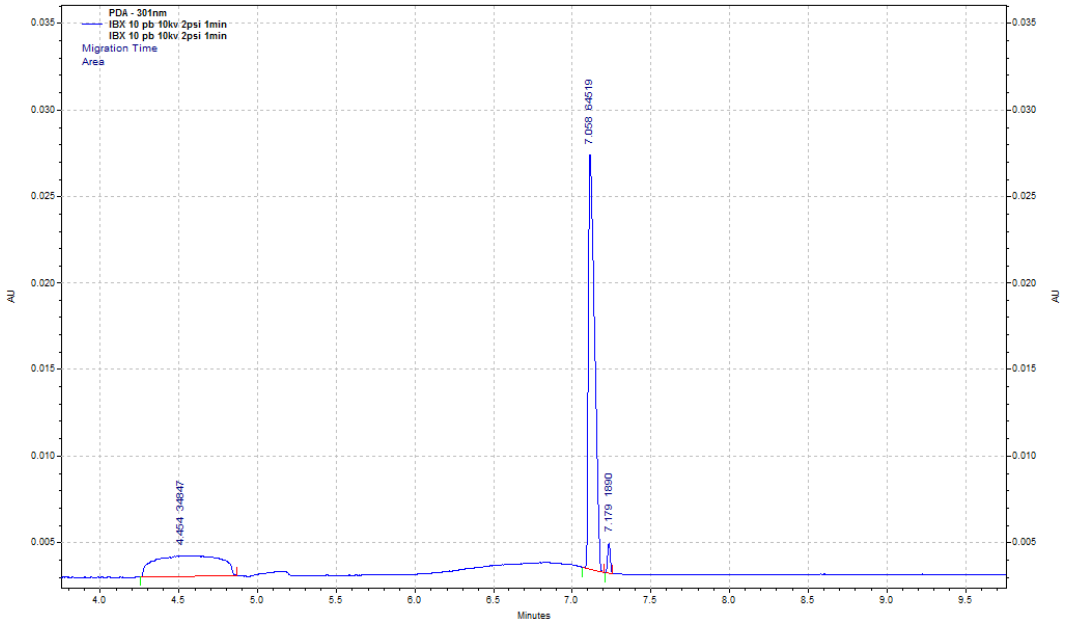


Figure 13: Electropherogram of isobutyl xanthate sample in concentration of 10 mg/L in process water, using method 2. Detection 301 nm.

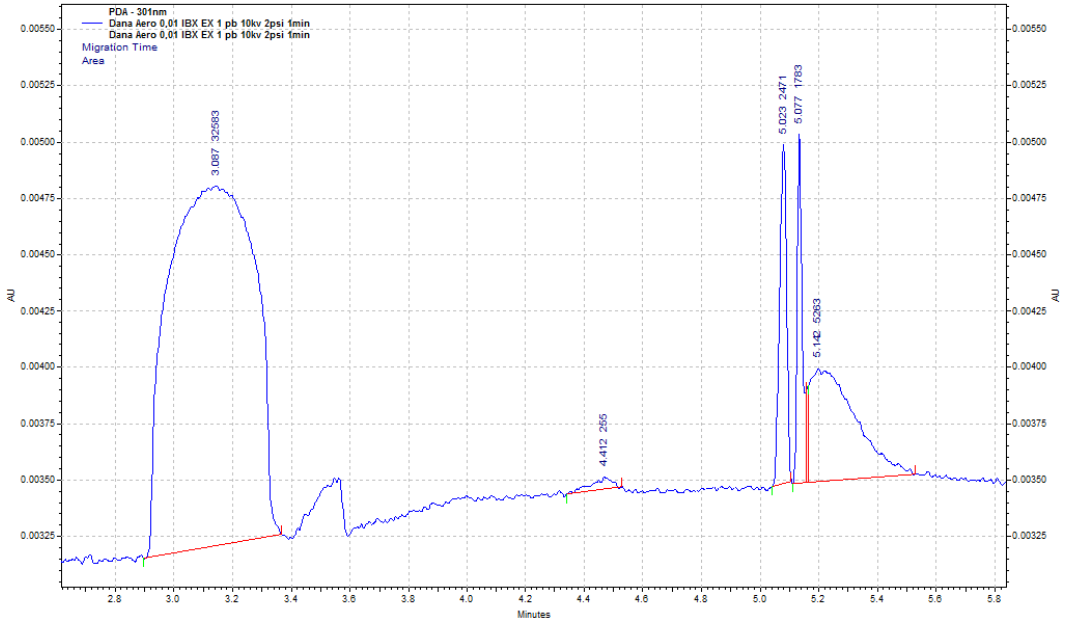


Figure 14: Electropherogram of sodium diisobutyldithiophosphate, sodium diisobutyldithiophosphinate, isobutyl xanthate and ethyl xanthate, using method 2. DTP and DTPI in the concentration of 10 mg/L; and both xanthates in the concentration of 1 mg/L in process water. Detection 301 nm.

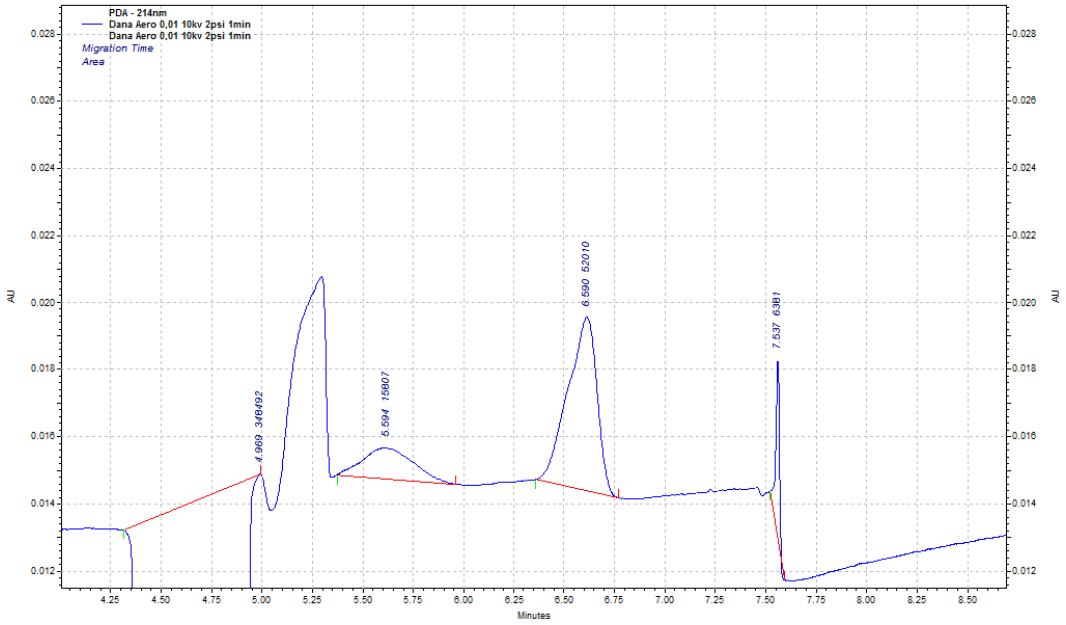


Figure 15: Electropherogram of DTP and DTPI sample in concentration of 10 mg/L in process water, using method 2. Detection 214 nm.

## 5.3 Results

In capillary electrophoresis mobility of the separated compounds are used for calculation of the analytical separation efficiency of the method. The apparent mobility ($\mu_{app}$) or sometimes total mobility of a analyte can be calculated from the following equation

$$\mu_{app} = \frac{L_t L_d}{tU} \tag{1}$$

where $L_t$ is the total capillary length, $L_d$ is the capillary length to detector, $t$ is the migration time and $U$ is the voltage applied between capillary ends. With the same equation (1) we can calculate the electro-osmotic mobility ($\mu_{eof}$) just by replacing the migration time with the time of the EOF peak.

Now we can calculate the electrophoretic mobilities ($\mu_{ep}$) for analytes using the next equation

$$\mu_{app} = \mu_{ep} + \mu_{eof} \tag{2}$$

Resolution ($R_s$) describes the separation between two analytes. It can be calculated directly from the electropherogram by the following equation

$$R_s = \frac{2(t_i - t_j)}{w_{b,i} + w_{b,j}} \tag{3}$$

where $w_b$ is the peak width at the baseline of a Gaussian peak and $t$ is the migration time of the analytes $i$ and $j$.

Quantification of the compounds was made by external standard method. Reference standard chemicals were used at specific concentrations for eight (method 1) and for six (method 2) level calibrations. The analysis results were used for fitting the parameters of a straight line $y = b + mx$, where $y$ is the peak area in the electropherogram and $x$ is the concentration of the reference compound.

### 5.3.1 Calibration

Calibration for Aerophine and Danafloat was done using the method 1 described earlier. Calibration samples were done by serial dilutions in the concentrations of 4.57, 13.7, 41.2, 123.5, 370.4, 1,110.0, 3,330.0 and 10,000 mgL$^{-1}$. To make sure the method would work in process conditions the calibrations were done using three different matrices. First calibration was simply done using the pure water from laboratory and two sequential calibrations were done using the process water samples analyzed previously with ICP-AES. By using the process water samples to dilute the analytes it is possible to get very close to the same ionic strength as in the process. All calibration samples were analyzed three times and the results were used to fit the calibration curves. The limits of detections (LOD) for the analytes were defined with signal to noise ratio 3 ($S/N = 3$) and for the limits of quantification (LOQ) a ratio of $S/N = 10$ was used. These ratios were calculated by comparing the peak heights to the height of the baseline variation.

As mentioned earlier in Table 7, the reagents were not pure and the exact concentration of the chemical used for the calibration is not known. This means that all of the measurements have more error than is otherwise calculated. One more thing to notice is that for both Danafloat and Aerophine the peak shapes were not good anymore at the concentration of 10,000 mgL$^{-1}$. The calibration was anyhow done to that concentration, as the peak areas still fitted the calibration curve quite well (seen Figure 16) and removing these data points did not improve the coefficient of determination noticeably.

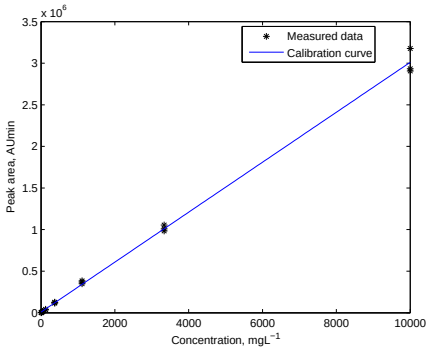


(a) Calibration curve of Aerophine in pure water.

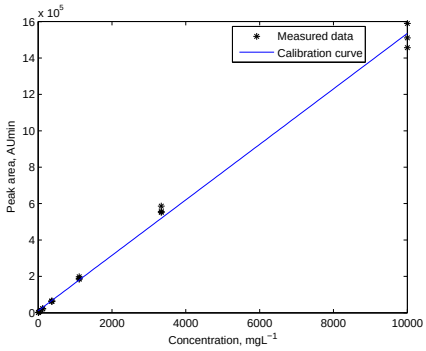


(b) Calibration curve of Danafloat in pure water

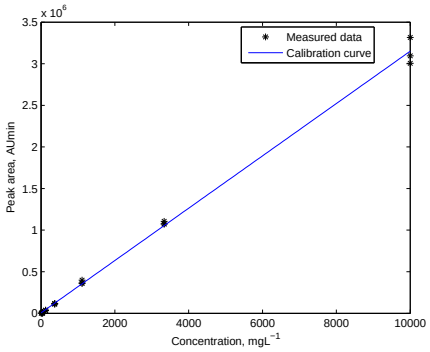


(c) Calibration curve of Aerophine in process water A

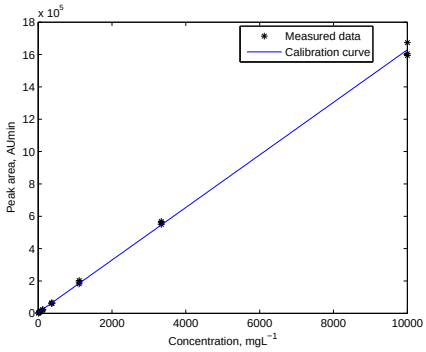


(d) Calibration curve of Danafloat in process water A

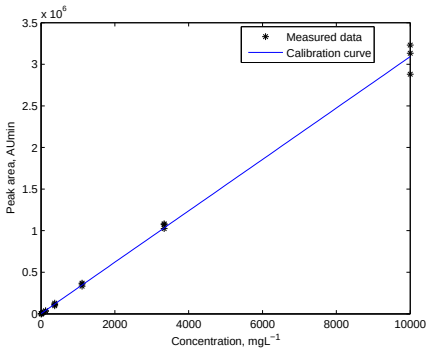


(e) Calibration curve of Aerophine in process water B

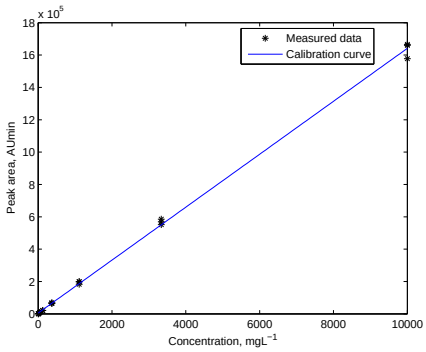


(f) Calibration curve of Danafloat in process water B

Figure 16: Calibration curves of Aerophine and Danafloat on three different matrices.

Results of Aerophine calibration are presented in Table 11. It can be seen that the LODs and LOQs are worse in the process waters and that electrophoretic mobilities also change a little. Comparison of the electropherograms made by spiking shows that the matrix compounds are not detectable, because the method is the most selective for Danafloat and Aerophine. However, there is a slight change in the electrophoretic mobilities of the above mentioned analytes that is probably caused by

difference in the ionic strength of the sample matrices. Therefore the calibration established in this study is usable for determining the concentrations of collectors that are simultaneously present in process waters, even though the ionic strength causes the analyte retention and its movement from the standardized migration time.

Table 11: Calibration results for Aerophine using method 1.

| Matrix | Calibration area, $mgL^{-1}$ | $R^2$ | LOD, $mgL^{-1}$ | LOQ, $mgL^{-1}$ | $\mu_{ep}$, $10^{-8}m^2V^{-1}s^{-1}$ |
|---|---|---|---|---|---|
| Pure water | 4.5 – 10000 | 0.998 | 2.7 | 9.0 | -0.186 $\pm$ 0.004 |
| Process water A | 4.5 – 10000 | 0.998 | 6.7 | 22.5 | -0.184 $\pm$ 0.005 |
| Process water B | 4.5 – 10000 | 0.997 | 6.7 | 22.5 | -0.183 $\pm$ 0.005 |

Results of Danafloat calibration are given in Table 12. From this table the same conclusions can be made as with Aerophine. The difference is the calculated LOD and LOQ values for process water A, as they are lower than even in pure water. This can be explained with the process water already containing some Danafloat, which makes the peaks bigger.

Table 12: Calibration results for Danafloat using method 1.

| Matrix | Calibration area, $mgL^{-1}$ | $R^2$ | LOD, $mgL^{-1}$ | LOQ, $mgL^{-1}$ | $\mu_{ep}$, $10^{-8}m^2V^{-1}s^{-1}$ |
|---|---|---|---|---|---|
| Pure water | 4.5 – 10000 | 0.997 | 4.5 | 45.0 | -0.179 $\pm$ 0.004 |
| Process water A | 4.5 – 10000 | 0.999 | 2.5 | 8.3 | -0.177 $\pm$ 0.003 |
| Process water B | 4.5 – 10000 | 0.999 | 6.7 | 22.5 | -0.177 $\pm$ 0.004 |

Calibrations using method 2 were only done for isobutyl xanthate and ethyl xanthate. This is because it was noticed during the method development, that DTP and DTPI did not give very good peaks using this method, as can be seen in Figure 15.

Calibration samples were done by serial dilutions and had the concentrations of 0.41, 1.23, 3.70, 11.11, 33.33 and 100 $mgL^{-1}$. Calibrations for this method were only done using pure water and process water. This is because during the calibration of the first method it was noticed that the results between calibrations done in process water and the water from thickener overflow did not differ noticeably. Calibration runs were repeated three times from the same sample vials.

It can be seen from the calibration data of IBX in Figure 18 and in Table 13 that the method seems to work better in the process water. The calibration for samples in process water gives a straight line with a good coefficient of determination

while data points from calibration in pure water seems to be nonlinear. In addition, Figure 18b shows that the repeated measurements have much more spread than the repetitions in process water in Figure 18a.

Starting from the concentration of 1.23 $mgL^{-1}$ in the electropherograms of the process water calibrations a unknown peak could be seen. This peak also grew linearly with the IBX concentration. This unknown peak can be seen in Figure 19.

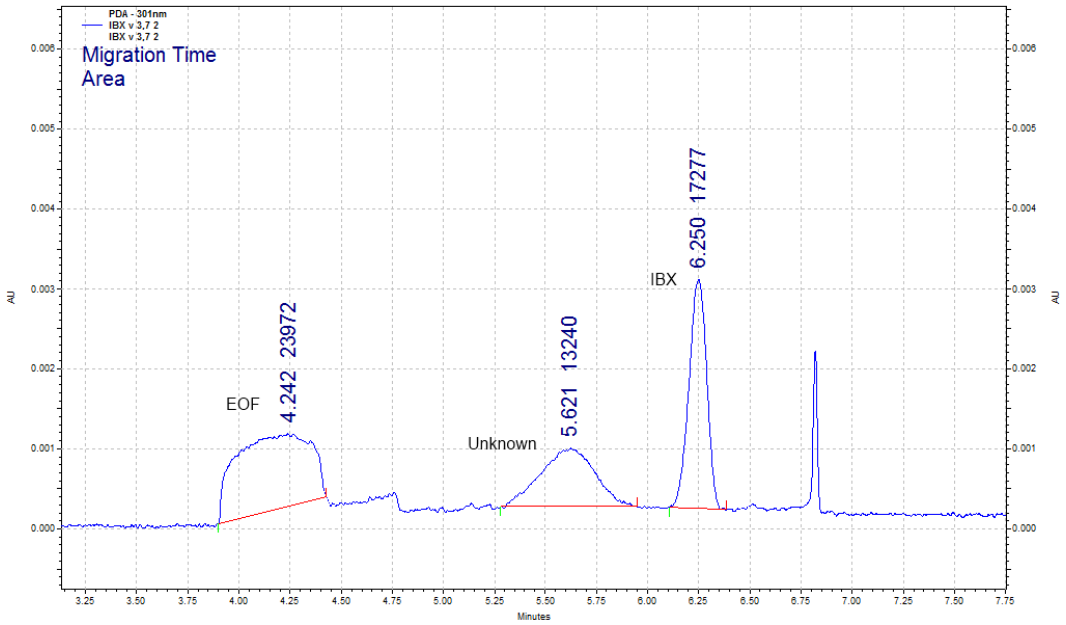


Figure 17: Electropherogram from the calibration runs for IBX in process water using method 2.

Table 13: Calibration results for isobutyl xanthate using method 2.

| Matrix | Calibration area, $mgL^{-1}$ | $R^2$ | LOD, $mgL^{-1}$ | LOQ, $mgL^{-1}$ | $\mu_{ep}$, $10^{-8}m^2V^{-1}s^{-1}$ |
|---|---|---|---|---|---|
| Pure water | 0.41 – 100 | – | 0.41 | 1.4 | -0.239 $\pm$ 0.021 |
| Process water B | 0.41 – 100 | 0.999 | 0.62 | 2.0 | -0.192 $\pm$ 0.008 |

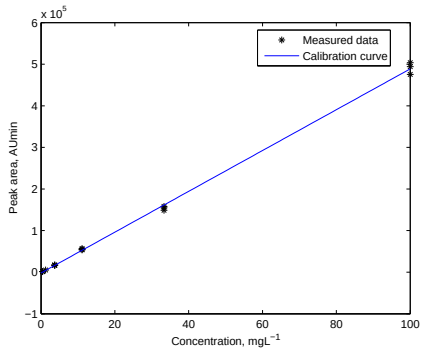


(a) Calibration curve of IBX in process water.

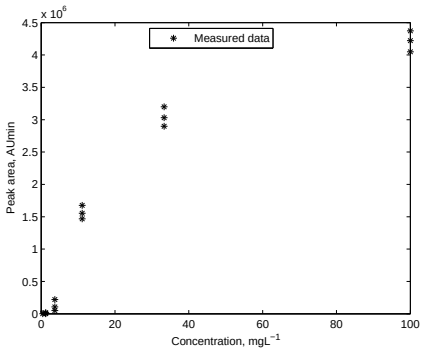


(b) Datapoints of IBX calibration in pure water.

Figure 18: Calibration results for IBX in two different sample matrices.

For ethyl xanthate similar results as for isobutyl xanthate were obtained from the calibration using method 2. The results can be seen in Table 14 and in Figure 20. The method seems to be working better with process water samples also in the case of EX . Although the LOD in water is much smaller and so doing the calibration in pure water with a different concentration range could yield better results because the data points at smaller concentrations seem quite linear in Figure 20b. Comparing the results from EX and IBX calibrations it can be seen that the LODs are smaller for EX. This is most likely caused by the fact that EX has a larger electrophoretic mobility ($\mu_{ep}$) than IBX, i.e. during the electrokinetic injection EX molecules migrate to the capillary faster and as a result the EX peaks are bigger, when the injection time is the same for both analytes.

Similarly to IBX a unknown peak appeared also in the electropherograms of EX calibrations in the process water, but for EX this peak was visible from the sample concentration of 0.41 $\text{mgL}^{-1}$. When the concentrations of the analytes were 100 $\text{mgL}^{-1}$, the peaks for both the EX and the unknown compound were so big that they did not separate well enough for quantitative determination. This is why the final calibration range of EX in process water was 0.41 – 33.3 $\text{mgL}^{-1}$.

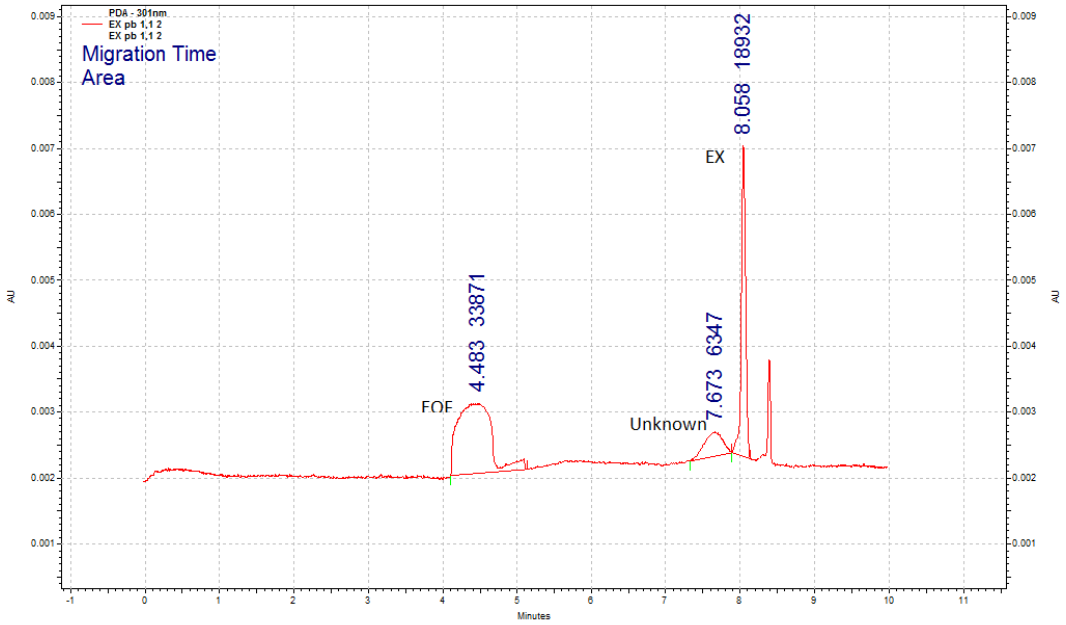


Figure 19: Electropherogram from the calibration runs for EX in process water using method 2.

Table 14: Calibration results for ethyl xanthate using method 2.

| Matrix | Calibration area, $mgL^{-1}$ | $R^2$ | LOD, $mgL^{-1}$ | LOQ, $mgL^{-1}$ | $\mu_{ep}$, $10^{-8}m^2V^{-1}s^{-1}$ |
|---|---|---|---|---|---|
| Pure water | 0.41 – 100 | – | 0.025 | 0.08 | -0.283 $\pm$ 0.027 |
| Process water B | 0.41 – 33.3 | 0.959 | 0.16 | 0.5 | -0.244 $\pm$ 0.013 |

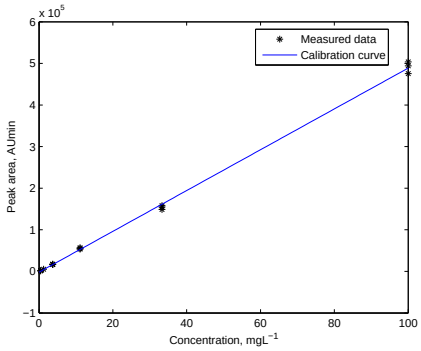


(a) Calibration curve of EX in process water.

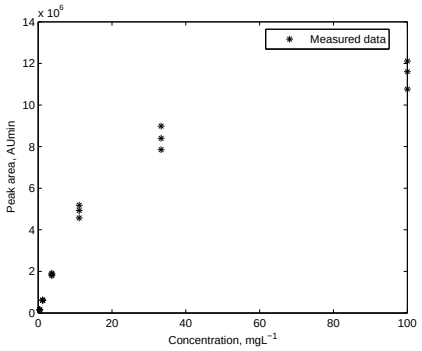


(b) Datapoints of EX calibration in pure water

Figure 20: Calibration results for EX in two different sample matrices.

### 5.3.2 Separation

With method 1 it is possible to separate Danafloat and Aerophine as can be seen in Figure 21. Similar separation happens also in samples prepared using the process waters for dilution. In all matrices tested Danafloat migrates first. From the same figure it is also possible to see that both of the analytes migrate before 10 minutes. Using equation (3) the resolutions were calculated between Danafloat and Aerophine in all of the matrices. Danafloat and Aerophine separated well enough in all of the matrices, because the resolution factor was larger than one.

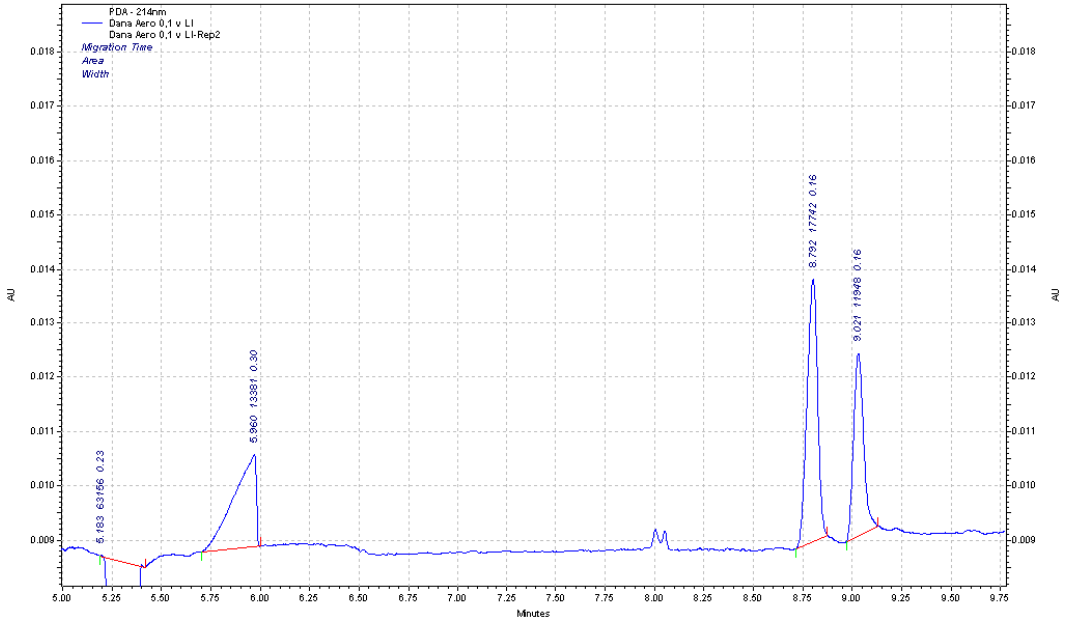


Figure 21: Electropherogram of Danafloat and Aerophine in pure water in the concentration of 100 mgL$^{-1}$. The negative peak at the start and the following peak are system peaks caused by the EOF, after that Danafloat migrates first followed by Aerophine. Conditions as in method 1.

Using method 2 all four compounds (DTP, DTPI, IBX and EX) could be separated in pure water (see Figure 10). Figure 14 shows that method 2 was not efficient for all of the compounds in process water, but has capacity to separate EX and IBX, even though the EX peak has some overlapping with one unknown compound.

### 5.3.3 Measurements at a gold concentrator

Vammala gold concentrator is owned by Dragon Mining and it is located in Sastamala, Finland. Ores from Orivesi and Jokisivu gold mines are processed there. The

process consists of crushing, grinding and flotation. The concentrate produced is further refined at the Harjavalta smelter. Flowchart of the process can be seen in Figure 23.

Measurements at Vammala gold concentrator were made during 6th and 7th of September 2012. Purpose of these measurements was to test the applicability of the developed methods for samples straight from different stages of the process. Prior to these test analyses at the concentrator both methods had been developed using water samples from the same concentrator. It was expected that these methods should work also at the plant and with fresh samples, but it is also known that the composition of the process waters change as the ore compositions change. In addition, the waters may change during different stages of the process. These kind of samples require some robustness from the analysis method. The plant changes the promoter used alongside IBX depending on the ore they are handling, Danafloat for Orivesi and Aerophine for Jokisivu -ore. During measurements ore from Orivesi gold mine was handled. The ore had changed two weeks before the measurement campaign.

During analyses there could be seen some sifting of the peaks between different samples. This is most likely caused by the difference in the ionic strengths at various stages of the process, still when calculated the electrophoretic mobilities were close to one another. Another reason for peaks sifting was the surroundings of the capillary electrophoresis machine, especially the ambient temperature. Because the machine was placed in a part of the plant with no heating system, the temperatures around the machine changed with the outside temperature. The analysis machine itself has temperature control for the capillary and the sample storage, but no doubt the temperature of environment has some effect on the buffers and samples on the buffer trays, because the trays are basically exposed directly to outside air. Picture of the measurement apparatus and setup in the concentrator plant can be seen in Figure 22.


Figure 22: Measurement setup at Vammala concentrator plant.

Samples were taken from 9 different points in the process. These points were cyclone overflow, cyclone underflow, rougher flotation, scavenger flotation, tails, concentrate, thickener overflow, thickener underflow and filtrate of the thickener underflow. Figure 23 shows a flowchart of the process for better understanding of the sampling points. All of these samples were studied using both method 1 and 2. As noted before the measurement conditions were a bit different than in the laboratory where the methods were developed and where the calibrations were done. Normally calibrations should have been done with the sample runs, but as the idea was just to test the applicability of the methods they were omitted to allow for more samples to be analyzed. For the same reason repeated analyses were done only for some samples with quite good reproducibility. For the above reasons the following results give more information about the methods rather than exact knowledge of the process. For example the concentrations calculated for different samples should be considered more as an orders of magnitude than the real concentrations.

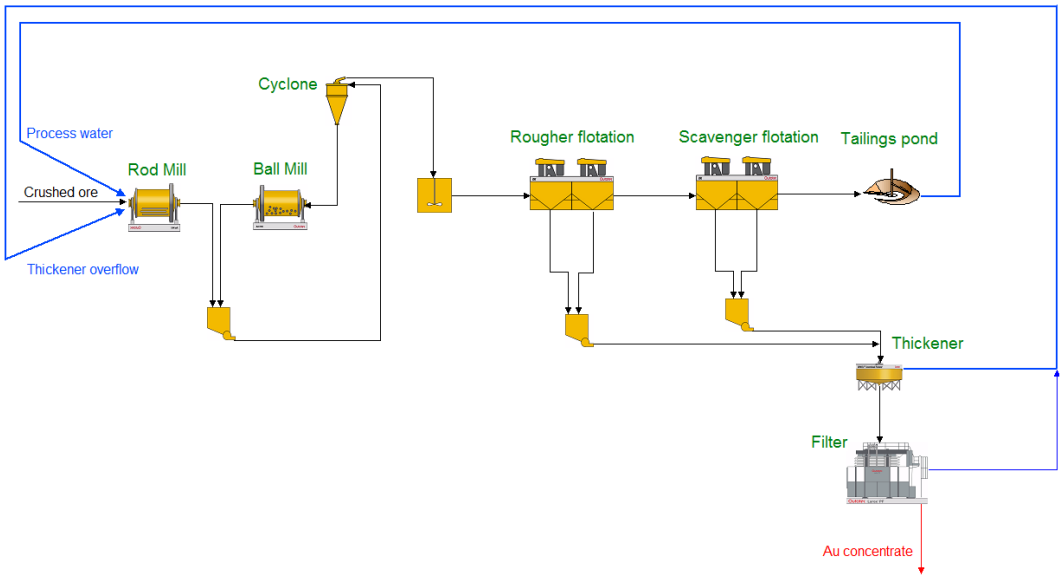


Figure 23: Flowchart of the Vammala gold concentrator plant showing all the main equipment and process streams from which the samples were taken.

Using method 1 small peaks could be detected in most of the process samples. Unfortunately, concentrations calculated from these peaks fall under the LODs of the analytes this method was calibrated for. Electrophoretic mobilities were calculated for the peaks found in the samples and compared to electrophoretic mobilities calculated from the calibrations of method 1. For all of the peaks found in the process samples using method 1 the electrophoretic mobilities were very close to the mobility calculated for Danafloat in process water. It was also known that during the measurements the concentrator plant was using Danafloat 245 in their process. According to the electrophoretic mobilities it can be said that the peaks found are very likely to be Danafloat, but the amounts fall under the detection limit of 6.7 $mgL^{-1}$. The calibration data for Danafloat can be seen in Table 12 and the results of method 1 from the concentrator in Table 15. In Figure 24 few electropherograms from samples are drawn together with a standard that was run between samples at Vammala.

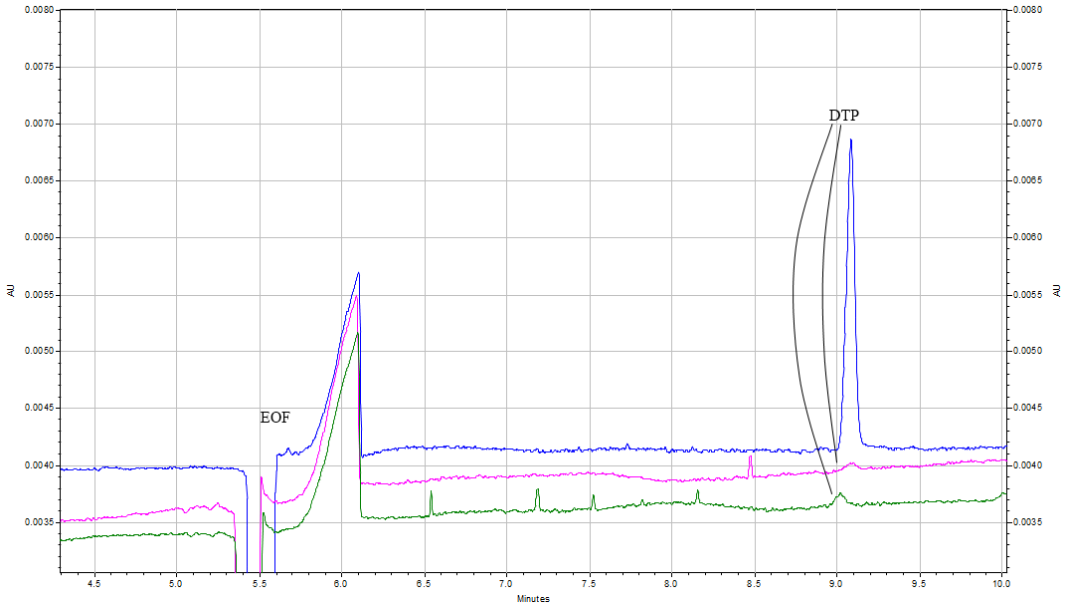


Figure 24: Electropherograms of Vammala samples cyclone overflow (pink) and thickener overflow (green) together with a 50 mgL$^{-1}$ standard (blue). Conditions as in method 1.

Table 15: Results for Danafloat 245 (DTP) measurements from Vammala concentrator process waters using method 1.

| Sample | Electrophoretic mobility ($\mu_{ep}$) $10^{-8}m^2V^{-1}s^{-1}$ | Concentration, mgL$^{-1}$ |
|---|---|---|
| Cyclone overflow | -0.1725 | Under LOD |
| Cyclone underflow | -0.1704 | " |
| Rougher flotation | -0.1724 | " |
| Scavenger flotation | -0.1718 | " |
| Tails | -0.1737 | " |
| Concentrate | -0.1723 | " |
| Thickener overflow | -0.1704 | " |
| Thickener underflow | -0.1738 | " |
| Filtrate | No peak detected | – |

In most of the samples Danafloat migrated to the detector in about 10 minutes. For some samples longer analyses of about 20 minutes were done. In these some additional peaks were detected as showed in Figure 25, where a electropherogram of a sample from the thickener underflow is presented. Similar results were obtained also for the filtrate. The thickener underflow and the filtrate are actually taken from

almost the same part of the process. The only difference is that the thickener underflow was filtrated in the laboratory before analysis and the filtrate sample came from the filter used in the process. One reason for these peaks could be that the filtration, either in the process or in the laboratory detaches some of the adsorbed collector species as complexes or decomposition products. At this point and with the data available it is impossible to say much else about these unknown peaks, but after further development the method could be used for gaining more information about the phenomena in the flotation process.

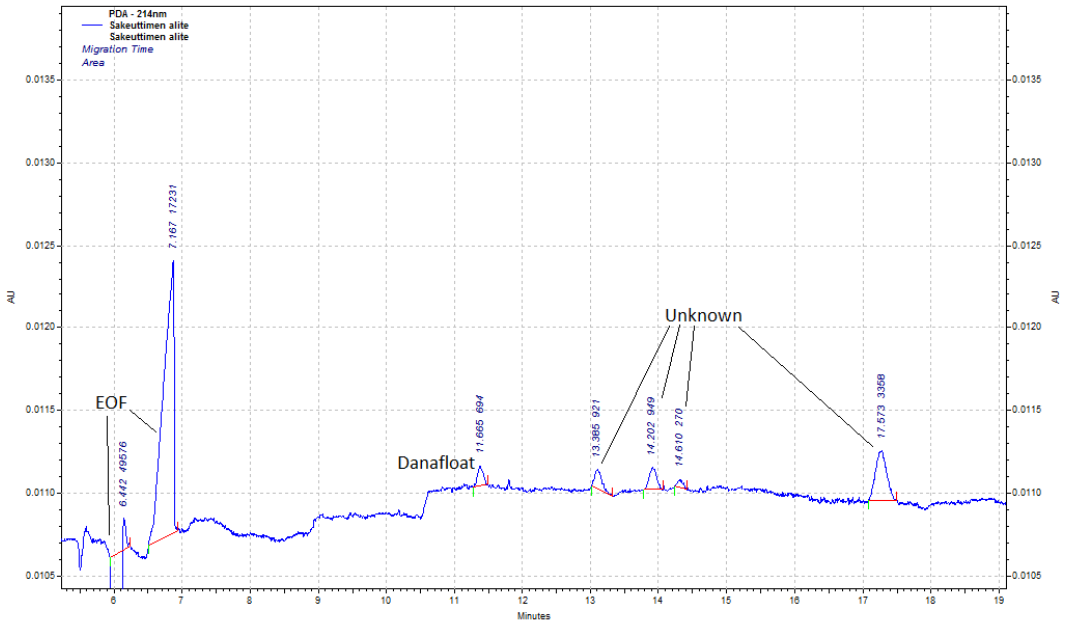


Figure 25: Electropherogram of a sample from thickener underflow using method 1.

Method 2 was used to study the presence of isobutyl xanthate in the process samples. From Table 16 it can be seen that IBX was not found in so many of the samples as Danafloat was. In addition, the electrophoretic mobilities do not match up against the values calculated from calibration quite so well as in samples analyzed with method 1. Still the mobilities are close to the value calculated from calibration in Table 13. This gives a reason to believe that the peaks detected were likely IBX. Most of the electropherograms of Vammala samples remind those attained from calibration runs, at least to a some extent. This can be seen from Figure 26 where results from laboratory are compared to those from the Vammala concentrator.

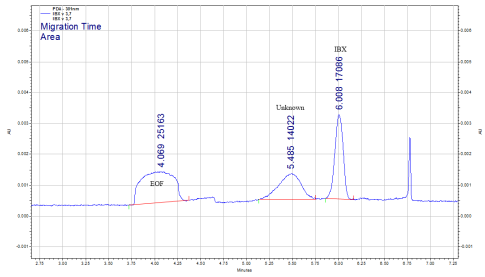


(a) Electropherogram from the calibration of IBX in process water, detection at 301 nm.

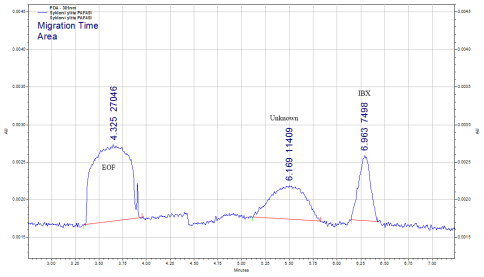


(b) Electropherogram from the cyclone overflow, detection at 301 nm.

Figure 26: Comparison of electropherograms gathered from laboratory calibrations and measurements at Vammala concentrator. Method 2 was used in both cases.

Even when the electropherograms of the samples remind the ones from calibration there are some differences. The main difference is that the peaks detected in the samples are larger when detected at wavelengths of 214 nm and 254 nm rather than 301 nm, where the absorption of of xanthates should have their maximum. Example of this is presented in Figure 27, where the first two peaks are clearly smaller at wavelength 214 nm while the third one clearly grows. The last peak in fact matches most closely the electrophoretic mobility of IBX. One reason could be that while Danafloat was determined using the method 1, it separates also with the method 2. Then the reason for the intensive signal at 214 nm and 254 nm, could be Danafloat comigrating with other compounds. At wavelength of 301 nm Danafloat does not appear, since due to the selective detection only xanthate peaks can be monitored. But the reason could well be entirely other, such as xanthate oxidation product comigrating, and in this case spiking the sample with IBX would be the best way to resolve this.

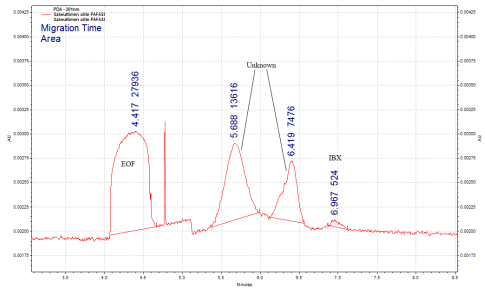


(a) Electropherogram from the thickener underflow, detection at 301 nm.

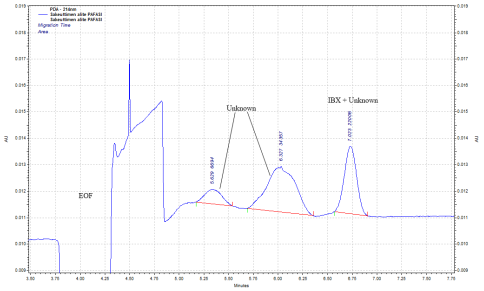


(b) Electropherogram from the thickener underflow, detection at 214 nm.

Figure 27: Electropherograms of thickener underflow recorded at two different wavelengths using method 2.

Table 16: Results for isobutyl xanthate (IBX) measurements from Vammala concentrator process waters using method 2.

| Sample | Electrophoretic mobility ($\mu_{ep}$) $10^{-8}m^2V^{-1}s^{-1}$ | Concentration, mgL$^{-1}$ |
|---|---|---|
| Cyclone overflow | -0.2190 | 2.0 |
| Cyclone underflow | -0.2172 | 1.5 |
| Rougher flotation | No peak detected | – |
| Scavenger flotation | No peak detected | – |
| Tails | -0.2166 | 1.0 |
| Concentrate | No peak detected | – |
| Thickener overflow | No peak detected | – |
| Thickener underflow | -0.2072 | 0.5 |
| Filtrate | -0.2088 | 0.5 |

In addition to the process samples, a few samples from Vammala concentrator's waters were analyzed using both methods. Samples were taken from from the first and second tailings bonds, the overflow drain, or the storm drain and from the fresh water well. From these samples no peaks were detected with either method.

### 5.3.4 Other remarks

During the development and calibration of method 2 and the measurements in Vammala, some peaks other than of the analytes were observed. In Table 17 migration times for peaks found from various samples are given. This includes a lot of unknown peaks, which are for future reference, so when for example oxidation products of xanthates are studied using this method, a comparison could be done between the migration times.

At the moment these unknown compounds can be either impurities from the industrial grade chemicals used, decomposition products or metal complexes. The peaks have been arranged to columns according to similar migration times, this does not mean that the peaks in different samples would be of the same origin. Still some conclusions can be made from Table 17. Firstly, by comparing the analyses of the 6th and 7th sample in the table it can be seen that five peaks have appeared to the older (7th) sample. This would implicate that the peaks that have appeared would be some kind of degradation products of one or both xanthates in the sample.

It could be assumed that the unknown peaks found in the samples that were analyzed just after preparation, are most likely impurities from the chemicals themselves, as decomposition has not had time to happen. At least in the case of higher concentration samples, as the 3rd sample, where also the impurity concentrations are higher. Lastly, the unknown peaks found in samples prepared in pure water are most likely not complexes, because there should not be any metal ions available to form complexes.

Table 17: Migration times of known and unknown peaks from various samples analyzed using method 2.

| Sample | EOF, min | Peak 1, min | DTP, min | DTPI, min | Peak 2, min | Peak 3, min | Peak 4, min | IBX, min | Peak 5, min | Peak 6, min | EX, min | Peak 7, min |
|---|---|---|---|---|---|---|---|---|---|---|---|---|
| EX 3.7 $mgL^{-1}$ in pure water | 4.890 | | | | | | | | 9.279 | 10.040 | 11.317 | |
| EX 10 $mgL^{-1}$ in pure water | 4.817 | | | | | | | | 9.519 | 9.785 | 11.221 | |
| IBX 100 $mgL^{-1}$ in pure water | 4.033 | 6.283 | | | 7.485 | 8.488 | | 6.504 | | | | |
| IBX 10 $mgL^{-1}$ in pure water | 4.808 | | | | | 8.500 | 9.023 | 9.250 | | 10.502 | | 12.027 |
| EX and IBX 5 $mgL^{-1}$ in pure water | 4.852 | | | | | | | 9.577 | | 10.781 | 11.971 | |
| DTP, DTPI at 10 $mgL^{-1}$ and EX, IBX at 1 $mgL^{-1}$ in pure water | 4.883 | | 7.694 | 7.871 | | | | 9.748 | | | 12.400 | |
| DTP, DTPI at 10 $mgL^{-1}$ and EX, IBX at 1 $mgL^{-1}$ in pure water, a few days old sample | 4.765 | 7.296 | 7.452 | 7.635 | 8.106 | 8.444 | 8.923 | 9.329 | 9.721 | 10.360 | 11.415 | |
| EX 1.1 $mgL^{-1}$ in process water | 4.483 | | | | | | | | | 7.673 | 8.058 | |
| IBX 3.7 $mgL^{-1}$ in process water | 4.069 | | | | | | 5.485 | 6.008 | | | | |
| Cyclone overflow | 4.325 | | | | | | 6.169 | 6.963 | | | | |
| Thickener underflow | 4.417 | | | | | 5.688 | 6.419 | 6.967 | | | | |

## 5.4 Conclusions

In this work two capillary electrophoresis methods were developed for analyzing flotation collectors from process waters. First method can be used for sodium diiosobutylditiophosphate and sodium diisobutyldithiophosphinate. The second for ethyl and isobutyl xanthates.

Phosphate method is able to separate and detect sodium diiosobutylditiophosphate (DTP) and sodium diisobutyldithiophosphinate (DTPI) in pure water as well as in flotation process water. For DTPI the detection limits were 2.7 $mgL^{-1}$ and 6.7 $mgL^{-1}$ in pure water and process water, respectively. For DTP the corresponding limits were 4.5 $mgL^{-1}$ and 6.7 $mgL^{-1}$. These components can be analyzed in 10 minutes using this method in both matrices. The method is also capable of separating ethyl and isobutyl xanthates, but in those analyses the detection limits were still so high that a separate method was developed for analyzing them.

Phosphate method was also used for analyzing samples from the flotation plant at Vammala. The method proved itself robust enough to handle samples from all stages of the process giving peaks with similar electrophoretic mobilities as DTP calibration peaks. Unfortunately, all of the peaks detected were under the limit of detection of the analytes. Additional optimization was studied to get lower LODs. The good separation efficiency and the many unknown compounds detected in the electropherograms may make possible the characterization of degradation products and complexes of collectors.

Xanthate method is used for separating isobutyl xanthate (IBX) and ethyl xanthate (EX) in pure water and flotation process water. The detection limits in pure water for isobutyl xanthate (IBX) and ethyl xanthate (EX) are 0.41 $mgL^{-1}$ and 0.025 $mgL^{-1}$, respectively. In process water the LODs were 0.62 $mgL^{-1}$ and 0.16 $mgL^{-1}$. Analysis of these compounds can be achieved in 10 minutes in process waters and in under 15 minutes in pure water. This method also shows response for DTP and DTPI, but they do not separate well from other compounds in process waters. Fortunately, these compounds do not have a high absorbance at 301 nm where xanthates are detected.

Xanthate method was used at Vammala gold concentrator. While the method seemed to be a little less robust than the phosphate method, it did give peaks in many of the samples. Concentrations were calculated for the peaks with similar electrophoretic mobilities as in IBX calibration. Although the conclusion was made that these peaks are most likely IBX, it is not so sure as with the phosphate method. Some

more development should be done with this method at least to get all the components to separate from each other and to increase robustness and thus applicability to process samples.

The next step in the method development could be the testing of other injection methods. For example stacking could improve the detection limits by introducing more analytes to the capillary. Buffer composition could also be changed or a organic modifier added to the buffer. These could help separating species for example in the case of the xanthate method.

These methods serve as a starting point for further development. They have the potential to be used for the study of decomposition products and complexes of collectors. Another application can be on-line measurements, either at a concentrator plant or in a laboratory scale flotation experiment. For these applications the methods need to be tested with synthesized complexes or decomposition products and most likely some more optimization is needed for these new analytes.

# References


[1] G.C. Allan and J.T. Woodcock. A review of the flotation of native gold and electrum. *Minerals Engineering*, 14(9):931 – 962, 2001.

[2] P. Somasundra and K.P. Ananthapadmanabhan. *Handbook of separation process technology*, chapter Bubble and Foam Separations - Ore Flotation, pages 775 – 805. Wiley-interscience publication. J. Wiley, 1987.

[3] B. Yarar. *Ullmann's Encyclopedia of Industrial Chemistry*, chapter Flotation, pages 238–267. Wiley-VCH Verlag GmbH & Co. KGaA, 2000.

[4] M.J. Pearse. An overview of the use of chemical reagents in mineral processing. *Minerals Engineering*, 18(2):139 – 149, 2005.

[5] N.O. Lotter and D.J. Bradshaw. The formulation and use of mixed collectors in sulphide flotation. *Minerals Engineering*, 23(11–13):945 – 951, 2010.

[6] Y. Vazifeh, E. Jorjani, and A. Bagherian. Optimization of reagent dosages for copper flotation using statistical technique. *Transactions of Nonferrous Metals Society of China*, 20(12):2371 – 2378, 2010.

[7] F. Hao, K.J. Davey, W.J. Bruckard, and J.T. Woodcock. Online analysis for xanthate in laboratory flotation pulps with a uv monitor. *International Journal of Mineral Processing*, 89(1–4):71 – 75, 2008.

[8] M.H. Jones and J.T. Woodcock. Dixanthogen determination in flotation liquors by solvent extraction and ultraviolet spectrometry. *Analytical Chemistry*, 58(3):588–591, 1986.

[9] S. Luukkanen, P. Parvinen, M. Miettinen, P. Stén, S. Lähteenmäki, and A. Tuikka. Monitoring the composition of water of flotation slurries with an on-line analyser. *Minerals Engineering*, 16(11):1075 – 1079, 2003.

[10] A.J. Vreugdenhil, J.A. Finch, I.S. Butler, and I. Paquin. Analysis of alkylxanthate collectors on sulphide minerals and flotation products by headspace analysis gas-phase infrared spectroscopy (hagis). *Minerals Engineering*, 12(7):745 – 756, 1999.

[11] H. Eggers and H. Rüssel. Liquid chromatography of xanthate complexes. *Chromatographia*, 17:486–490, 1983.

[12] C. Zhou, A. Bahr, and G. Schwedt. Separation and determination of xanthates in mixtures as dixanthogens by normal-phase hplc on a diol-phase. *Fresenius' Journal of Analytical Chemistry*, 338:908–911, 1990.

[13] C. Zhou, A. Bahr, and G. Schwedt. Studies on the hplc determination of xanthates via copper(i) xanthates and dixanthogens. *Fresenius' Journal of Analytical Chemistry*, 334:527–533, 1989.

[14] F.P. Hao, E. Silvester, and G. David Senior. Spectroscopic characterization of ethyl xanthate oxidation products and analysis by ion interaction chromatography. *Analytical Chemistry*, 72(20):4836–4845, 2000.

[15] D. E. Barnes and C. Pohlandt-Watson. Separation and determination of the sulph-hydryl flotation collectors using ion-interaction chromatography. *Fresenius' Journal of Analytical Chemistry*, 345:36–42, 1993.

[16] A. K. Malik and W. Faubel. Capillary electrophoretic determination of dithiocarbamates and ethyl xanthate. *Fresenius' Journal of Analytical Chemistry*, 367:211–214, 2000.

[17] F. Hissner, B. Daus, J. Mattusch, and K. Heinig. Determination of flotation reagents used in tin-mining by capillary electrophoresis. *Journal of Chromatography A*, 853(1–2):497 – 502, 1999.

[18] C.H. Keller. Concentration of gold, sulphide minerals and uranium oxide minerals by flotation from ores and metallurgical plant products, 1925.

[19] R.D. Crozier. *Flotation: Theory, Reagents and Ore Testing*. Pergamon, 1992.

[20] A.J. Vreugdenhil, S.H.R. Brienne, I.S. Butler, J.A. Finch, and R.D. Markwell. Infrared spectroscopic determination of the gas-phase thermal decomposition products of metal-ethyldithiocarbonate complexes. *Spectrochimica Acta Part A: Molecular and Biomolecular Spectroscopy*, 53(12):2139 – 2151, 1997.

[21] A. López Valdivieso, A.A. Sánchez López, and S. Song. On the cathodic reaction coupled with the oxidation of xanthates at the pyrite/aqueous solution interface. *International Journal of Mineral Processing*, 77(3):154 – 164, 2005.

[22] J.O. Leppinen. Ftir and flotation investigation of the adsorption of ethyl xanthate on activated and non-activated sulfide minerals. *International Journal of Mineral Processing*, 30(3–4):245 – 263, 1990.

[23] J. Leja. *Surface chemistry of froth flotation*. Plenum Press, 1982.

[24] M. Trudgett. The ultra-trace levels analysis of xanthates by high performance liquid chromatography. Master's thesis, University of Western Sydney, 2005.

[25] Z. Sun and W. Forsling. The degradation kinetics of ethyl-xanthate as a function of ph in aqueous solution. *Minerals Engineering*, 10(4):389 – 400, 1997.

[26] I. Iwasaki and S. R. B. Cooke. The decomposition of xanthate in acid solution. *Journal of the American Chemical Society*, 80(2):285–288, 1958.

[27] Y. Hu, W. Sun, and D. Wang. General review of electrochemistry of flotation of sulphide minerals. In *Electrochemistry of Flotation of Sulphide Minerals*, pages 1–19. Springer Berlin Heidelberg, 2009.

[28] R. Tipman and J. Leja. Reactivity of xanthate and dixanthogen in aqueous solutions of different ph. *Colloid & Polymer Science*, 253:4–10, 1975.

[29] A.J. Vreugdenhil, S.H.R. Brienne, R.D. Markwell, I.S. Butler, and J.A. Finch. Headspace analysis gas-phase infrared spectroscopy: a study of xanthate decomposition on mineral surfaces. *Journal of Molecular Structure*, 405(1):67 – 77, 1997.

[30] J.G. Eckhardt, K. Stetzenbach, M.F. Burke, and J.L. Moyers. Studies on the separation of xanthate related compounds using high performance liquid chromatography. *Journal of Chromatographic Science*, 16(11):510–513, 1978.

[31] A. Ivaska and J. Leppinen. Determination of trace amounts of the flotation collectors ethyl xanthate and diethyl dithiophosphate in aqueous solutions by cathodic stripping voltammetry. *Talanta*, 33(10):801 – 806, 1986.

[32] J. Leppinen and S. Vahtila. Differential pulse polarographic determination of thiol flotation collectors and sulphide in waters. *Talanta*, 33(10):795 – 799, 1986.

[33] O. M. Zakharova and M. S. Zakharov. Determination of potassium xanthate in aqueous solutions by cathodic stripping voltammetry at a silver electrode. *Journal of Analytical Chemistry*, 58:573–576, 2003.

[34] J. Bugajski and H. Gamsjäger. A new xanthate ion-specific electrode. *Fresenius' Journal of Analytical Chemistry*, 327:362–363, 1987.

[35] W. J. Cabrera, E. S. Maldonado, and H. E. Ríos. Effect of dodecyl alcohol on the potentiometric response of an isopropyl xanthate ion-selective electrode. *Journal of Colloid and Interface Science*, 237(1):76 – 79, 2001.

[36] N. Huang, A. Mao, D. Wang, B. Li, and S. Sun. On-line determination of remained xanthate concentration in pulp. *Journal of Central South University of Technology*, 5:11–13, 1998.

[37] D.A. Skoog, F.J. Holler, and T.A. Nieman. *Principles of instrumental analysis*. Saunders golden sunburst series. Saunders College Pub., 1998.

[38] Y. Nagaosa and T. Mizuyuki. Determination of cu(ii) and ni(ii) as chelates with butyl xanthate by liquid chromatography with electrochemical and spectrophotometric detection. *Analytica Chimica Acta*, 311(2):225 – 229, 1995.

[39] K. W. Weissmahr, C. L. Houghton, and D. L. Sedlak. Analysis of the dithiocarbamate fungicides ziram, maneb, and zineb and the flotation agent ethylxanthogenate by ion-pair reversed-phase hplc. *Analytical Chemistry*, 70(22):4800–4804, 1998.

[40] R. Kuhn and S. Hofstetter-Kuhn. *Capillary electrophoresis: principles and practice*. Springer laboratory. Springer-Verlag, 1993.

[41] B. A. Siles. *Capillary Electrophoresis*. John Wiley & Sons, Ltd, 2006.

[42] H. H. Lauer and G. P. Rozing. *High Performance Capillary Electrophoresis*. Agilent Technologies, second completely revised edition edition, 2010.

[43] V. R. A. Thibon, K. D. Bartle, D. J. Abbott, and K. A. Mccormack. Analysis of zinc dialkyl dithiophosphates by nonaqueous capillary electrophoresis and application to lubricants. *Journal of Microcolumn Separations*, 11(1):71–80, 1999.

[44] P. Stén, P. Parvinen, M. Miettinen, S. Luukkanen, V. Kaskiniemi, and J. Aaltonen. On-line analysis of flotation process waters at Siilinjärvi (Finland) apatite concentrating plant. *Minerals Engineering*, 16(3):229 – 236, 2003.

[45] E. Fuguet, M. Reta, C. Gibert, M. Rosés, E. Bosch, and C. Ràfols. Critical evaluation of buffering solutions for pka determination by capillary electrophoresis. *ELECTROPHORESIS*, 29(13):2841–2851, 2008.

[46] Xin Xu and R.J. Hurtubise. Influence of organic solvents in the capillary zone electrophoresis of polycyclic aromatic hydrocarbon metabolites. *Journal of Chromatography A*, 829(1–2):289 – 299, 1998.

# A Electropherograms of DTPI calibration in pure water

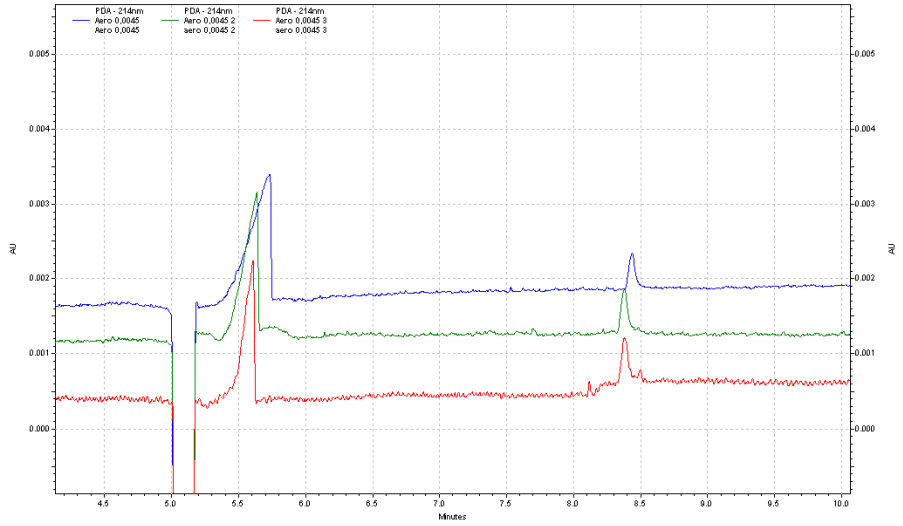


(a) Sample concentration 4.57 $mgL^{-1}$. Blue: 1st injection, green: 2nd injection and red: 3rd injection.

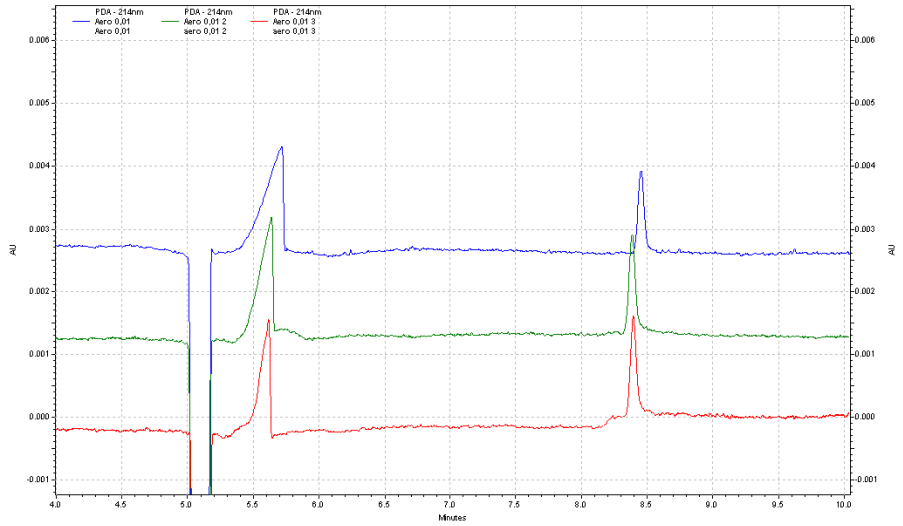


(b) Sample concentration 13.7 $mgL^{-1}$. Blue: 1st injection, green: 2nd injection and red: 3rd injection.

Figure 28: Electropherograms used for calibration of DTPI using method 1.

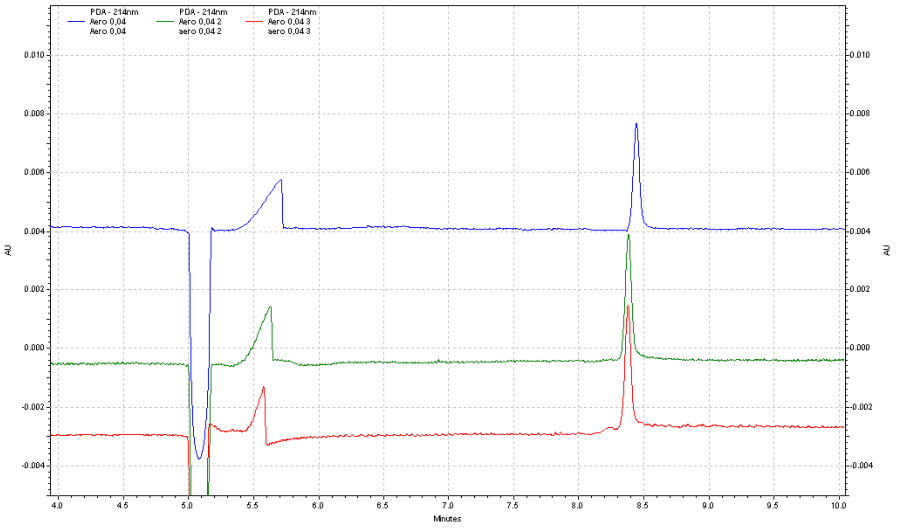


(a) Sample concentration 41.2 $mgL^{-1}$. Blue: 1st injection, green: 2nd injection and red: 3rd injection.

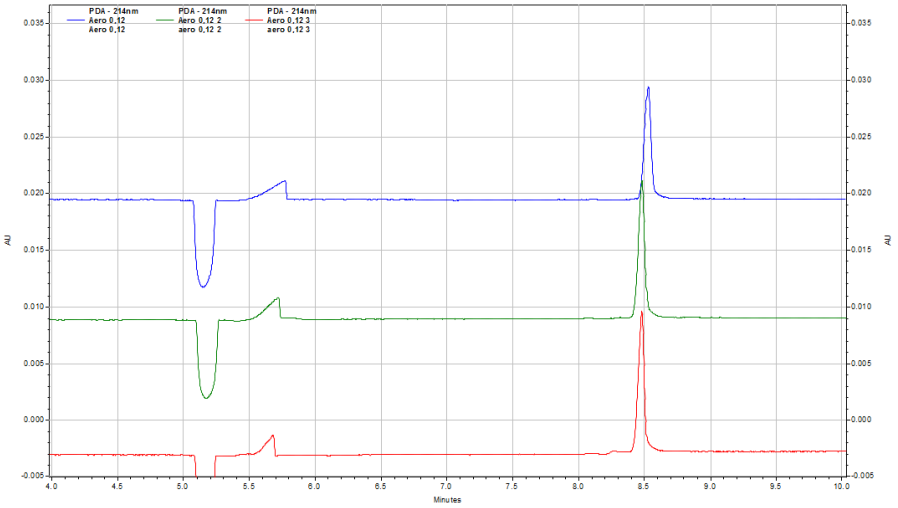


(b) Sample concentration 123.5 $mgL^{-1}$. Blue: 1st injection, green: 2nd injection and red: 3rd injection.

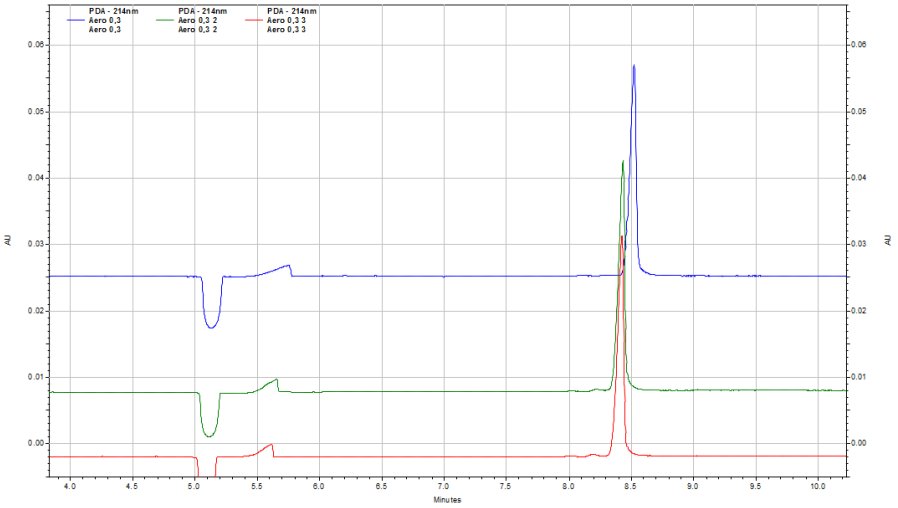


(c) Sample concentration 370.4 $mgL^{-1}$. Blue: 1st injection, green: 2nd injection and red: 3rd injection.

Figure 29: Electropherograms used for calibration of DTPI using method 1.

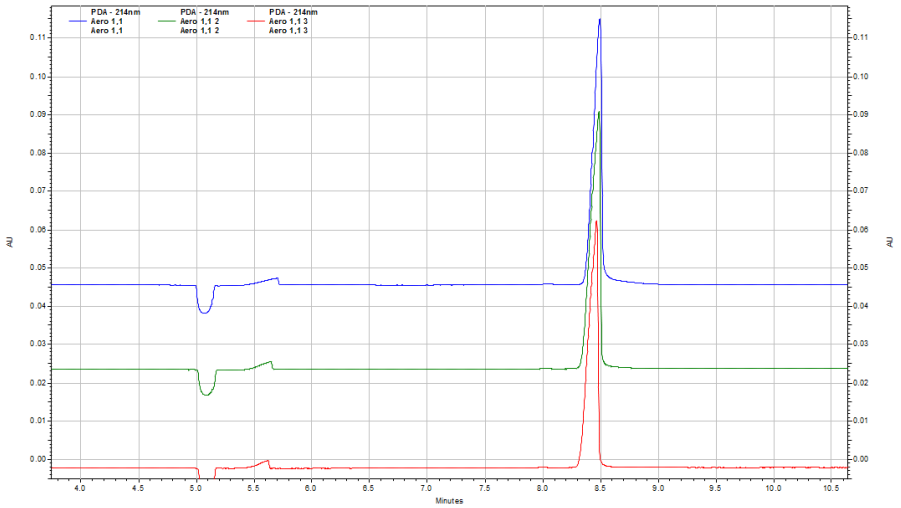


(a) Sample concentration 1,110.0 $mgL^{-1}$. Blue: 1st injection, green: 2nd injection and red: 3rd injection.

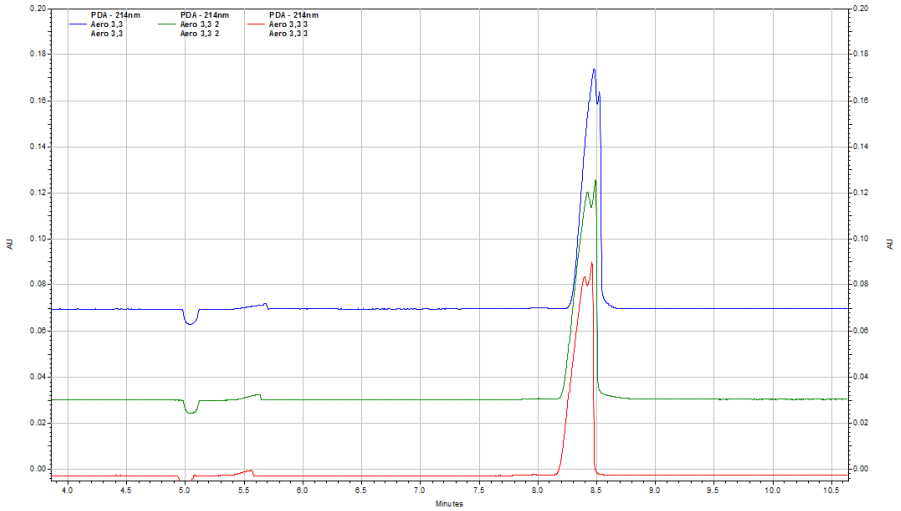


(b) Sample concentration 3,330.0 $mgL^{-1}$. Blue: 1st injection, green: 2nd injection and red: 3rd injection.

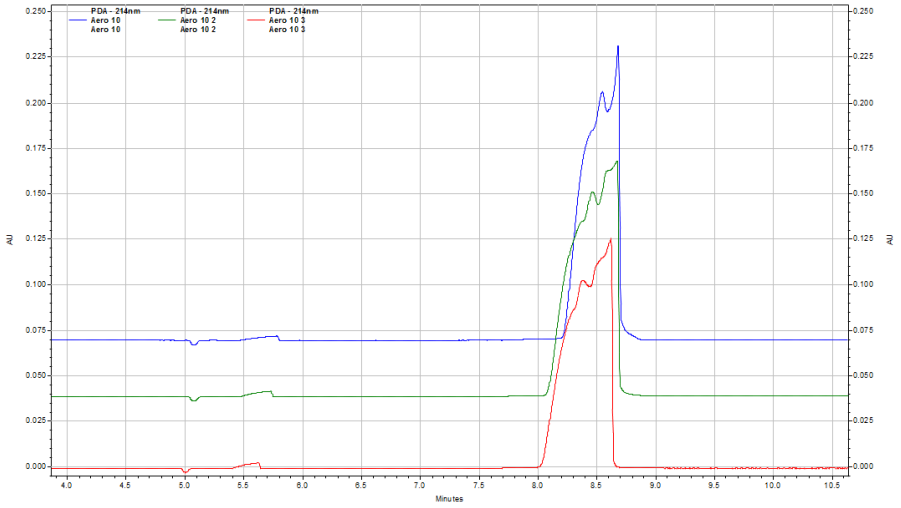


(c) Sample concentration 10,000 $mgL^{-1}$. Blue: 1st injection, green: 2nd injection and red: 3rd injection.

Figure 30: Electropherograms used for calibration of DTPI using method 1.

# B Electropherograms of DTP calibration pure water

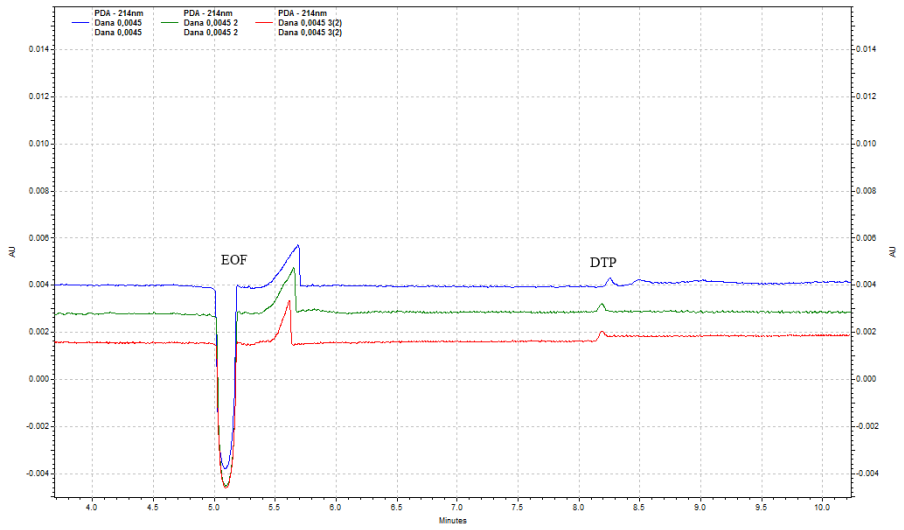


(a) Sample concentration 4.57 $\mathrm{mgL}^{-1}$. Blue: 1st injection, green: 2nd injection and red: 3rd injection.

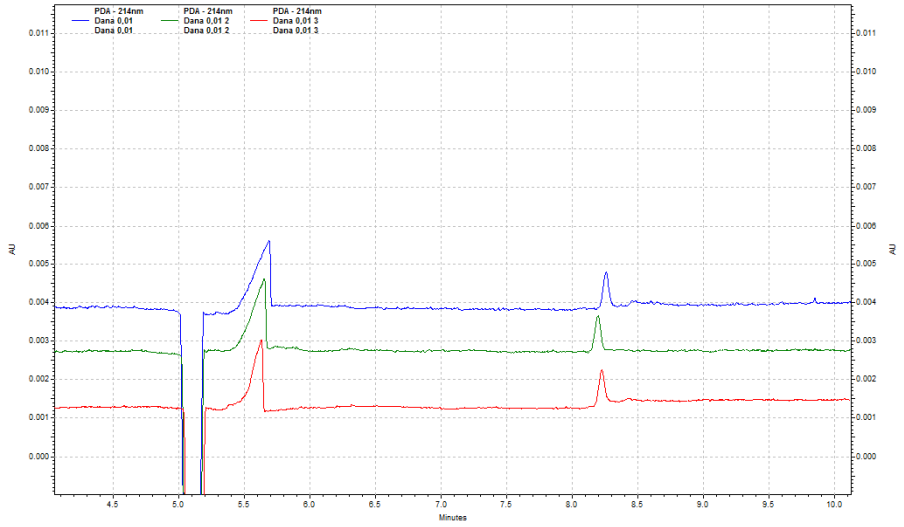


(b) Sample concentration 13.7 $\mathrm{mgL}^{-1}$. Blue: 1st injection, green: 2nd injection and red: 3rd injection.

Figure 31: Electropherograms used for calibration of DTP using method 1.

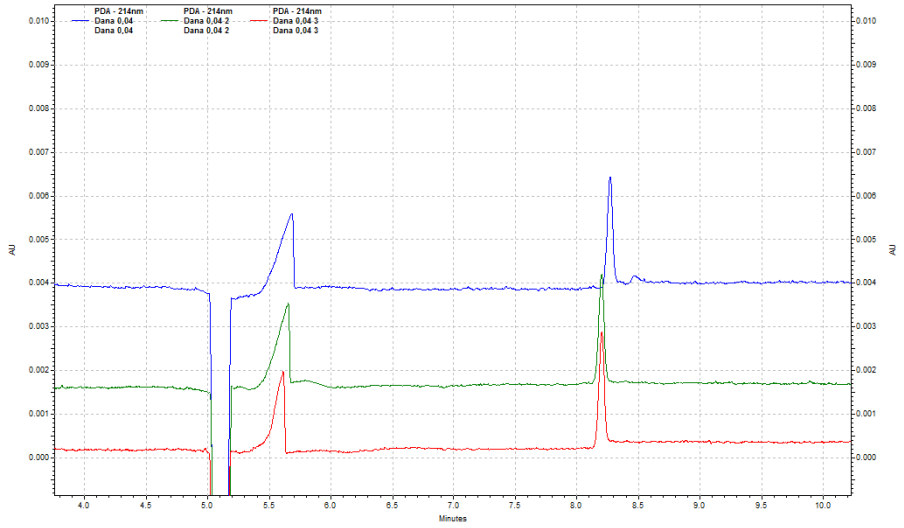


(a) Sample concentration 41.2 $mgL^{-1}$. Blue: 1st injection, green: 2nd injection and red: 3rd injection.

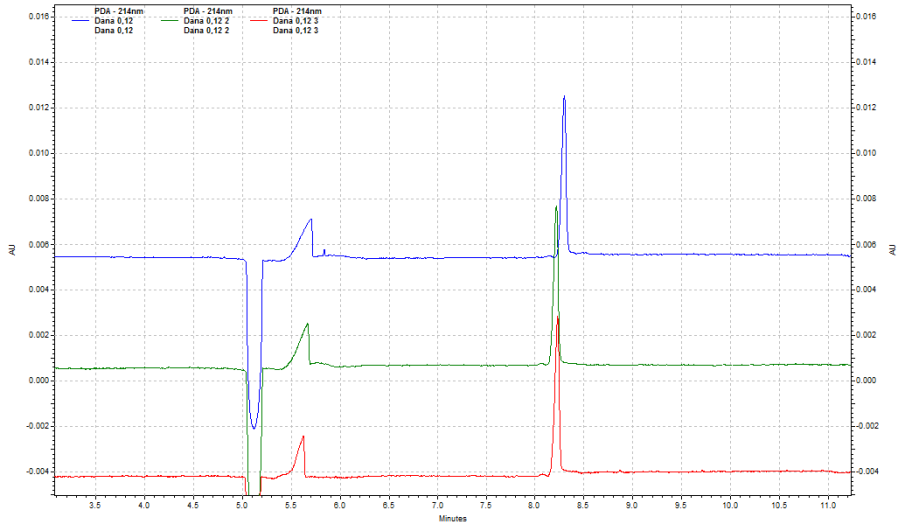


(b) Sample concentration 123.5 $mgL^{-1}$. Blue: 1st injection, green: 2nd injection and red: 3rd injection.

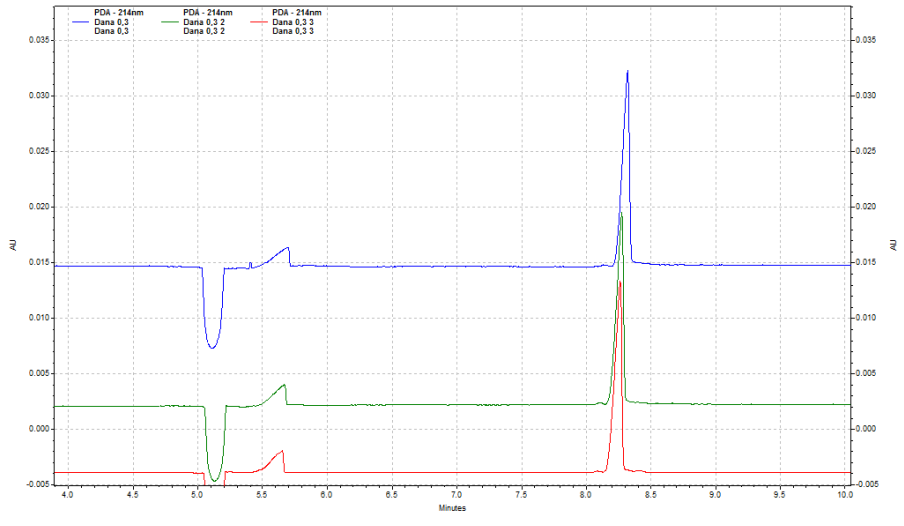


(c) Sample concentration 370.4 $mgL^{-1}$. Blue: 1st injection, green: 2nd injection and red: 3rd injection.

Figure 32: Electropherograms used for calibration of DTP using method 1.

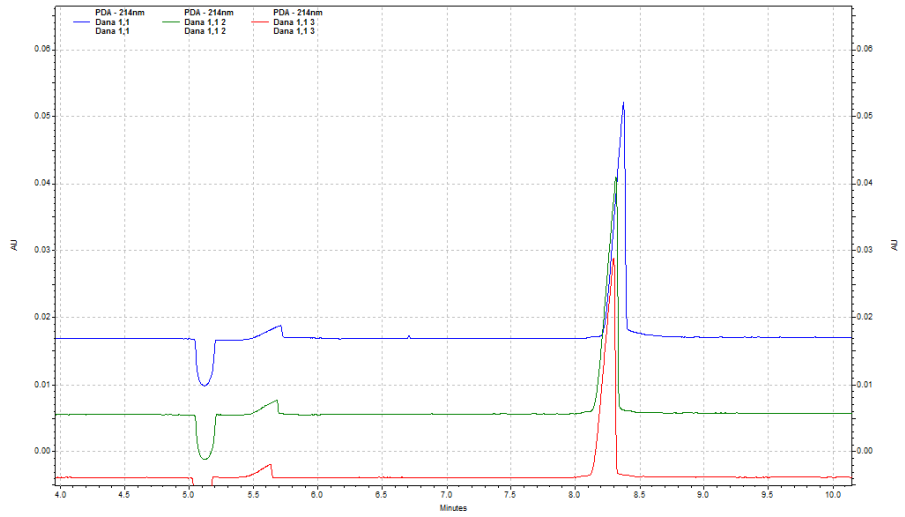


(a) Sample concentration 1,110.0 $mgL^{-1}$. Blue: 1st injection, green: 2nd injection and red: 3rd injection.

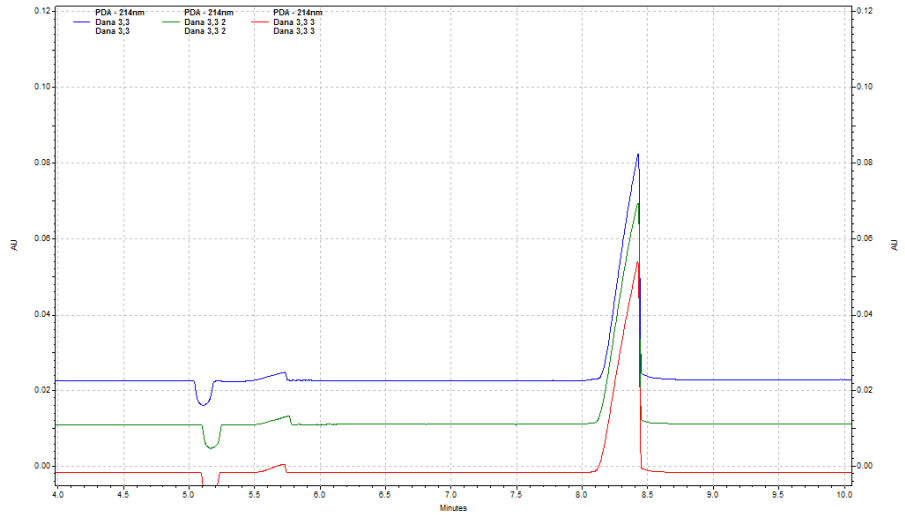


(b) Sample concentration 3,330.0 $mgL^{-1}$. Blue: 1st injection, green: 2nd injection and red: 3rd injection.

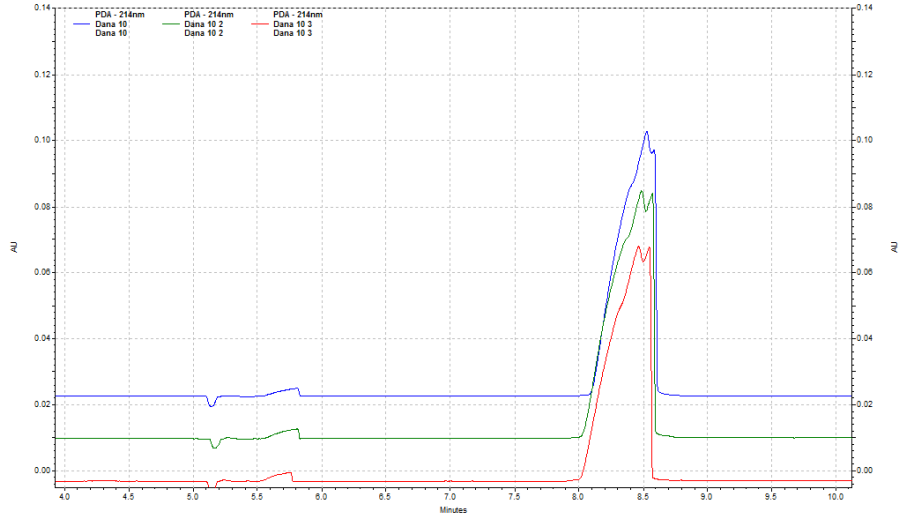


(c) Sample concentration 10,000 $mgL^{-1}$. Blue: 1st injection, green: 2nd injection and red: 3rd injection.

Figure 33: Electropherograms used for calibration of DTP using method 1.

# C Electropherograms of DTPI calibration in process water A

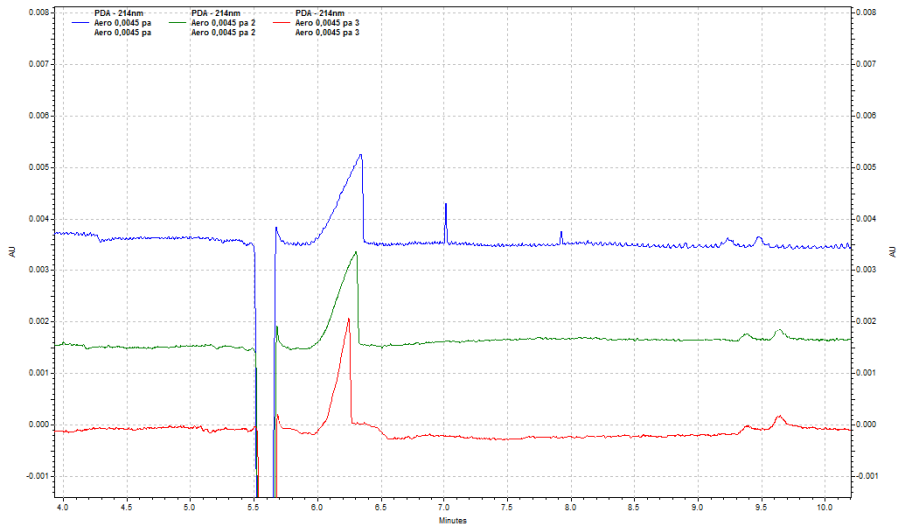


(a) Sample concentration 4.57 $mgL^{-1}$. Blue: 1st injection, green: 2nd injection and red: 3rd injection.

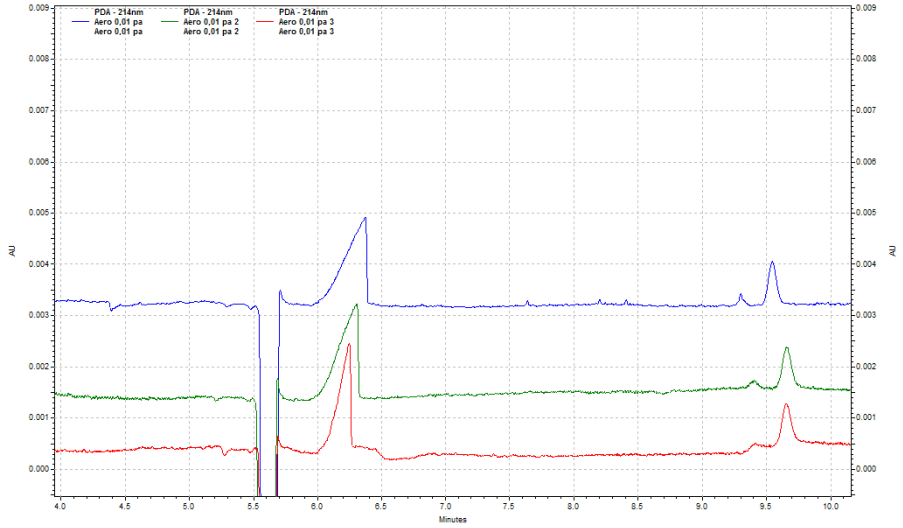


(b) Sample concentration 13. $mgL^{-1}$. Blue: 1st injection, green: 2nd injection and red: 3rd injection.

Figure 34: Electropherograms used for calibration of DTPI using method 1.

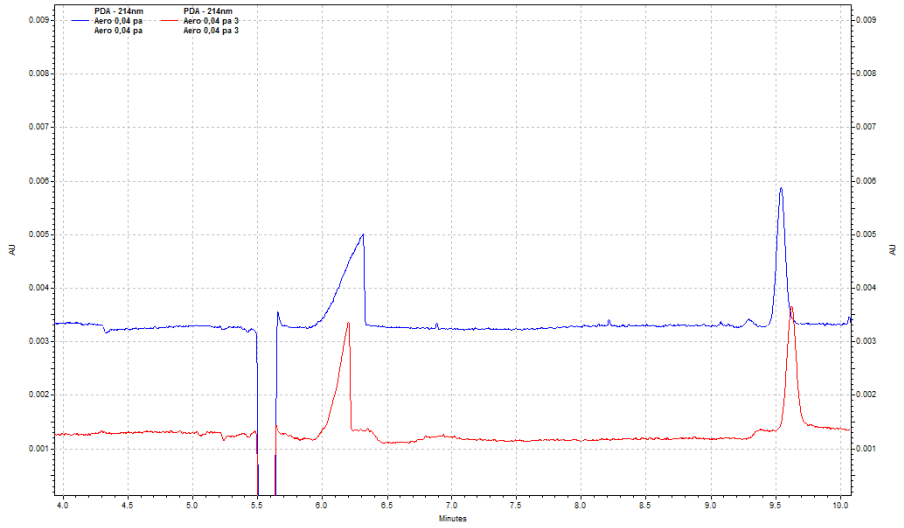


(a) Sample concentration 41.2 $mgL^{-1}$. Blue: 1st injection, green: 2nd injection and red: 3rd injection.

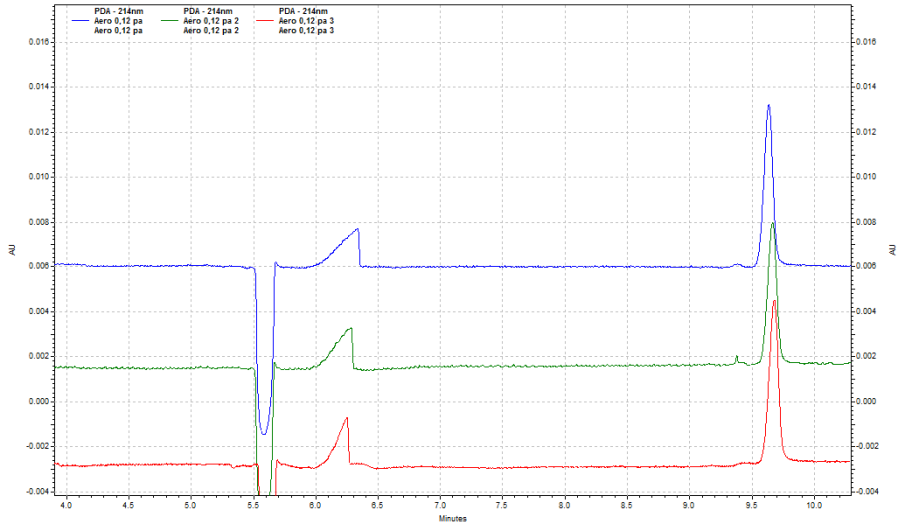


(b) Sample concentration 123.5 $mgL^{-1}$. Blue: 1st injection, green: 2nd injection and red: 3rd injection.

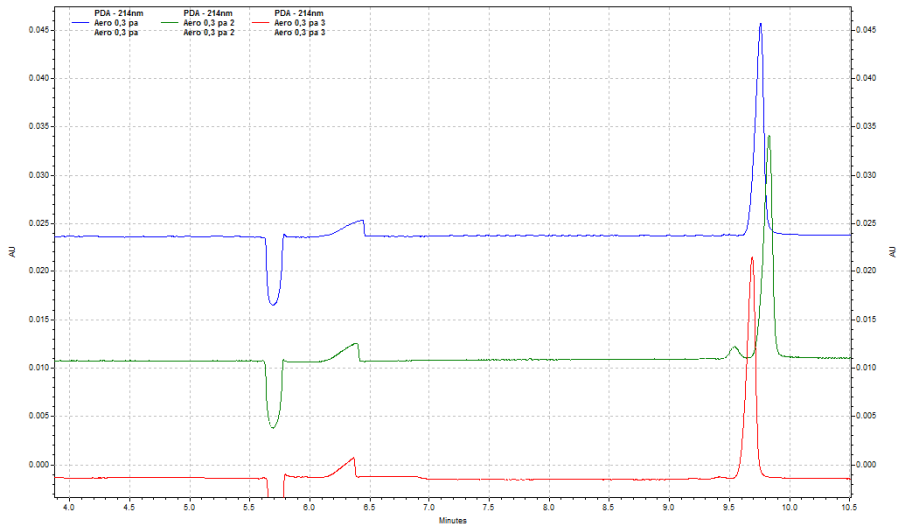


(c) Sample concentration 370.4 $mgL^{-1}$. Blue: 1st injection, green: 2nd injection and red: 3rd injection.

Figure 35: Electropherograms used for calibration of DTPI using method 1.

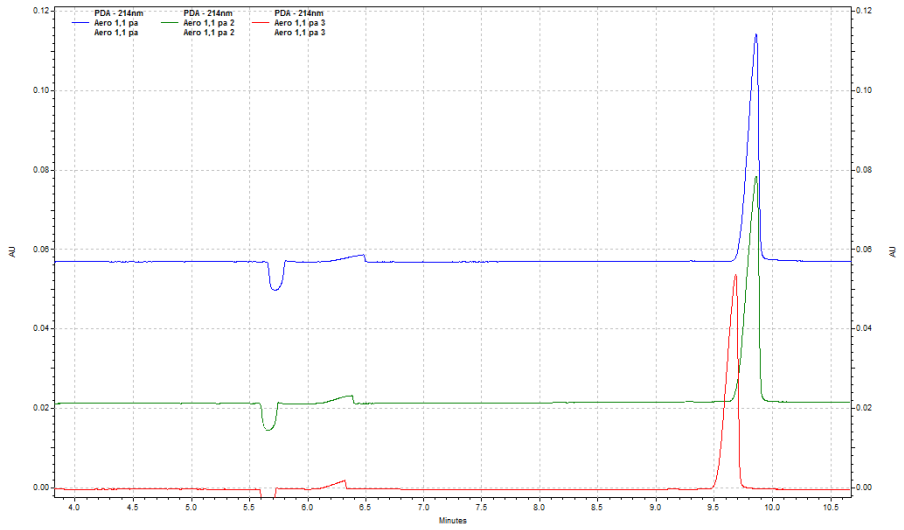


(a) Sample concentration 1,110.0 $mgL^{-1}$. Blue: 1st injection, green: 2nd injection and red: 3rd injection.

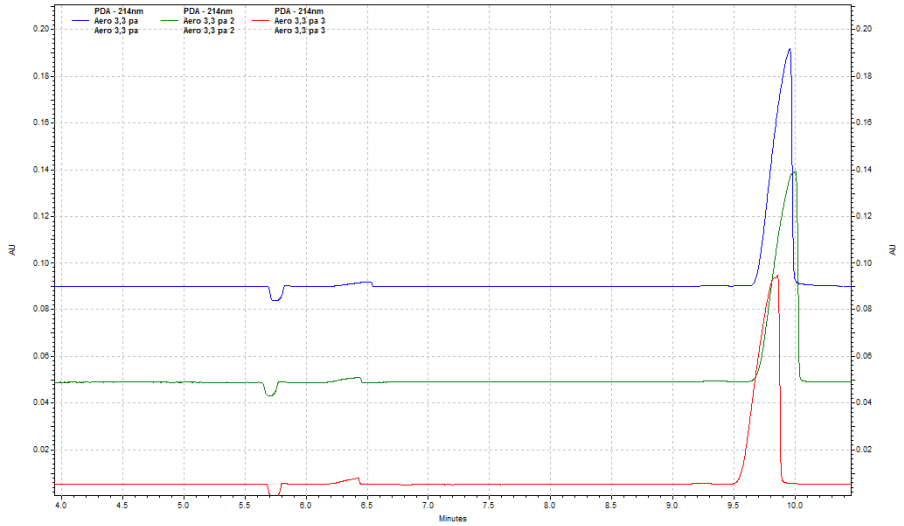


(b) Sample concentration 3,330.0 $mgL^{-1}$. Blue: 1st injection, green: 2nd injection and red: 3rd injection.

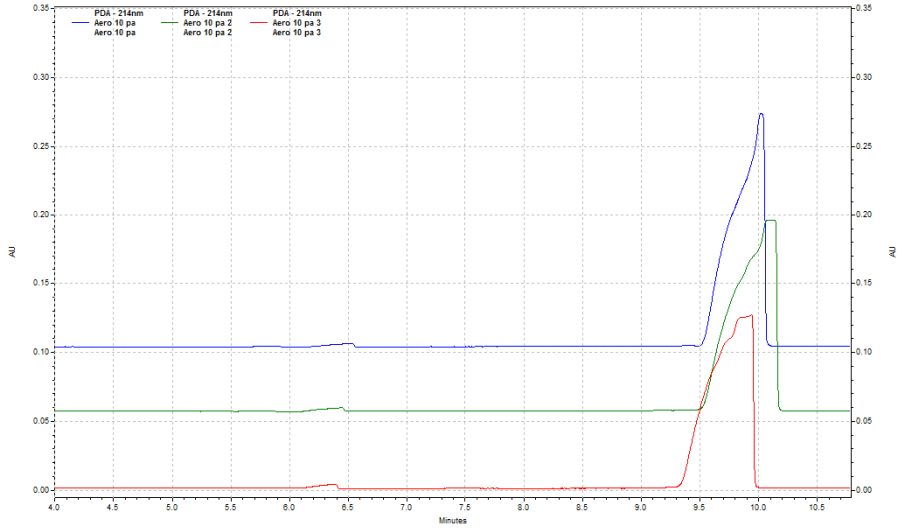


(c) Sample concentration 10,000 $mgL^{-1}$. Blue: 1st injection, green: 2nd injection and red: 3rd injection.

Figure 36: Electropherograms used for calibration of DTPI using method 1.

# D Electropherograms of DTP calibration in process water A

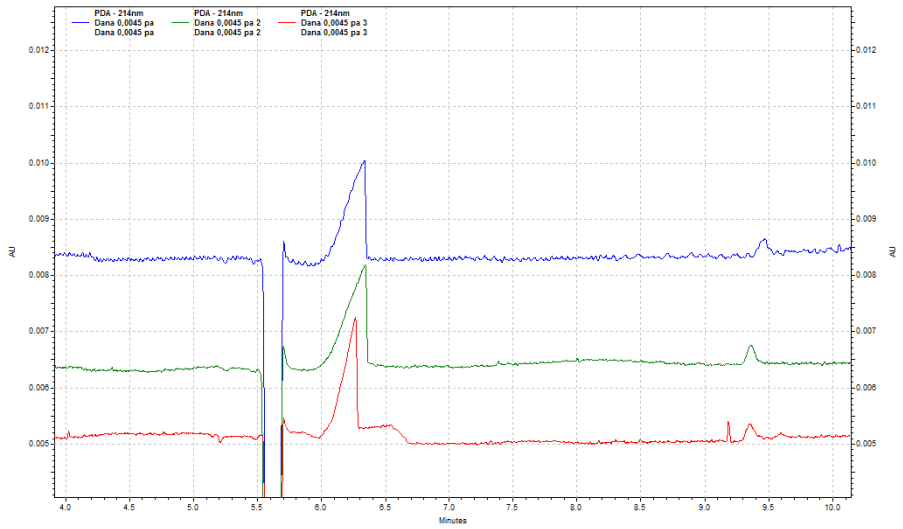


(a) Sample concentration 4.57 $mgL^{-1}$. Blue: 1st injection, green: 2nd injection and red: 3rd injection.

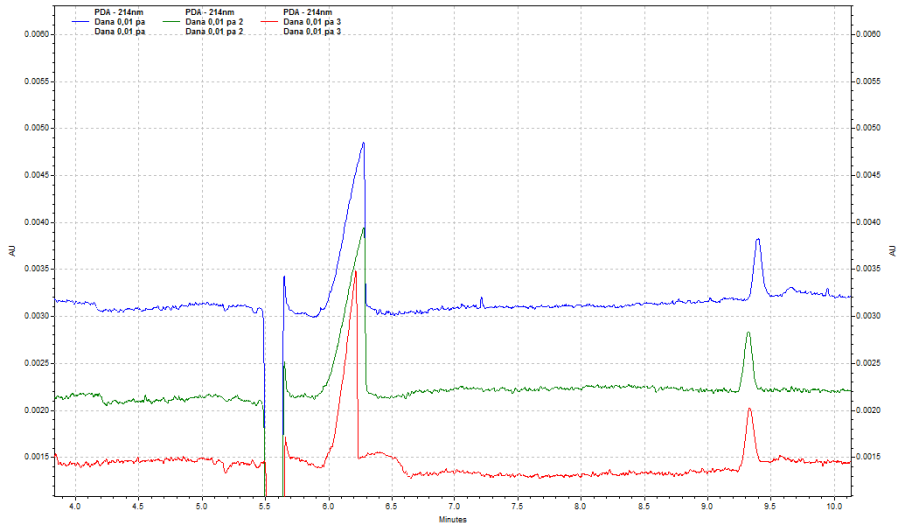


(b) Sample concentration 13.7 $mgL^{-1}$. Blue: 1st injection, green: 2nd injection and red: 3rd injection.

Figure 37: Electropherograms used for calibration of DTP using method 1.

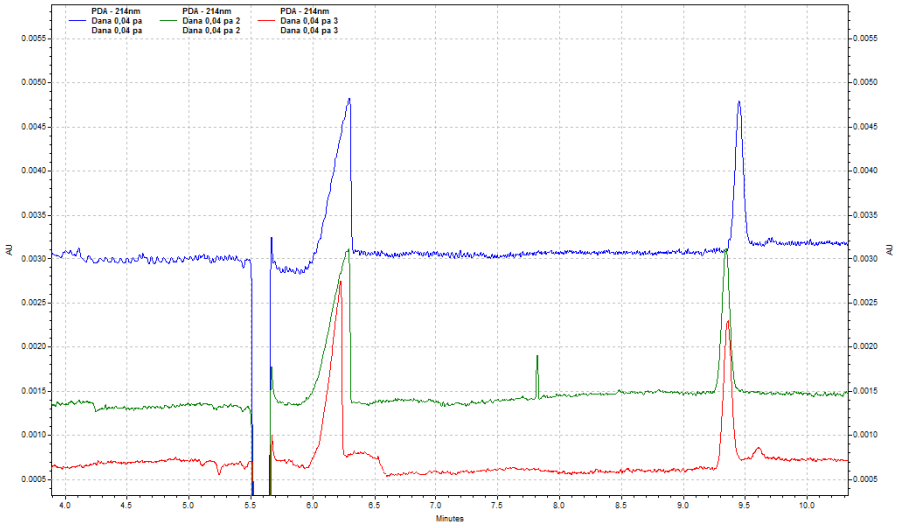


(a) Sample concentration 41.2 $mgL^{-1}$. Blue: 1st injection, green: 2nd injection and red: 3rd injection.

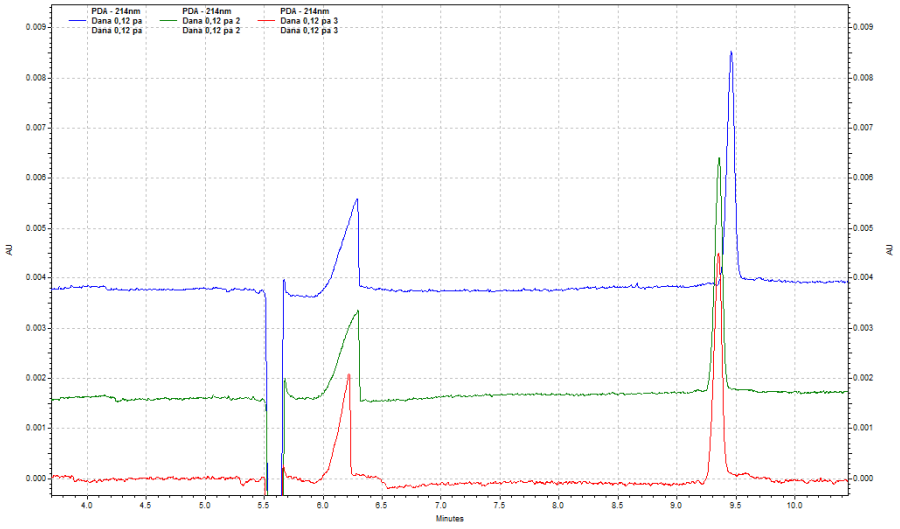


(b) Sample concentration 123.5 $mgL^{-1}$. Blue: 1st injection, green: 2nd injection and red: 3rd injection.

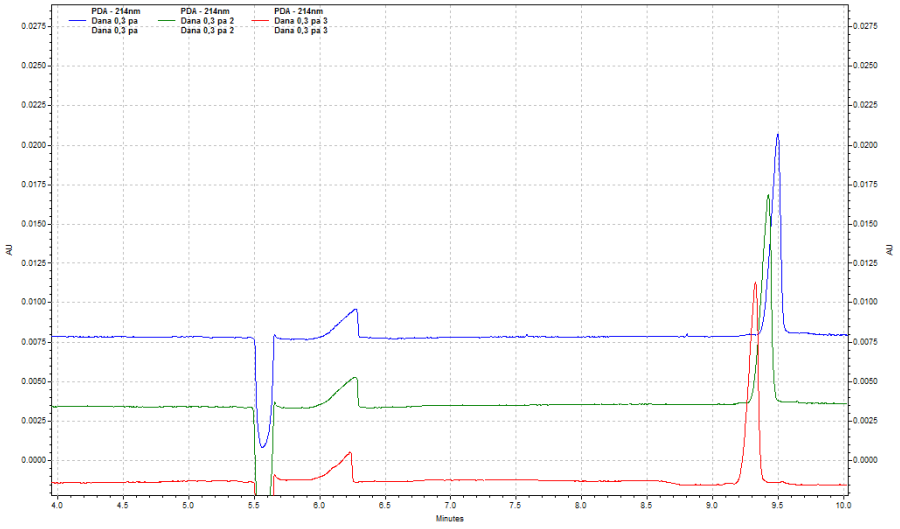


(c) Sample concentration 370.4 $mgL^{-1}$. Blue: 1st injection, green: 2nd injection and red: 3rd injection.

Figure 38: Electropherograms used for calibration of DTP using method 1.

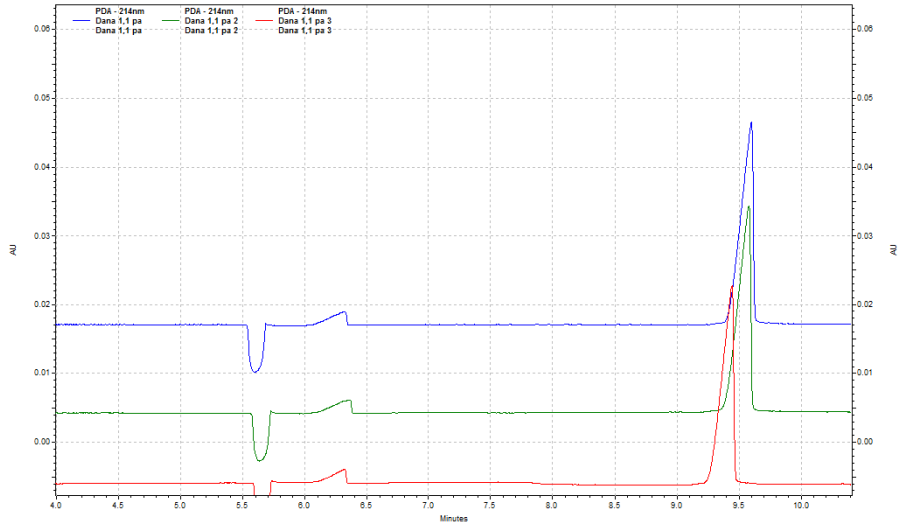


(a) Sample concentration 1,110.0 $mgL^{-1}$. Blue: 1st injection, green: 2nd injection and red: 3rd injection.

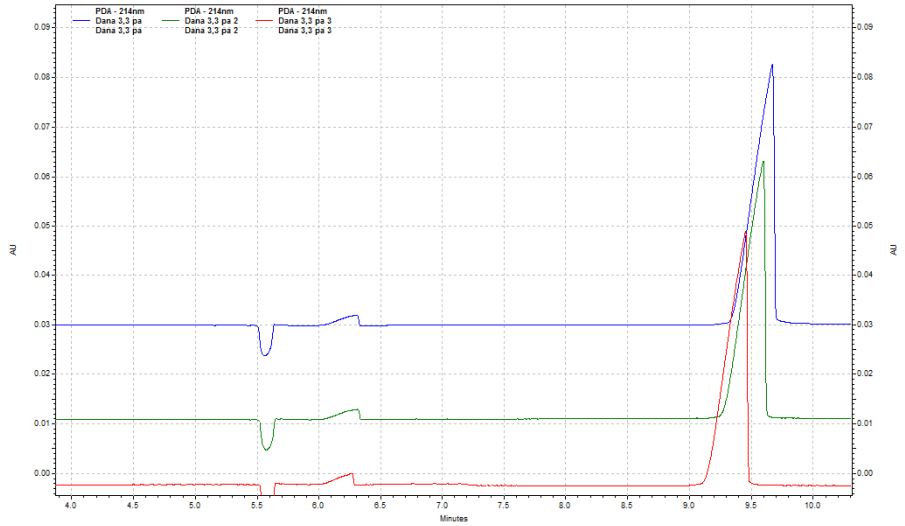


(b) Sample concentration 3,330.0 $mgL^{-1}$. Blue: 1st injection, green: 2nd injection and red: 3rd injection.

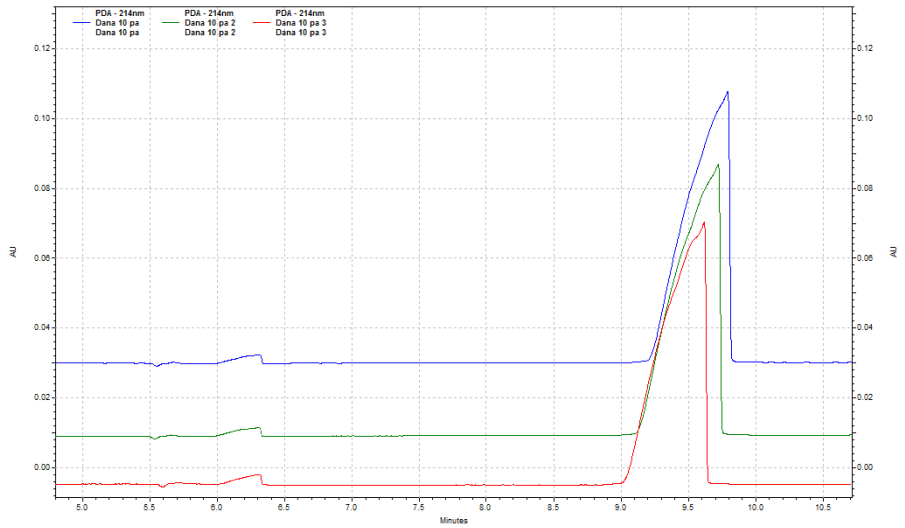


(c) Sample concentration 10,000 $mgL^{-1}$. Blue: 1st injection, green: 2nd injection and red: 3rd injection.

Figure 39: Electropherograms used for calibration of DTP using method 1.

# E Electropherograms of DTPI calibration in process water B

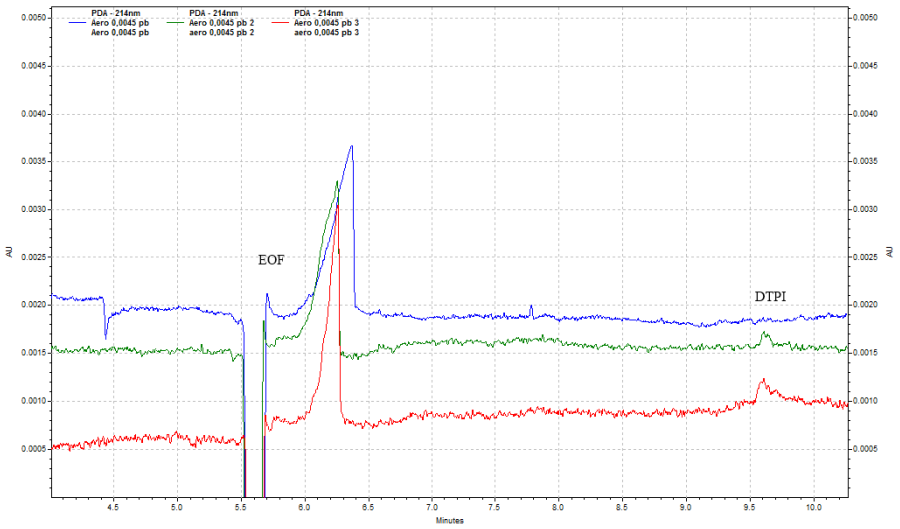


(a) Sample concentration 4.57 $mgL^{-1}$. Blue: 1st injection, green: 2nd injection and red: 3rd injection.

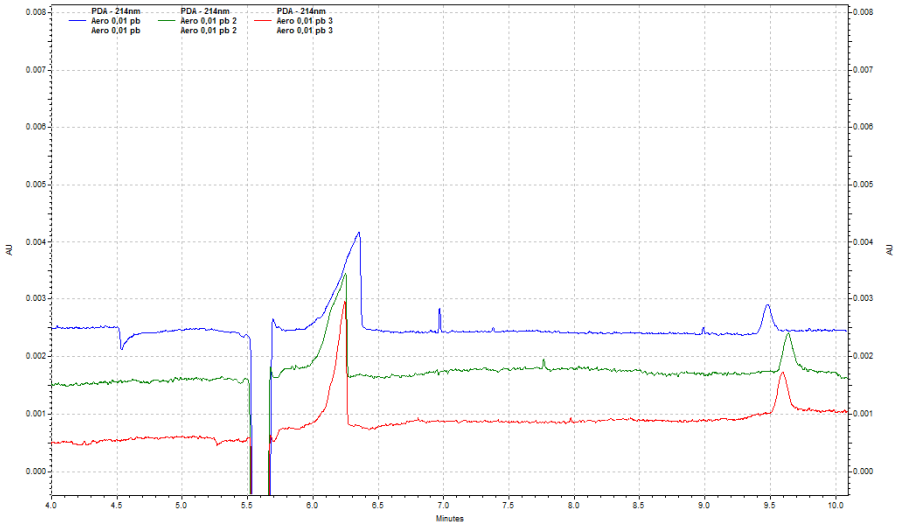


(b) Sample concentration 13.7 $mgL^{-1}$. Blue: 1st injection, green: 2nd injection and red: 3rd injection.

Figure 40: Electropherograms used for calibration of DTPI using method 1.

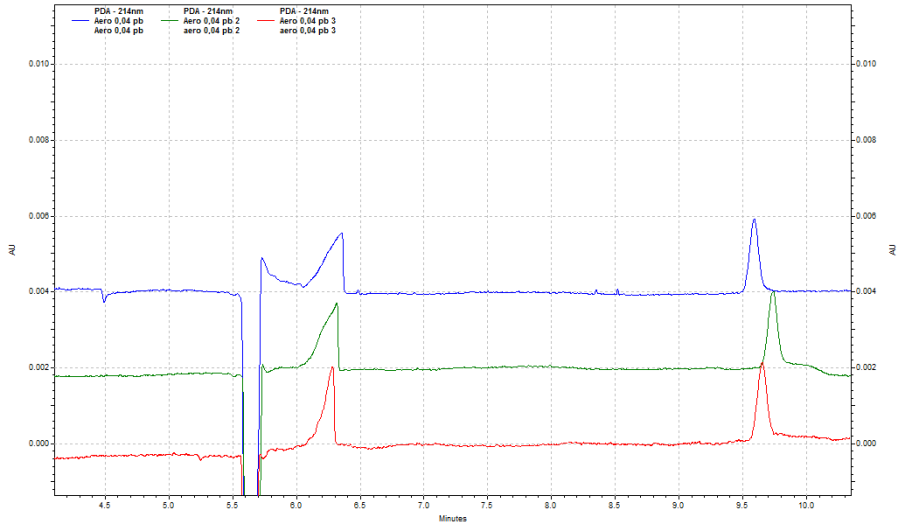


(a) Sample concentration 41.2 $mgL^{-1}$. Blue: 1st injection, green: 2nd injection and red: 3rd injection.

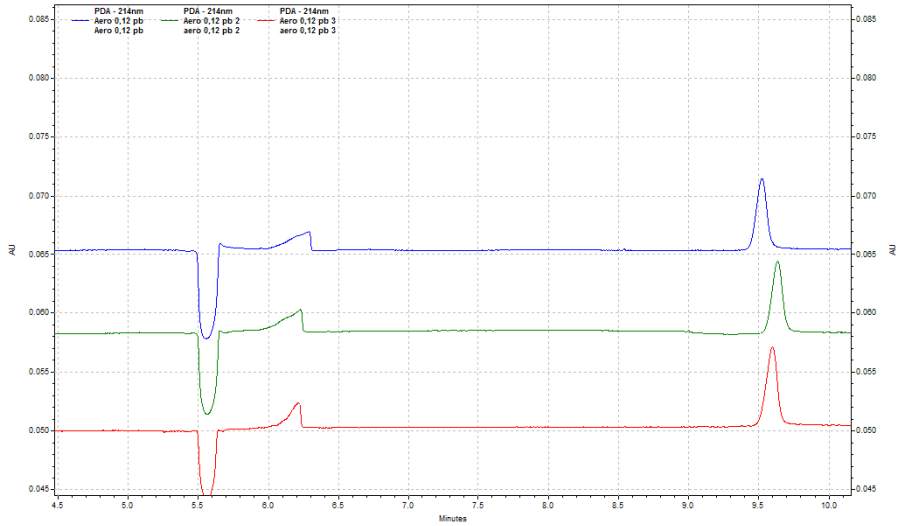


(b) Sample concentration 123.5 $mgL^{-1}$. Blue: 1st injection, green: 2nd injection and red: 3rd injection.

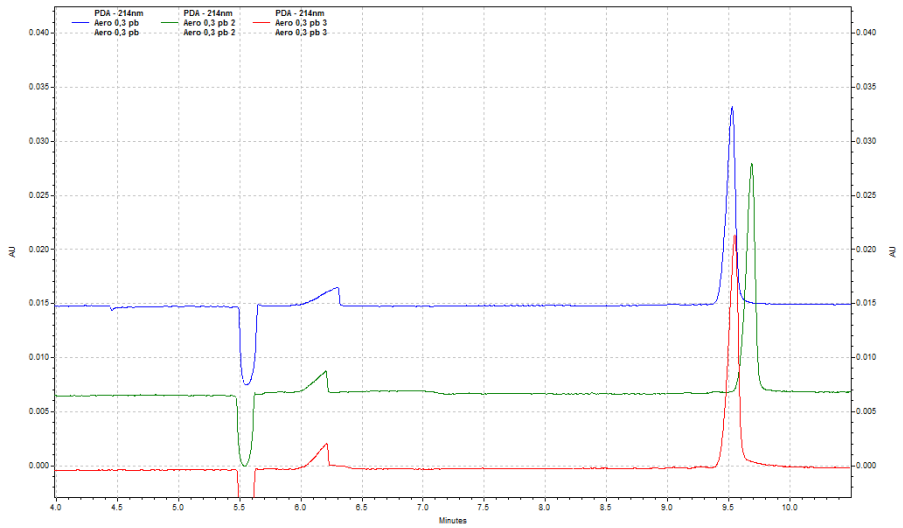


(c) Sample concentration 370.4 $mgL^{-1}$. Blue: 1st injection, green: 2nd injection and red: 3rd injection.

Figure 41: Electropherograms used for calibration of DTPI using method 1.

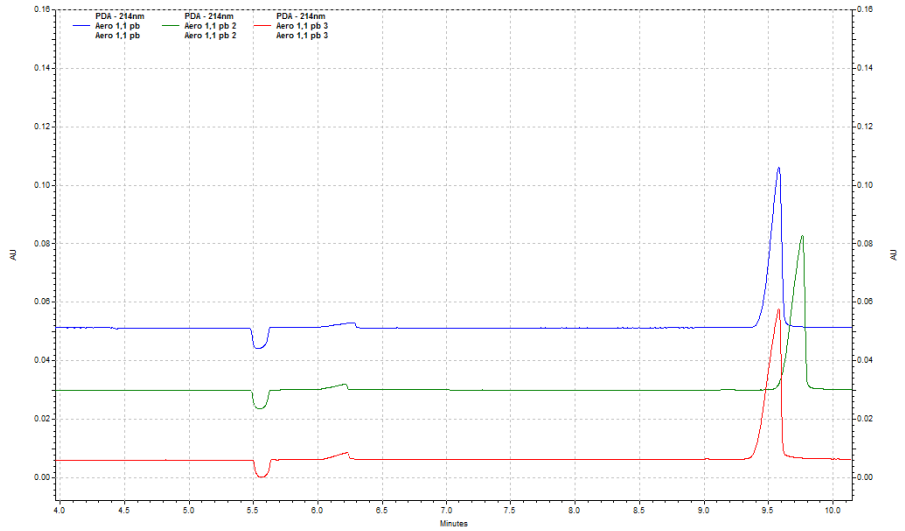


(a) Sample concentration 1,110.0 $mgL^{-1}$. Blue: 1st injection, green: 2nd injection and red: 3rd injection.

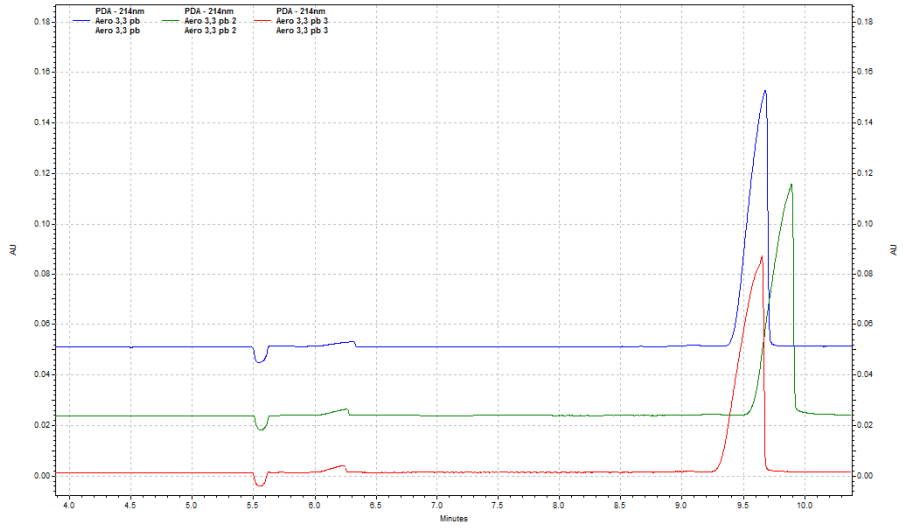


(b) Sample concentration 3,330.0 $mgL^{-1}$. Blue: 1st injection, green: 2nd injection and red: 3rd injection.

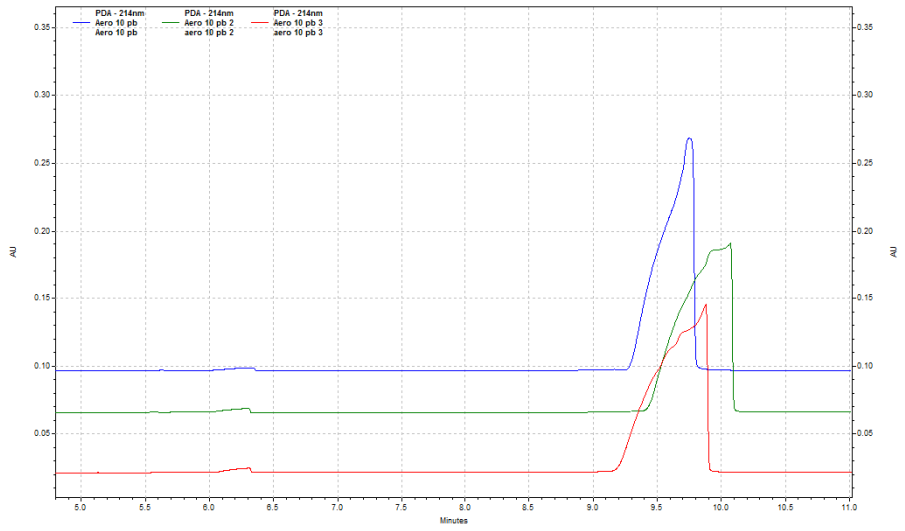


(c) Sample concentration 10,000 $mgL^{-1}$. Blue: 1st injection, green: 2nd injection and red: 3rd injection.

Figure 42: Electropherograms used for calibration of DTPI using method 1.

# F Electropherograms of DTP calibration in process water B

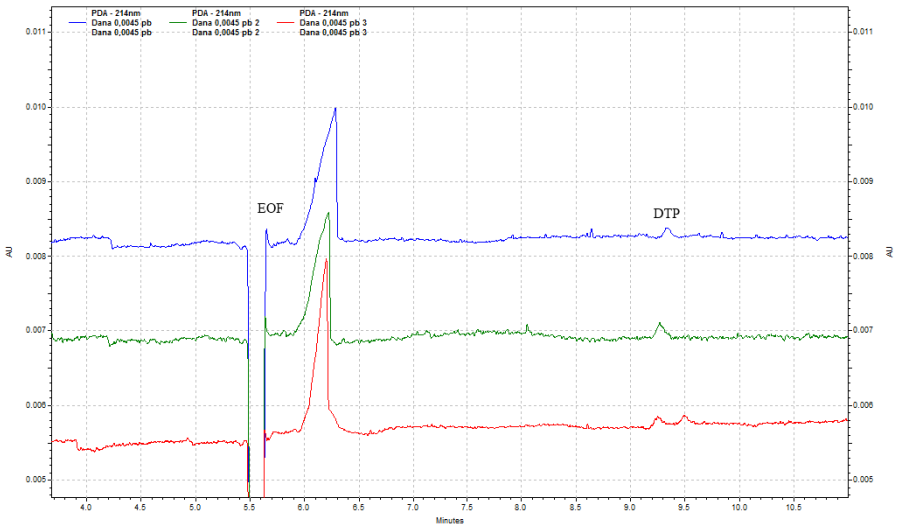


(a) Sample concentration 4.57 $mgL^{-1}$. Blue: 1st injection, green: 2nd injection and red: 3rd injection.

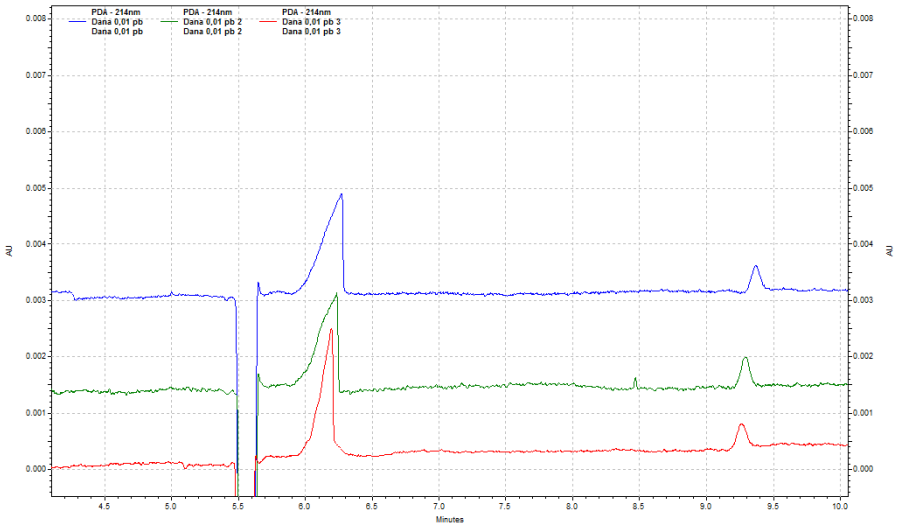


(b) Sample concentration 13.7 $mgL^{-1}$. Blue: 1st injection, green: 2nd injection and red: 3rd injection.

Figure 43: Electropherograms used for calibration of DTP using method 1.

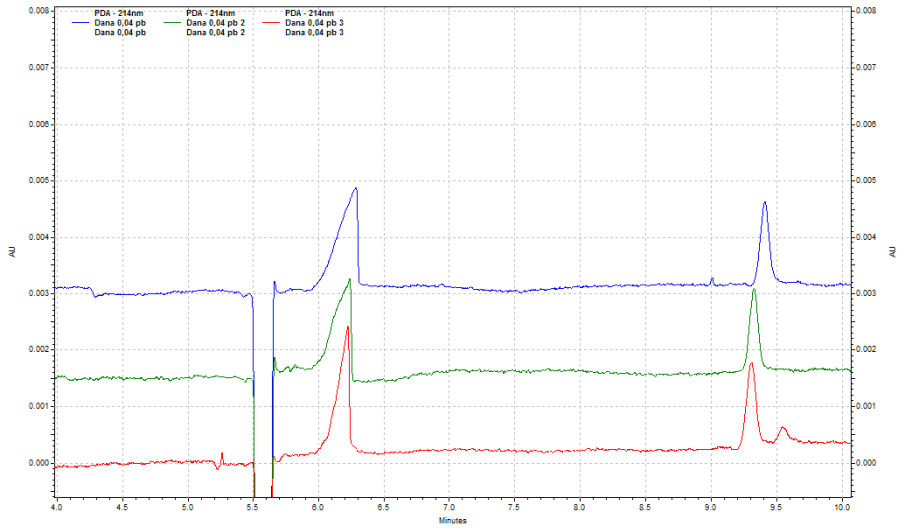


(a) Sample concentration 41.2 $mgL^{-1}$. Blue: 1st injection, green: 2nd injection and red: 3rd injection.

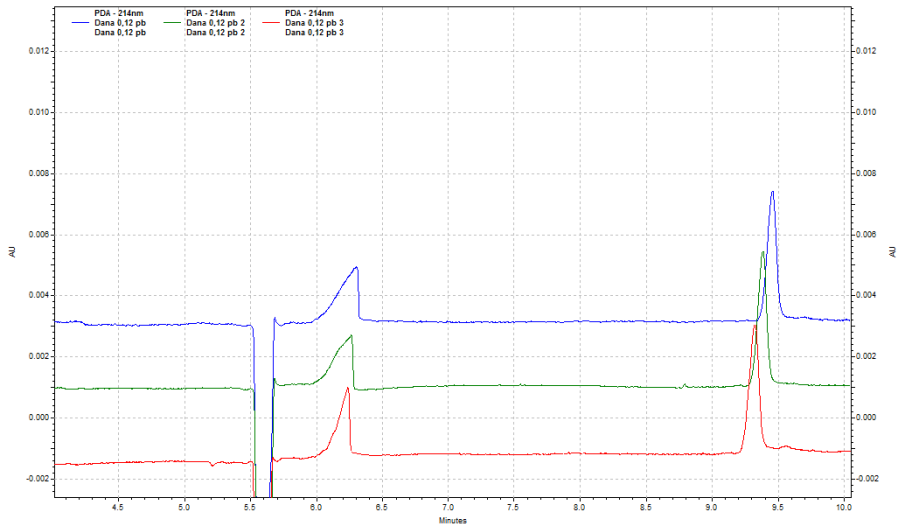


(b) Sample concentration 123.5 $mgL^{-1}$. Blue: 1st injection, green: 2nd injection and red: 3rd injection.

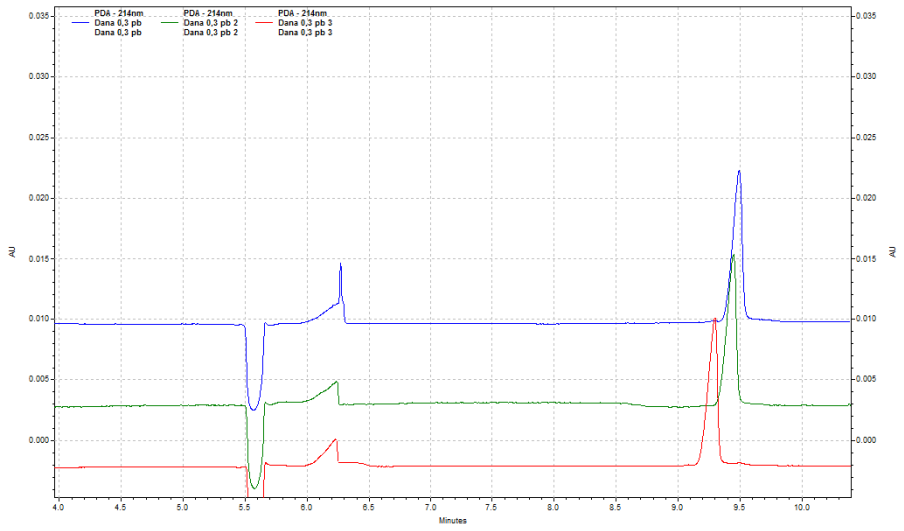


(c) Sample concentration 370.4 $mgL^{-1}$. Blue: 1st injection, green: 2nd injection and red: 3rd injection.

Figure 44: Electropherograms used for calibration of DTP using method 1.

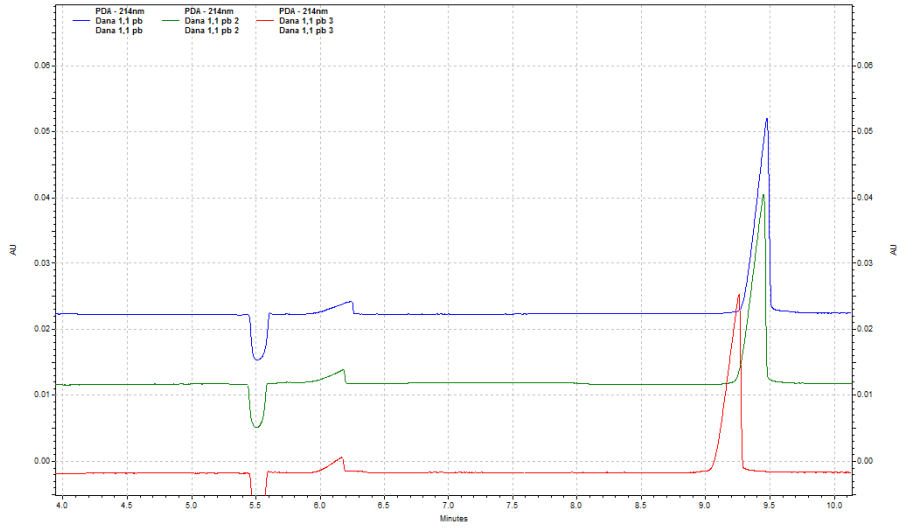


(a) Sample concentration 1,110.0 $mgL^{-1}$. Blue: 1st injection, green: 2nd injection and red: 3rd injection.

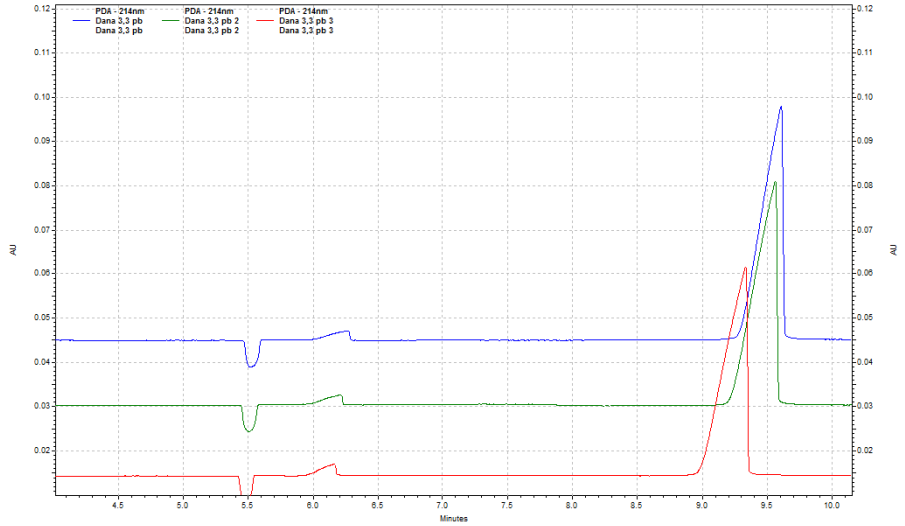


(b) Sample concentration 3,330.0 $mgL^{-1}$. Blue: 1st injection, green: 2nd injection and red: 3rd injection.

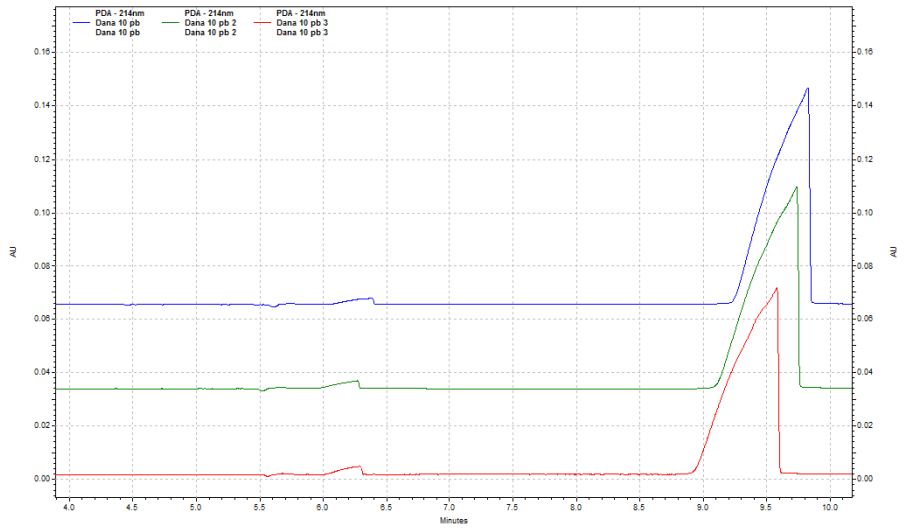


(c) Sample concentration 10,000 $mgL^{-1}$. Blue: 1st injection, green: 2nd injection and red: 3rd injection.

Figure 45: Electropherograms used for calibration of DTP using method 1.

# G Electropherograms of EX calibration in pure water

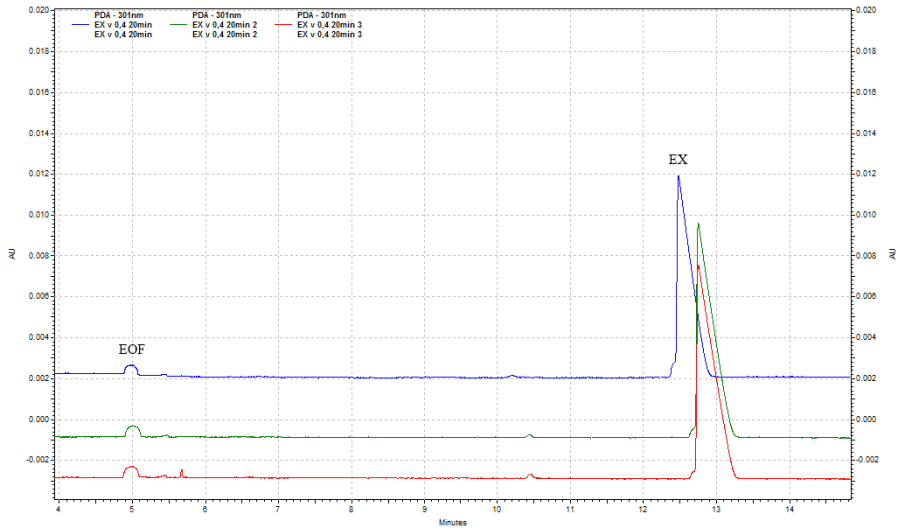


(a) Sample concentration 0.41 $mgL^{-1}$. Blue: 1st injection, green: 2nd injection and red: 3rd injection.

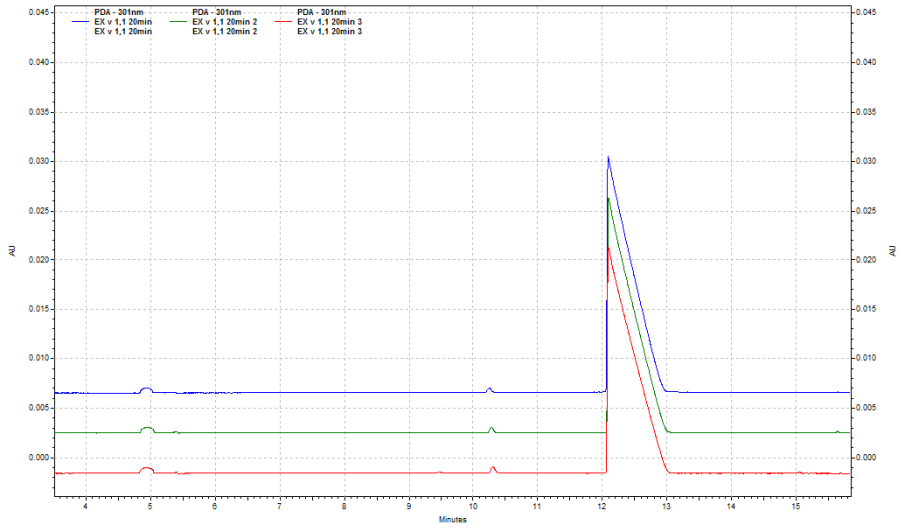


(b) Sample concentration 1.23 $mgL^{-1}$. Blue: 1st injection, green: 2nd injection and red: 3rd injection.

Figure 46: Electropherograms used for calibration of EX using method 2.

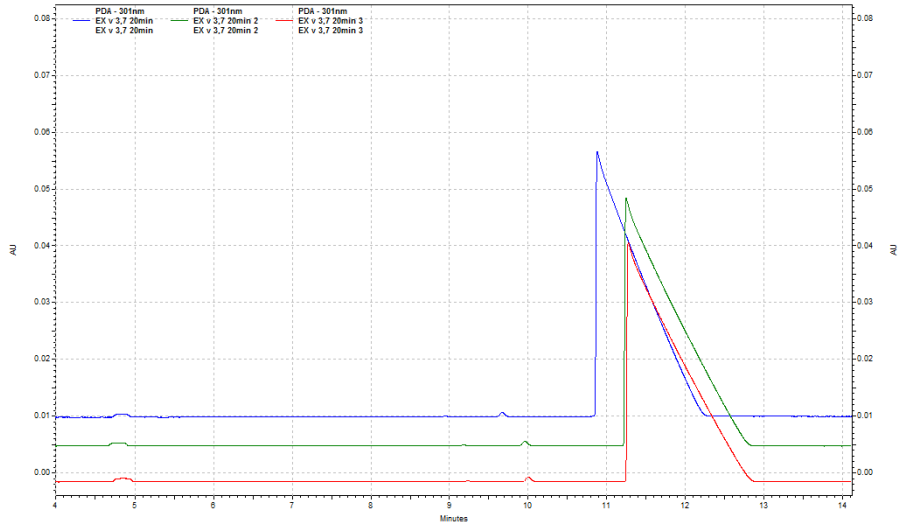


(a) Sample concentration 3.70 $mgL^{-1}$. Blue: 1st injection, green: 2nd injection and red: 3rd injection.

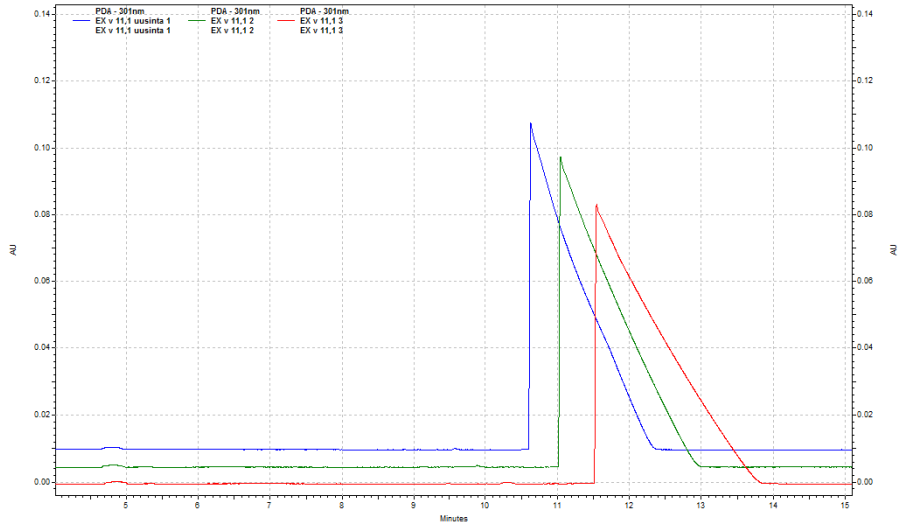


(b) Sample concentration 11.11 $mgL^{-1}$. Blue: 1st injection, green: 2nd injection and red: 3rd injection.

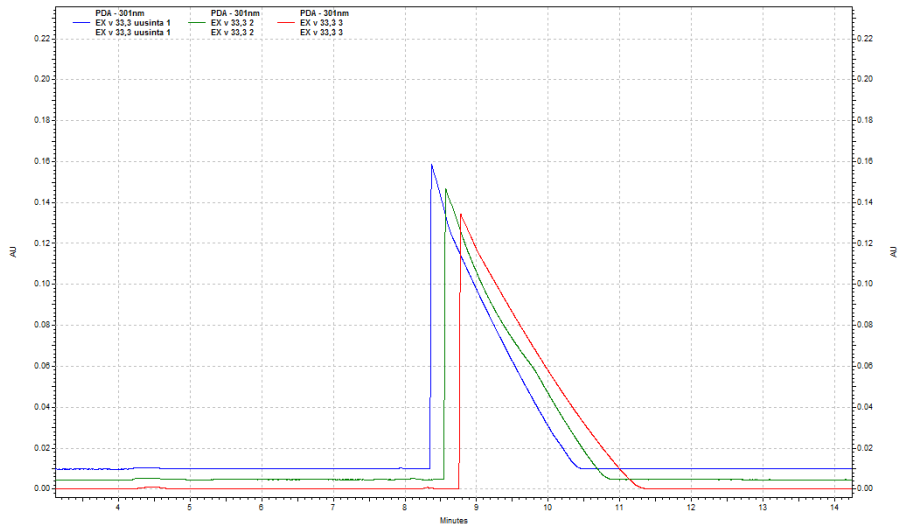


(c) Sample concentration 33.33 $mgL^{-1}$. Blue: 1st injection, green: 2nd injection and red: 3rd injection.

Figure 47: Electropherograms used for calibration of EX using method 2.

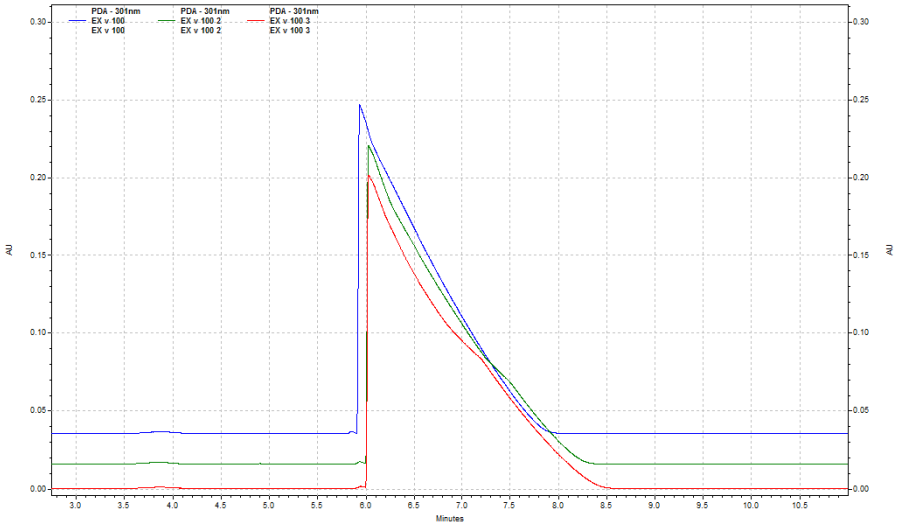


(a) Sample concentration 100 $mgL^{-1}$. Blue: 1st injection, green: 2nd injection and red: 3rd injection.

Figure 48: Electropherograms used for calibration of EX using method 2.

# H Electropherograms of IBX calibration in pure water

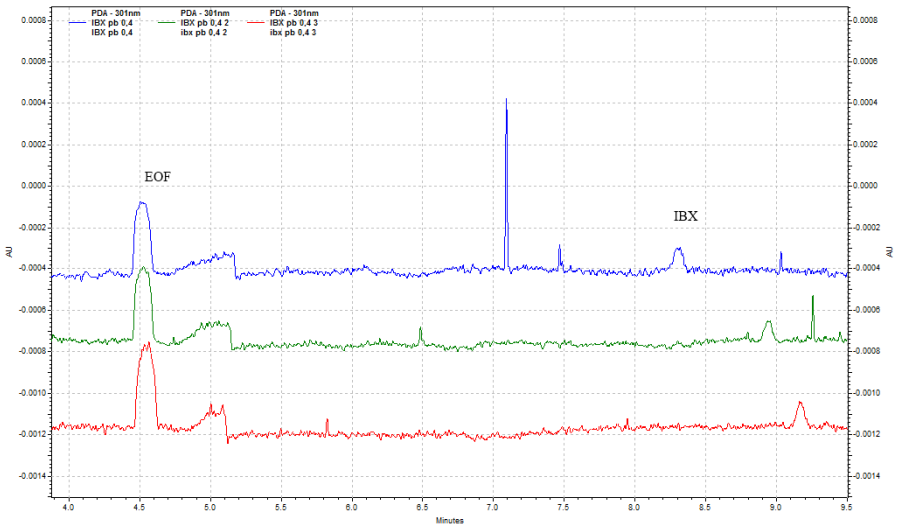


(a) Sample concentration 0.41 $mgL^{-1}$. Blue: 1st injection, green: 2nd injection and red: 3rd injection.

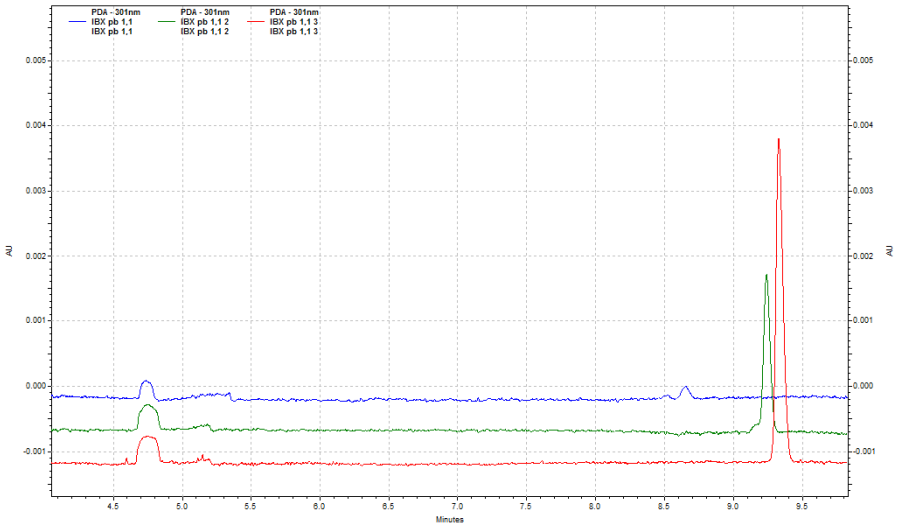


(b) Sample concentration 1.23 $mgL^{-1}$. Blue: 1st injection, green: 2nd injection and red: 3rd injection.

Figure 49: Electropherograms used for calibration of IBX using method 2.

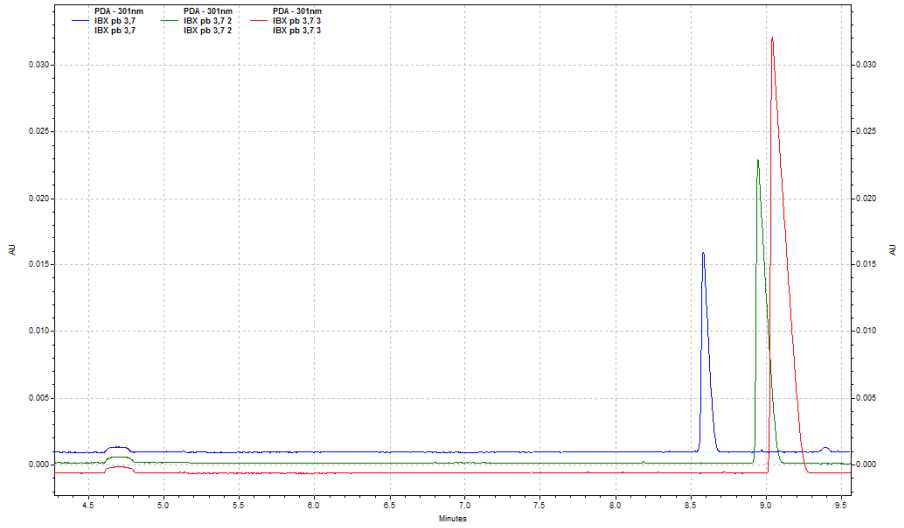


(a) Sample concentration 3.70 mgL$^{-1}$. Blue: 1st injection, green: 2nd injection and red: 3rd injection.

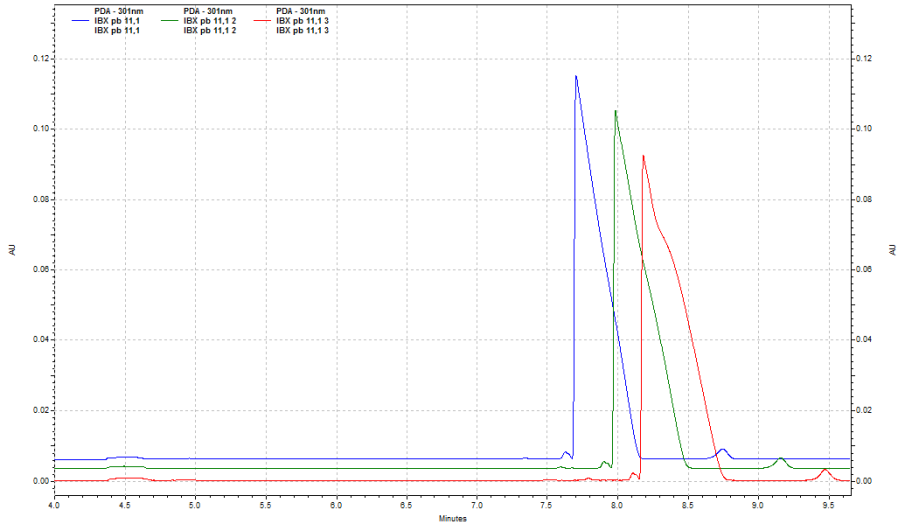


(b) Sample concentration 11.11 mgL$^{-1}$. Blue: 1st injection, green: 2nd injection and red: 3rd injection.

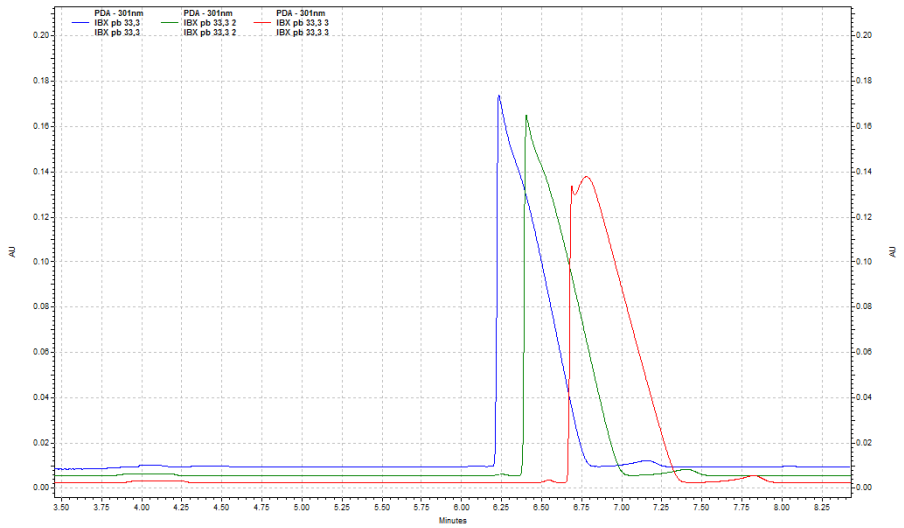


(c) Sample concentration 33.33 mgL$^{-1}$. Blue: 1st injection, green: 2nd injection and red: 3rd injection.

Figure 50: Electropherograms used for calibration of IBX using method 2.

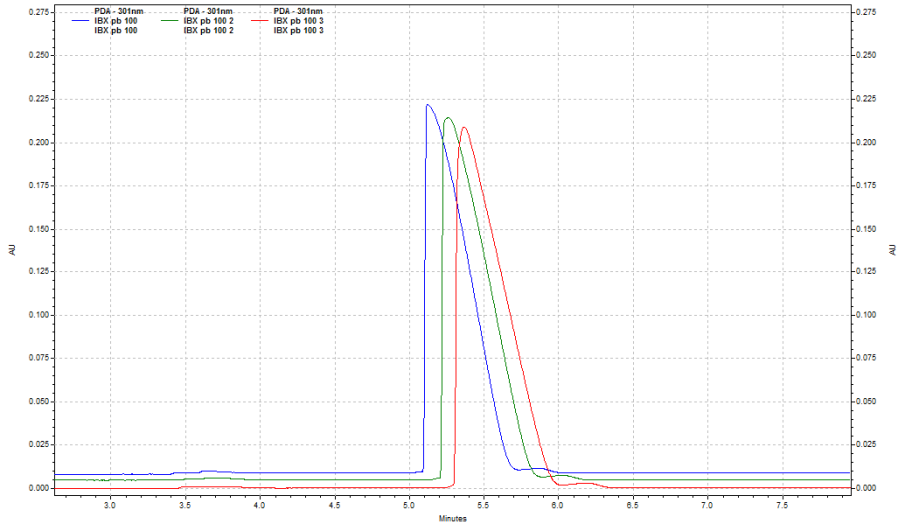


(a) Sample concentration 100 $mgL^{-1}$. Blue: 1st injection, green: 2nd injection and red: 3rd injection.

Figure 51: Electropherograms used for calibration of IBX using method 2.

# I Electropherograms of EX calibration in process water B

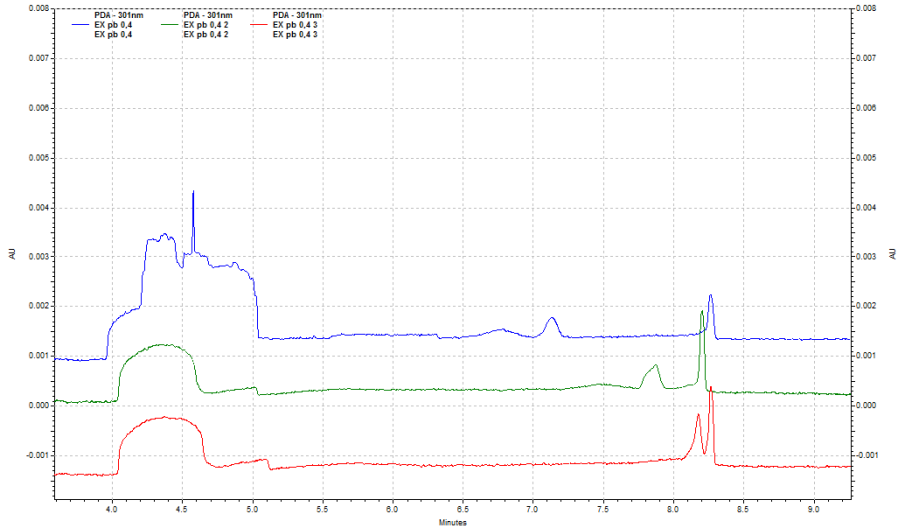


(a) Sample concentration 0.41 $mgL^{-1}$. Blue: 1st injection, green: 2nd injection and red: 3rd injection.

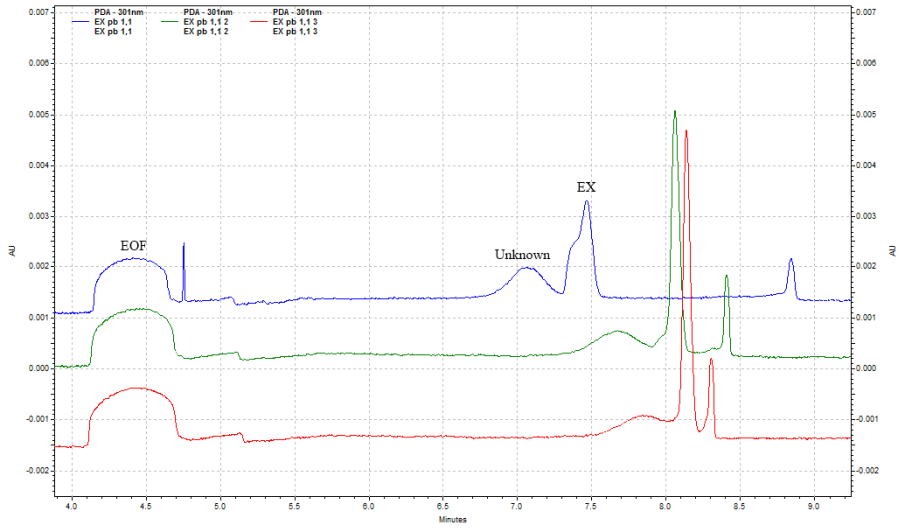


(b) Sample concentration 1.23 $mgL^{-1}$. Blue: 1st injection, green: 2nd injection and red: 3rd injection.

Figure 52: Electropherograms used for calibration of EX using method 2.

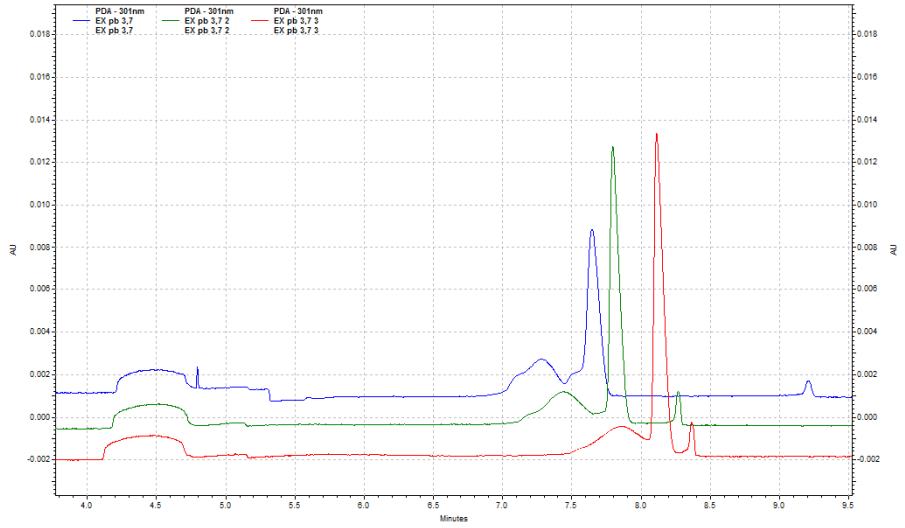


(a) Sample concentration 3.70 $mgL^{-1}$. Blue: 1st injection, green: 2nd injection and red: 3rd injection.

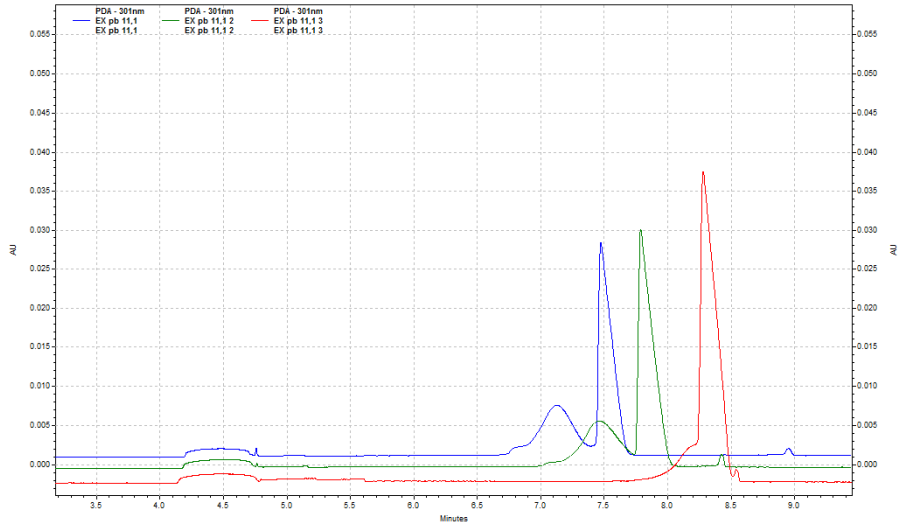


(b) Sample concentration 11.11 $mgL^{-1}$. Blue: 1st injection, green: 2nd injection and red: 3rd injection.

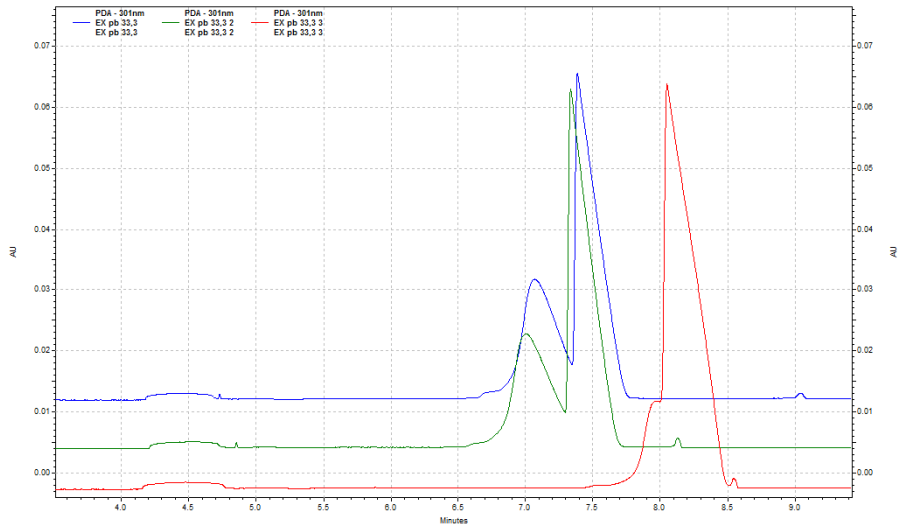


(c) Sample concentration 33.33 $mgL^{-1}$. Blue: 1st injection, green: 2nd injection and red: 3rd injection.

Figure 53: Electropherograms used for calibration of EX using method 2.

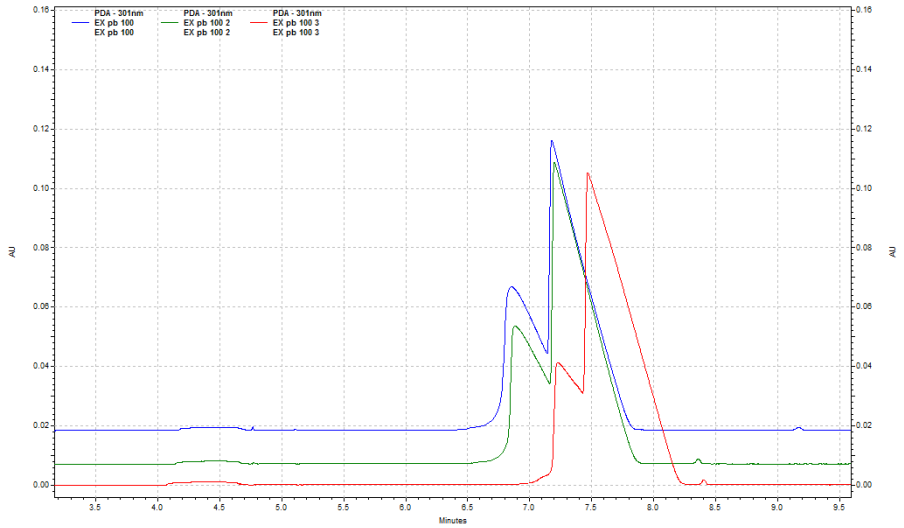


(a) Sample concentration 100 $mgL^{-1}$. Blue: 1st injection, green: 2nd injection and red: 3rd injection.

Figure 54: Electropherograms used for calibration of EX using method 2.

# J Electropherograms of IBX calibration in process water B

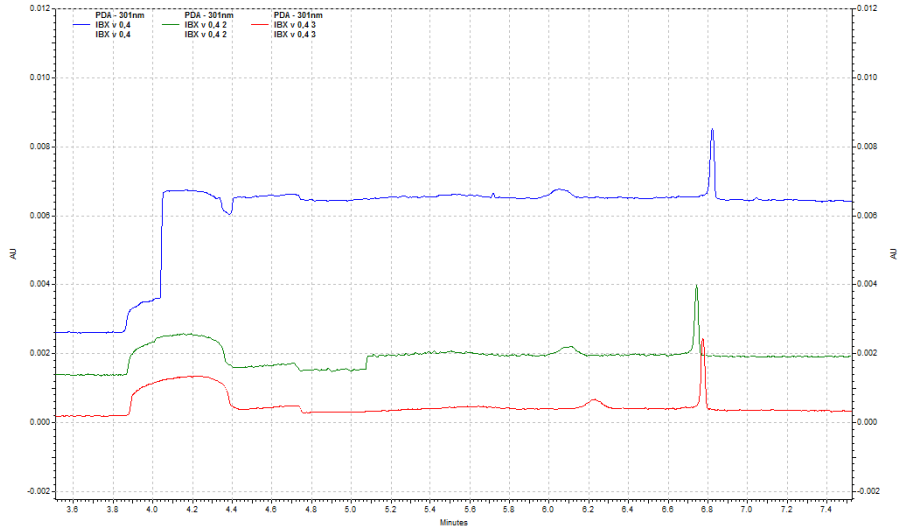


(a) Sample concentration 0.41 $mgL^{-1}$. Blue: 1st injection, green: 2nd injection and red: 3rd injection.

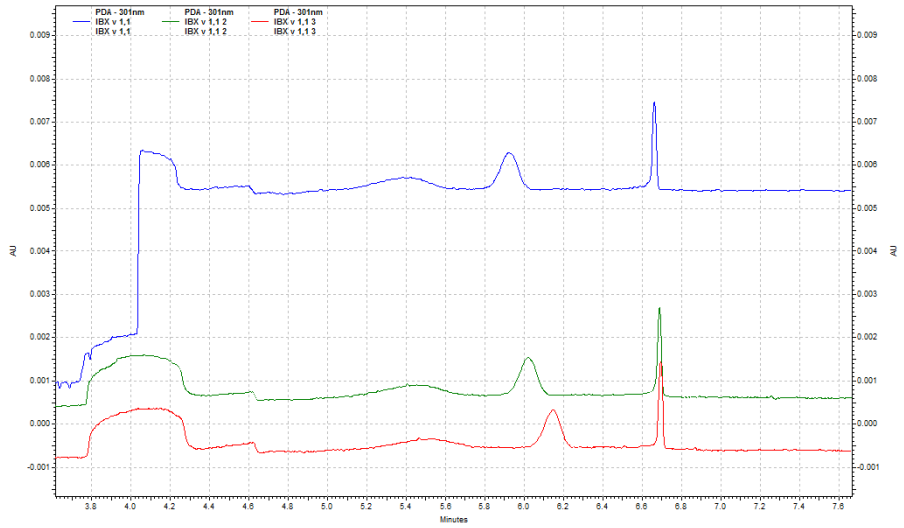


(b) Sample concentration 1.23 $mgL^{-1}$. Blue: 1st injection, green: 2nd injection and red: 3rd injection.

Figure 55: Electropherograms used for calibration of IBX using method 2.

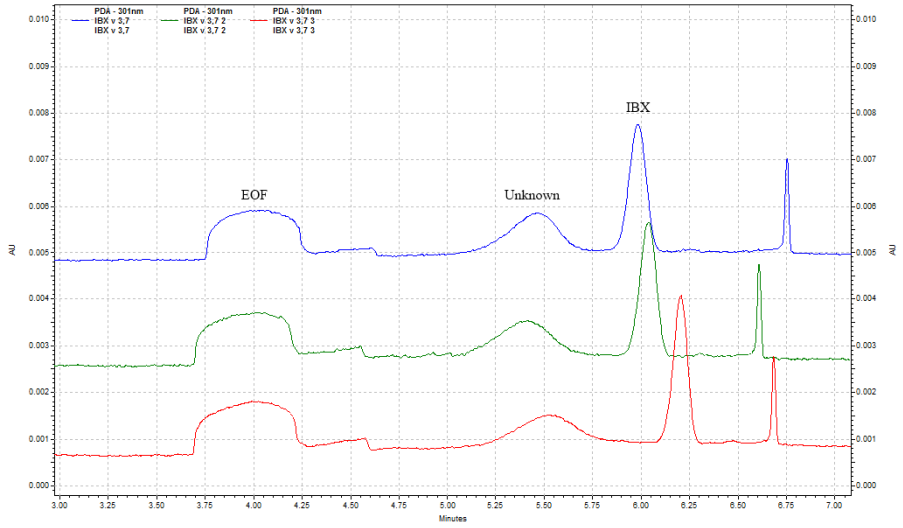


(a) Sample concentration 3.70 $mgL^{-1}$. Blue: 1st injection, green: 2nd injection and red: 3rd injection.

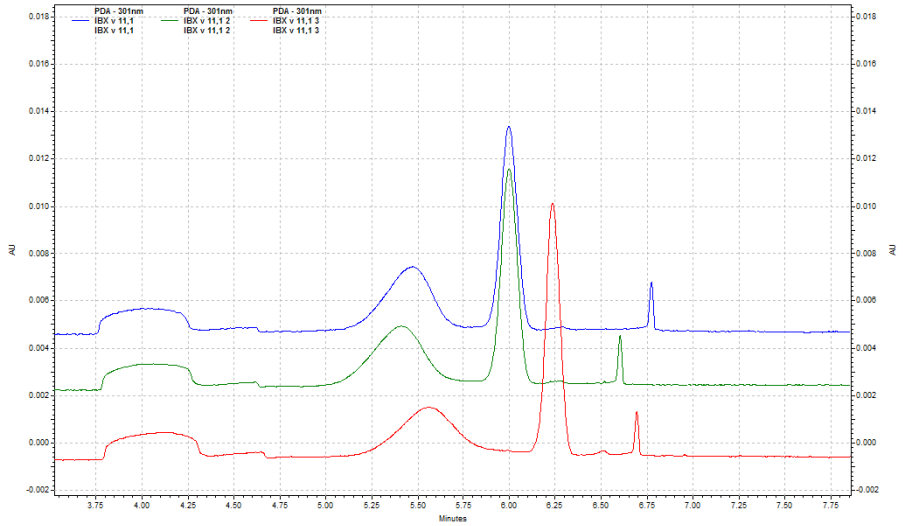


(b) Sample concentration 11.11 $mgL^{-1}$. Blue: 1st injection, green: 2nd injection and red: 3rd injection.

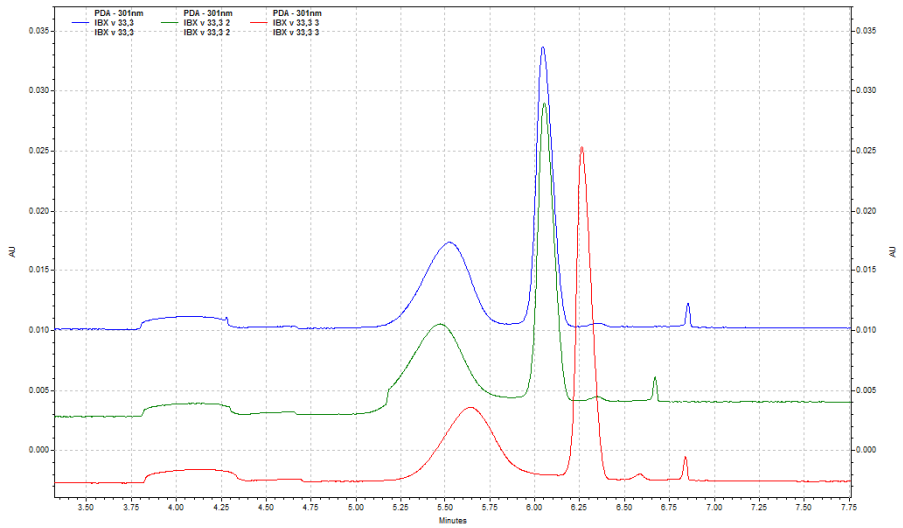


(c) Sample concentration 33.33 $mgL^{-1}$. Blue: 1st injection, green: 2nd injection and red: 3rd injection.

Figure 56: Electropherograms used for calibration of IBX using method 2.

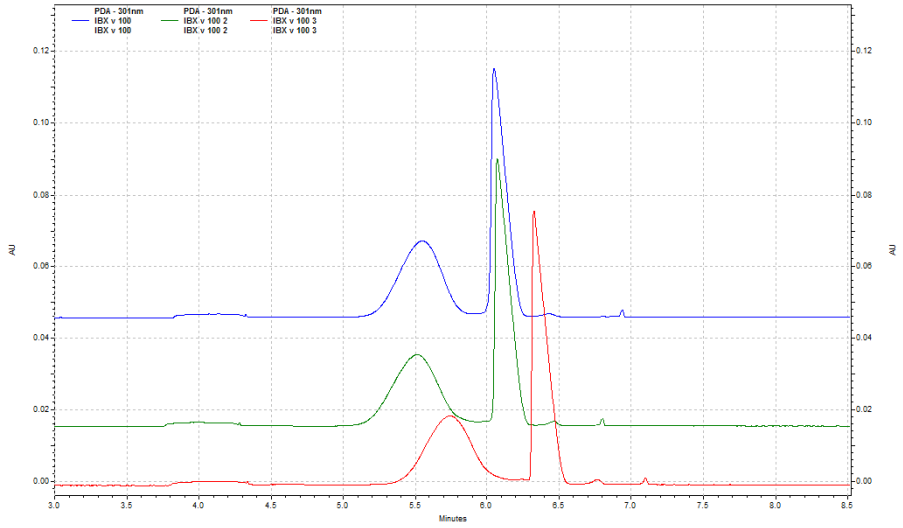


(a) Sample concentration 100 $mgL^{-1}$. Blue: 1st injection, green: 2nd injection and red: 3rd injection.

Figure 57: Electropherograms used for calibration of IBX using method 2.

# K Electropherograms from the measurements at Vammala gold concentrator

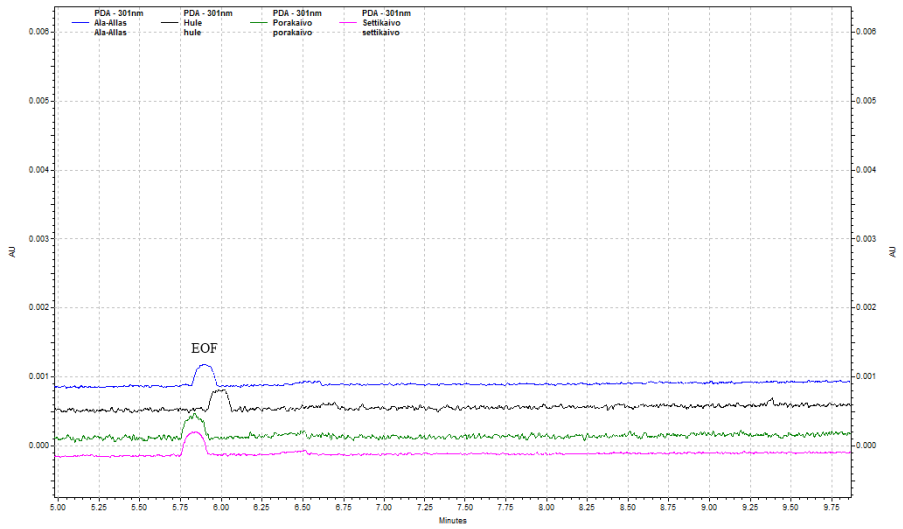


(a) Samples from the tailings bond (pink), fresh water well (green), overflow drain (black) and the second tailings bond (blue) analyzed using method 1.

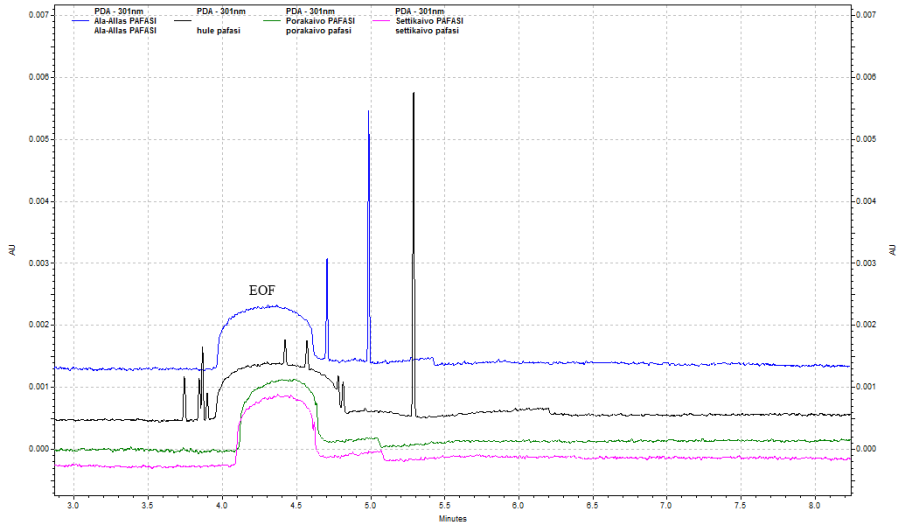


(b) Samples from the tailings bond (pink), fresh water well (green), overflow drain (black) and the second tailings bond (blue) analyzed using method 2.

Figure 58: Electropherograms of samples from the tailings bond (pink), fresh water well (green), overflow drain (black) and the second tailings bond (blue).

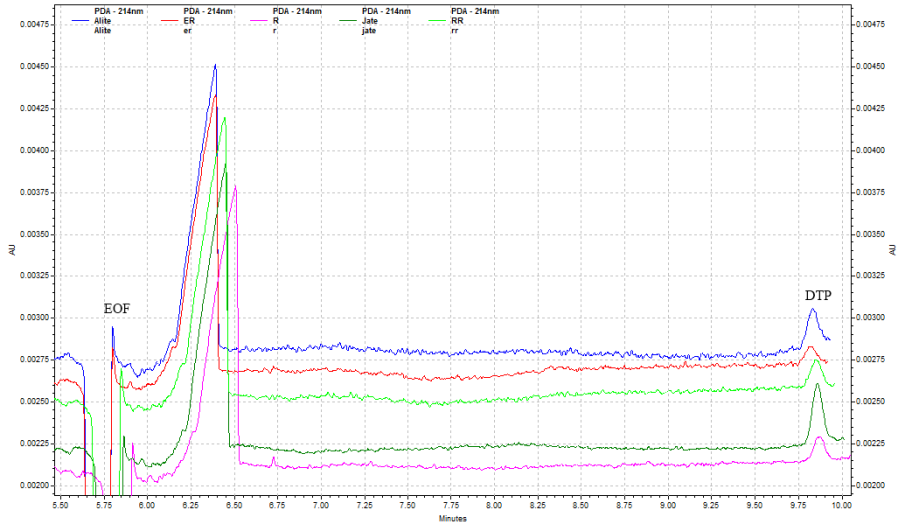


(a) Samples from cyclone underflow (blue), rougher flotation (red), concentrate (pink), tails (green) and scavenger flotation (light green).

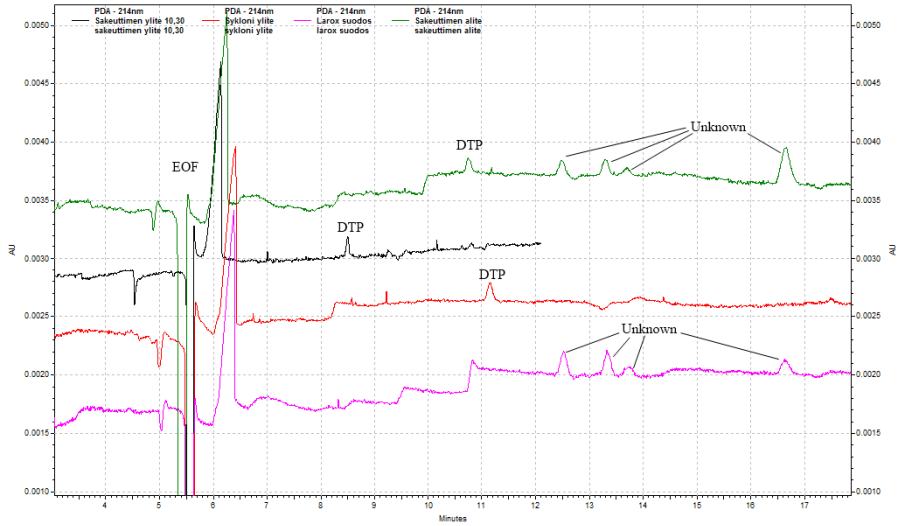


(b) Samples from thickener underflow (green), thickener overflow (black), cyclone overflow (red) and filtrate (pink).

Figure 59: Electropherograms of samples from the flotation process at Vammala. All samples analyzed using method 1.

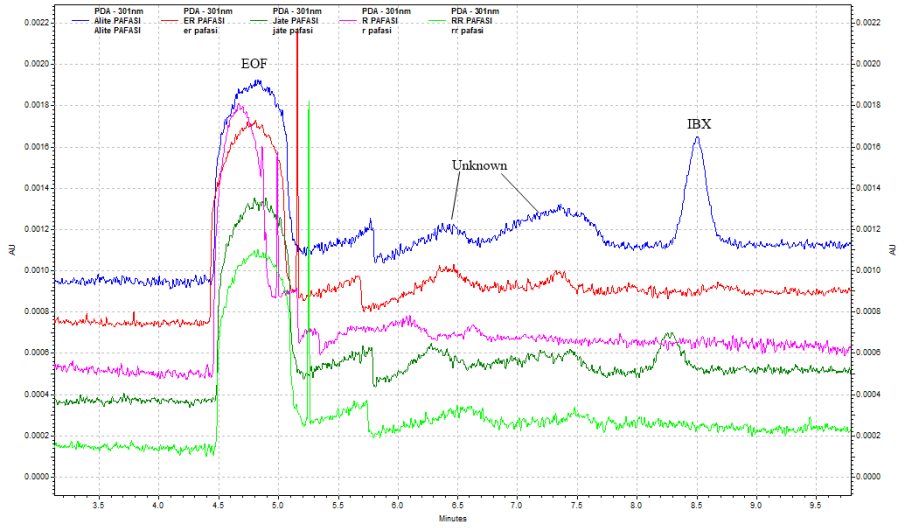


(a) Samples from cyclone underflow (blue), rougher flotation (red), concentrate (pink), tails (green) and scavenger flotation (light green).

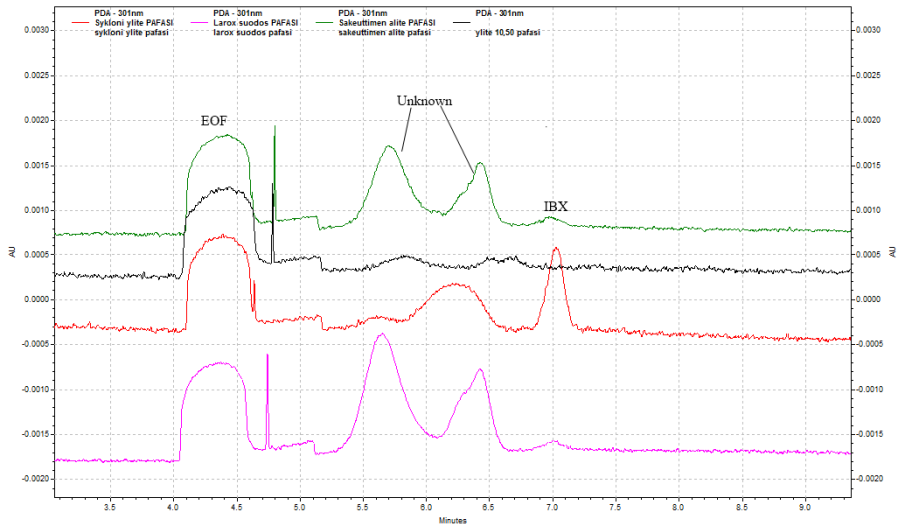


(b) Samples from thickener underflow (green), thickener overflow (black), cyclone overflow (red) and filtrate (pink).

Figure 60: Electropherograms of samples from the flotation process at Vammala. All samples analyzed using method 2.